# THE QUARTERLY JOURNAL OF
# MECHANICS AND APPLIED MATHEMATICS

VOLUME XII PART 1
FEBRUARY 1959

OXFORD
AT THE CLARENDON PRESS
1959

*Price* 18*s. net*

PRINTED IN GREAT BRITAIN BY VIVIAN RIDLER AT THE UNIVERSITY PRESS, OXFORD

# THE QUARTERLY JOURNAL OF MECHANICS AND APPLIED MATHEMATICS




THE QUARTERLY JOURNAL OF MECHANICS AND APPLIED MATHEMATICS is published at 18*s.* net for a single number with an annual subscription (for four numbers) of 60*s.* post free.


## NOTICE TO CONTRIBUTORS

1. *Communication.* Papers should be communicated to Dr. D. M. A. Leggett, Department of Mathematics, King's College, Strand, London, W.C. 2.

**If possible, to expedite publication, papers should be submitted in duplicate.**

2. *Presentation.* Papers should be typewritten (double spacing) and should be preceded by a summary not exceeding 300 words in length. References to literature should be given in standard order, *author, title of journal, volume number, date, page.* These should be placed at the end of the paper and arranged according to the order of reference in the paper.

3. *Diagrams.* The number of diagrams should be kept to the minimum consistent with clarity. The lines of the figures should be drawn in ink either on draughtsman's paper or on good quality white paper. Each individual line in the figure should bear reducing to one-half of the size of the original, and great care should be exercised to see that the lines are regular in thickness, especially where they meet. Lettering of the figure should be in pencil and should be sufficient to define clearly the lines and curves in it. The writing of formulæ or of explanations on the diagram itself should be avoided. All explanations of symbols, etc., should be given in underline. Contributors should indicate on their manuscripts where figures should be inserted.

4. *Tables.* Tables should preferably be arranged so that they can be printed with the columns parallel to the longer edge of the page.

5. *Notation.* All single letters used to denote vectors in the manuscript should be marked by underlining with a wavy line. Scalar and vector products should be denoted by $\underset{\sim}{a} . \underset{\sim}{b}$ and $\underset{\sim}{a} \wedge \underset{\sim}{b}$ respectively. Real and imaginary parts of complex quantities should be denoted by re and im respectively.

6. *Offprints.* Authors of papers will be entitled to 25 free offprints. This number is available for sharing between authors of joint papers.

7. All correspondence other than that dealing with contributions should be addressed to the publishers:


OXFORD UNIVERSITY PRESS
AMEN HOUSE, LONDON, E.C. 4

# ON THE SEPARATION OF GAS MIXTURES BY SUCTION OF THE THERMAL-DIFFUSION BOUNDARY LAYER

*By* V. C. LIU

*(The University of Michigan, Ann Arbor, Michigan)*

[Received 21 November 1957]

SUMMARY

This paper discusses the formation and characteristics of the boundary layer of thermal diffusion existing along the surface of a heated wall over which flows a mixture of gases of unequal molecular weights. Due to the existence of a temperature gradient in the boundary layer, a thermal-diffusion flux is set up such that the lighter gas tends to move to the hotter region and the heavier gas to the colder region. When the temperature of the surface is maintained at a much higher level than that of the free stream, the concentration of the lighter gas increases monotonically from its free-stream value at the outer edge of the boundary layer to a maximum value at the plate.

The existence of an extremely high temperature gradient makes it possible to obtain significant diffusive separation of gas mixtures in the boundary layer of a laminar flow. From this consideration a new method of separating gas mixtures by suction of the thermal-diffusion boundary layer was conceived. An analysis of the thermal-diffusion boundary layer is made, using a flat plate with constant suction as a model and assuming that the concentration of the lighter gas is much smaller than unity. The strong stabilizing effect of suction on the laminar flow is discussed briefly. A limiting ratio of suction against free-stream velocity for the maintenance of laminar flow is derived. An estimation of the rate of attaining the equilibrium-concentration profile is also made.

## 1. Introduction

The Clusius and Dickel method (1) for separating gas mixtures with an appropriate combination of thermal diffusion and natural convection has proved to be exceedingly effective in many cases. The principle of this method can be described as follows: a vertical tube has an electrically heated wire along its axis and is filled with a mixture of two gases of different molecular weights. On account of the temperature difference between the heated wire and the cooled wall, the resulting thermal-diffusion flux makes the concentration of the heavier constituent greater near the wall and that of the lighter constituent greater near the wire. Natural convection produces a flow of the cold gas downward near the wall and of the hot gas upward along the wire. These two processes combine

[Quart. Journ. Mech. and Applied Math., Vol. XII, Pt. 1, 1959]

# THE QUARTERLY JOURNAL OF MECHANICS AND APPLIED MATHEMATICS




THE QUARTERLY JOURNAL OF MECHANICS AND APPLIED MATHEMATICS is published at 18*s.* net for a single number with an annual subscription (for four numbers) of 60*s.* post free.


## NOTICE TO CONTRIBUTORS

1. *Communication.* Papers should be communicated to Dr. D. M. A. Leggett, Department of Mathematics, King's College, Strand, London, W.C. 2.

If possible, to expedite publication, papers should be submitted in duplicate.

2. *Presentation.* Papers should be typewritten (double spacing) and should be preceded by a summary not exceding 300 words in length. References to literature should be given in standard order, *author, title of journal, volume number, date, page.* These should be placed at the end of the paper and arranged according to the order of reference in the paper.

3. *Diagrams.* The number of diagrams should be kept to the minimum consistent with clarity. The lines of the figures should be drawn in ink either on draughtsman's paper or on good quality white paper. Each individual line in the figure should bear reducing to one-half of the size of the original, and great care should be exercised to see that the lines are regular in thickness, especially where they meet. Lettering of the figure should be in pencil and should be sufficient to define clearly the lines and curves in it. The writing of formulae or of explanations on the diagram itself should be avoided. All explanations of symbols, etc., should be given in underline. Contributors should indicate on their manuscripts where figures should be inserted.

4. *Tables.* Tables should preferably be arranged so that they can be printed with the columns parallel to the longer edge of the page.

5. *Notation.* All single letters used to denote vectors in the manuscript should be marked by underlining with a wavy line. Scalar and vector products should be denoted by $\underline{a} \cdot \underline{b}$ and $\underline{a} \times \underline{b}$ respectively. Real and imaginary parts of complex quantities should be denoted by re and im respectively.

6. *Offprints.* Authors of papers will be entitled to 25 free offprints. This number is available for sharing between authors of joint papers.

7. All correspondence other than that dealing with contributions should be addressed to the publishers:


OXFORD UNIVERSITY PRESS
AMEN HOUSE, LONDON, E.C. 4

# ON THE SEPARATION OF GAS MIXTURES BY SUCTION OF THE THERMAL-DIFFUSION BOUNDARY LAYER

*By* V. C. LIU

(*The University of Michigan, Ann Arbor, Michigan*)

[Received 21 November 1957]

SUMMARY

This paper discusses the formation and characteristics of the boundary layer of thermal diffusion existing along the surface of a heated wall over which flows a mixture of gases of unequal molecular weights. Due to the existence of a temperature gradient in the boundary layer, a thermal-diffusion flux is set up such that the lighter gas tends to move to the hotter region and the heavier gas to the colder region. When the temperature of the surface is maintained at a much higher level than that of the free stream, the concentration of the lighter gas increases monotonically from its free-stream value at the outer edge of the boundary layer to a maximum value at the plate.

The existence of an extremely high temperature gradient makes it possible to obtain significant diffusive separation of gas mixtures in the boundary layer of a laminar flow. From this consideration a new method of separating gas mixtures by suction of the thermal-diffusion boundary layer was conceived. An analysis of the thermal-diffusion boundary layer is made, using a flat plate with constant suction as a model and assuming that the concentration of the lighter gas is much smaller than unity. The strong stabilizing effect of suction on the laminar flow is discussed briefly. A limiting ratio of suction against free-stream velocity for the maintenance of laminar flow is derived. An estimation of the rate of attaining the equilibrium-concentration profile is also made.

## 1. Introduction

THE Clusius and Dickel method (1) for separating gas mixtures with an appropriate combination of thermal diffusion and natural convection has proved to be exceedingly effective in many cases. The principle of this method can be described as follows: a vertical tube has an electrically heated wire along its axis and is filled with a mixture of two gases of different molecular weights. On account of the temperature difference between the heated wire and the cooled wall, the resulting thermal-diffusion flux makes the concentration of the heavier constituent greater near the wall and that of the lighter constituent greater near the wire. Natural convection produces a flow of the cold gas downward near the wall and of the hot gas upward along the wire. These two processes combine

to increase the concentration of the heavier constituent at the bottom and of the lighter constituent at the top of the tube.

From the hydrodynamic point of view, a limitation of this separation method by convection and thermal diffusion is that the critical Reynolds number of transition from laminar to turbulent flow must not be reached. According to Onsager and Watson (**2**), the magnitude of the transition Reynolds number of the Clusius and Dickel separation column is of order one-tenth the values obtainable for pure pressure flow through pipes. As a result of the low transition Reynolds number, the efficiency of production of concentrated material is limited (Jones and Furry, **3**).

The purpose of this paper is to point out a method of separating gas mixtures which might possibly be a more efficient method because of its inherently higher transition Reynolds number and higher rate of separation. The method originates from the theory of laminar boundary layers, a phenomenon of fluid dynamics. It is most simply described by stating that if a forced convection stream at high Reynolds number flows along a stationary solid wall which is maintained at an elevated temperature, a very thin layer of laminar flow exists in contact with the wall. It is in this layer that the velocity of flow rises from zero at the wall to its free-stream value at the other edge of the boundary layer. Coexisting with the velocity boundary layer is a thermal boundary layer in which the temperature difference $(T-T_\infty)$ varies from $(T_0-T_\infty)$ at the wall to zero at the free stream. With a flow of ordinary gases, the thicknesses of these two boundary layers are of the same order of magnitude. For example, a temperature gradient of the order of $3\times10^4$ °C per cm can be obtained at the inner edge of the boundary layer with a forced convection of air under normal conditions, at a free-stream velocity of 30 m per sec, and a wall temperature of 300° C above the free-stream air temperature. Therefore, one might expect that if the flow medium is a mixture of gases of unequal molecular weights, diffusive separation will occur in the boundary layer, especially near the wall. The amount of separation after equilibrium is attained will depend on the local temperature gradient, the molecular-mass ratio, and the law of mutual interaction of the gases. Concentration of the lighter constituent will increase near the wall. This increase of concentration over the free-stream concentration diminishes to zero as the other edge of the boundary layer is approached. Thus, a concentration (or thermal-diffusion) boundary layer is formed. To collect the more concentrated mixture near the plate, one may use the method of boundary-layer suction through a porous plate, a technique already in use for the control of boundary-layer flow in attaining the optimum lift and drag characteristics of an airfoil (**4**).

The Clusius and Dickel method differs from the present one in the use of the convection stream and the collection of the concentrated mixture. The convective flow in the thermal-diffusion column of Clusius and Dickel is caused solely by the density gradients created by the temperature differences in the horizontal direction. The convective flow in the system here proposed is created by external causes (e.g. a pump). Such a flow is generally called a *forced* convection as distinguished from the *natural* convection caused by temperature differences and buoyancy forces. The forced convection is directly responsible for boosting the temperature gradient in the boundary layers.

Another asset of the present method is its inherently higher transition Reynolds number due to the large stabilizing effect of suction on the boundary-layer flow. The stabilizing effect of suction makes it possible to use a higher temperature difference for thermal diffusion.

The analysis that follows is to establish the validity and feasibility of the present method. The emphasis will be mainly on the concepts and on the general features of the problem rather than on the computation of details in specific cases.

## 2. Notation

The notation of Chapman and Cowling (**5**) has been used with the following exceptions:

$\mathbf{V}$ velocity vector of mean mass flow.

$u, v$ mean mass-flow velocity components parallel to the $x$- and $y$-axes.

$\nu$ kinematic viscosity $(\mu/\rho)$.

$D$ ordinary coefficient of diffusion of binary gas-mixtures.

$a$ $(T_0-T_\infty)/T_\infty$.

$\psi(\xi)$ logarithmic derivative of the gamma function.

$\sigma$ Prandtl number $(\mu c_p/\lambda)$. [$\sigma$ is assumed constant for a given gas or gas mixture.]

$S$ $\nu/D$ [$S$ is assumed constant for a given gas mixture].

$\Lambda$ $\lambda/\rho c_p D$ [$\Lambda$ is assumed constant for a given gas mixture].

$\beta$ $m_2/(m_2-m_1)$.

$\zeta$ suction boundary-layer parameter $\left[\zeta = -\rho_0 v_0 \int_0^y (1/\mu)\, dy\right]$.

$s$ viscosity- and diffusion-coefficient exponent

$$\mu/\mu_\infty = (T/T_\infty)^s; \qquad nD/(nD)_\infty = (T/T_\infty)^s.$$

$Z$ separation efficiency (see equation (5.1)).

$G$ $(1/T)(\partial T/\partial\zeta)$.

$M$ Mach number.

$R$ Reynolds number ($u_\infty L/\nu_\infty$).
$L$ a characteristic linear dimension of the system.
$R_t$ $u_\infty \delta^*/\nu_\infty$ (transition Reynolds number).

*Subscripts*

$_0$ at wall.
$_\infty$ at free stream.
$_c$ at suction chamber.
$_1$ constituent '1' of a binary gas mixture.
$_2$ constituent '2'.

## 3. Convective-diffusive equation

Consider a non-uniform binary gas mixture. Let $\bar{\mathbf{C}}_1$ denote the mean molecular velocity of constituent 1 relative to a coordinate system moving with the mean mass flow velocity $\mathbf{V}$. By applying the principle of conservation of molecules to the first constituent, one obtains

$$\frac{\partial n_1}{\partial t}+\nabla.(n_1\mathbf{V}+n_1\bar{\mathbf{C}}_1)=0. \tag{3.1}$$

On adding (3.1) to the corresponding equation for the second constituent, and noting that $\rho_1\bar{\mathbf{C}}_1+\rho_2\bar{\mathbf{C}}_2=0$, one gets the equation of mass conservation for the mixture

$$\frac{\partial \rho}{\partial t}+\nabla.(\rho\mathbf{V})=0. \tag{3.2}$$

For definiteness, suppose $m_2>m_1$. Let $\theta=n_1/n$ and $\beta=m_2/(m_2-m_1)$. Substituting $\theta$ and $\beta$ in (3.1) and (3.2) and then eliminating $\rho$, one has

$$n\frac{\partial\theta}{\partial t}+n\mathbf{V}.\nabla\theta+\frac{\beta-\theta}{\beta}\nabla.(n_1\bar{\mathbf{C}}_1)=0. \tag{3.3a}$$

The diffusive flux, given by

$$n_1\bar{\mathbf{C}}_1=-nD\left[\nabla\theta+\frac{\theta(1-\theta)}{\beta-\theta}\nabla\ln p-\alpha\theta(1-\theta)\nabla\ln T\right], \tag{3.3b}$$

includes contributions from gradients of concentration, pressure, and temperature, respectively; here $\alpha$ is the thermal diffusion factor. The diffusive flux due to external forces is taken to be negligible. The formulation of the total diffusive flux in (3.3) is based on the Chapman–Enskog theory of diffusion (**5**, note that the lighter gas is labelled 1 here).

The diffusion coefficient $D$ is inversely proportional to $n$ if the temperature is constant and $nD$ is a function of $T$ only. For many gas mixtures it can be assumed (**5**) that

$$nD/(nD)_\infty=(T/T_\infty)^s, \tag{3.4}$$

where $s$ is a constant depending upon the molecular models employed.

For ordinary gases $s$ lies between the extreme values $\frac{1}{2}$ and 1. The value of $s$ for a mixture of $H_2$ or He in air is 0·77.

The dependence of the thermal-diffusion factor $\alpha$ on $T$ and $n_1/n_2$ is small and here neglected. A list of measured values of $\alpha$ for various mixtures of gases has been compiled by Grew and Ibbs (**6**). Strictly, the functions $V$, $n$, and $T$ appearing in the differential equation (3.3) for $\theta$ depend, in turn, on $\theta$. This dependence is negligible when $\theta$ is small.

## 4. Boundary layer with suction

The boundary layer theory deals with the velocity and temperature distributions in the immediate neighbourhood of a solid surface along which there is convective flow of a slightly viscous medium. In the case of a flat plate with constant and continuous suction distributed over the whole plate, the Navier–Stokes equations of motion possess a particular solution for which the velocity distribution is independent of $x$, a coordinate measured along the plate (**4**). It can be shown for the case of an incompressible flow (**7**) that this special velocity profile, known as the asymptotic suction profile, is attained after an initial plate length of

$$x_s = 4u_\infty \nu / v_0^2 \tag{4.1}$$

measured from the leading edge, $v_0$ being the normal velocity at the plate. The corresponding problem for a compressible flow with heat transfer was treated by Liu (**8**). A brief résumé of the results of the asymptotic suction profile considering heat transfer and compressibility is reproduced here since the cited reference is unpublished. The equations of motion, continuity, and energy of boundary-layer flow along a flat plate are respectively (**9**)

$$\rho u \frac{\partial u}{\partial x} + \rho v \frac{\partial u}{\partial y} = \frac{\partial}{\partial y}\left(\mu \frac{\partial u}{\partial y}\right), \tag{4.2}$$

and

$$\frac{\partial}{\partial x}(\rho u) + \frac{\partial}{\partial y}(\rho v) = 0, \tag{4.3}$$

and

$$\rho u \frac{\partial}{\partial x}(c_p T) + \rho v \frac{\partial}{\partial y}(c_p T) = \frac{\partial}{\partial y}\left(\lambda \frac{\partial T}{\partial y}\right) + \mu\left(\frac{\partial u}{\partial y}\right)^2. \tag{4.4}$$

The associated boundary conditions for the case of a flat plate with constant suction $v_0$ are

$$u = 0, \quad v = -v_0, \quad T = T_0 \quad \text{at } y = 0, \tag{4.5a}$$

and

$$u = u_\infty, \quad T = T_\infty \quad \text{at } y = \infty. \tag{4.5b}$$

In view of the asymptotic assumption, i.e. $\partial u/\partial x = 0$ and $\partial T/\partial x = 0$, one can integrate (4.3) immediately, giving

$$\rho v = \text{constant} = \rho_0 v_0 = \rho_\infty v_\infty. \tag{4.6}$$

For many gases, the variation of $\mu$ with $T$ can be adequately represented by

$$(\mu/\mu_\infty) = (T/T_\infty)^s, \tag{4.7}$$

where the values of $s$ lie between $\frac{1}{2}$ and 1. For air $s$ is about 0·76. The values of $s$ in (3.4) and (4.7) are assumed identical. Introduce and substitute

$$\zeta = -\rho_0 v_0 \int_0^y (1/\mu)\, dy \tag{4.8}$$

in (4.2) and (4.4). One obtains after simple calculation

$$u = u_\infty(1-e^{-\zeta}), \tag{4.9}$$

and

$$\frac{T}{T_\infty}-1 = \left(\frac{T_0}{T_\infty}-1\right)e^{-\sigma\zeta}+\tfrac{1}{2}(\gamma-1)M_\infty^2\frac{\sigma}{2-\sigma}(e^{-\sigma\zeta}-e^{-2\zeta}), \tag{4.10}$$

where the Prandtl number $\sigma = \mu c_p/\lambda$ is assumed constant. It should be noted that the corresponding solution in the case of an insulated plate was given by Young (**10**).

It is significant that the essential variation of $u$ and $T$ is restricted to a very thin boundary-layer zone, the thickness of which is of the order of $\nu/(-v_0)$. Hence, it is justifiable to introduce the usual boundary-layer assumptions $u \gg v$ and $\partial/\partial y \gg \partial/\partial x$. For the case $\theta \ll 1$, the convective-diffusion equation (3.3) is simplified (by boundary layer approximations) to

$$n\frac{\partial\theta}{\partial t}+nu\frac{\partial\theta}{\partial x}+nv\frac{\partial\theta}{\partial y} = \frac{\partial}{\partial y}\left[nD\left(\frac{\partial\theta}{\partial y}-\alpha\theta\frac{\partial \ln T}{\partial y}\right)\right]. \tag{4.11}$$

After the velocity and temperature distributions in the boundary layer attain their respective asymptotic profiles, (4.9) and (4.10), along a flat plate with constant suction, the concentration distribution $\theta$ will adjust itself suitably.

Assume now that the origin of the $x$-axis coincides with the point at which the asymptotic suction profiles have been essentially attained (see (4.1)). Let† $x = u_\infty t$; then by substituting (4.8) in (4.11), this becomes

$$\rho\mu S\left(1+\frac{u}{u_\infty}\right)\frac{\partial\theta}{\partial t}-\rho_0^2 v_0^2\left[S\frac{\partial\theta}{\partial\zeta}+\frac{\partial}{\partial\zeta}\left(\frac{\partial\theta}{\partial\zeta}-\alpha\theta\frac{\partial \ln T}{\partial\zeta}\right)\right] = 0, \tag{4.12}$$

where $S = \nu/D$, which is assumed constant for a given gas mixture.

## 5. The steady-state solution

Consider a flat porous plate, on one side of which is a suction chamber. The suction-chamber pressure is maintained at a constant value $p_c$, which is less than the free-stream pressure $p_0$ on the other side of the plate. A binary gas mixture, with $\theta \ll 1$, flows along the plate with a free-stream

† This is feasible because the asymptotic profiles are independent of $x$.

velocity $u_\infty$. The plate temperature is maintained at $T_0$, which is higher than the free-stream temperature $T_\infty$. It is further assumed that the composition of the gas in the suction chamber remains constant, i.e. $\theta_c = \text{constant}$.

The gas mixture, while seeping through a porous plate or an equivalent array of capillary tubes, is subjected to a diffusive-separation process. For a given $p_0$ and $p_c$, the diffusive separation factor

$$\theta_c(1-\theta_0)/\theta_0(1-\theta_c) \approx \theta_c/\theta_0$$

depends primarily on the ratio of the mean free path of the inlet mixture $l$, to the radius $r$, of the equivalent capillary tubes. When $l \gg r$, the flow through the porous plate obeys the well-known Knudsen formula (11); hence, $\theta_c/\theta_0$ at $p_c = 0$ has its maximum value $(m_2/m_1)^{\frac{1}{2}}$. As the ratio $l/r$ decreases, the intermolecular collisions which transfer momentum between the lighter faster and the heavier slower molecules become more frequent; consequently, both constituents of the mixture tend to move with a common mass velocity. As $l \ll r$, the flow pattern gradually conforms to viscous tube flow of the Poiseuille type, for which the diffusive-separation effect is insignificant. In the intermediate region, $\theta_c/\theta_0$ varies between these extreme values. Let the separation efficiency $Z$ be the ratio of the actual enrichment (increase in concentration) to the ideal enrichment at constant back composition, namely (12)

$$\frac{\theta_c-\theta_0}{\theta_0} = Z\frac{(m_2/m_1)^{\frac{1}{2}}-1}{(m_2/m_1)^{\frac{1}{2}}}, \tag{5.1}$$

where $Z$ depends on $p_0$, $p_c$, and $l/r$ (see Appendix).

The best porosity size for the experiment depends on the limiting suction velocity for stabilizing the boundary-layer flow (see Section 7), the separation efficiency $Z$, and economy of operation. An optimum value for $r$ can be determined from these considerations. The use of a dual system of suction, a combination of porous surface and slit orifices, might possibly provide the optimum condition for efficient separation.

In the case of the steady state, (4.12) becomes

$$\frac{d^2\theta}{d\zeta^2} + S\frac{d\theta}{d\zeta} - \alpha\frac{d}{d\zeta}\left(\theta\frac{d\ln T}{d\zeta}\right) = 0, \tag{5.2}$$

with the boundary conditions

$$\theta = \theta_\infty; \quad d\theta/d\zeta = 0 \quad \text{at } \zeta = \infty. \tag{5.3}$$

After elementary integration, (5.2) and (5.3) give

$$\theta(\zeta)/\theta_\infty = 1 - \alpha T^\alpha e^{-S\zeta}\int_\zeta^\infty e^{S\xi}(dT/d\xi)T^{-(\alpha+1)}\,d\xi. \tag{5.4}$$

The diffusive separation factor for the thermal-diffusion boundary layer, $\theta_0/\theta_\infty$, in the case of incompressible flow ($M_\infty \ll 1$), becomes

$$\left[\frac{\theta_0}{\theta_\infty}\right]_b = 1+\alpha a(1+a)^\alpha \int_0^1 z^{-\Lambda}(1+az)^{-(1+\alpha)}\,dz, \tag{5.5a}$$

provided $0 \leqslant \Lambda < 1$ where $\Lambda = S/\sigma$ which is constant for a given gas mixture. It is of interest to note that the definite integral in (5.5a) can be expressed in terms of hypergeometric functions (**13**); consequently,

$$\left[\frac{\theta_0}{\theta_\infty}\right]_b = 1+\alpha a(1+a)^\alpha(1-\Lambda)^{-1}F(1+\alpha, 1-\Lambda; 2-\Lambda; -a). \tag{5.5b}$$

The advantage of the form (5.5b) is that in special cases a simple formula for $[\theta_0/\theta_\infty]_b$ can be obtained in closed form (in view of the considerable amount of knowledge concerning special forms of hypergeometric functions).

The factor $\Lambda$, defined as $\lambda/\rho c_p D$, needs further explanation. The parameter $\lambda/\rho c_p$ which appears in Fourier's equation of unsteady heat flow is sometimes called the thermal diffusivity (following Kelvin). It has the dimension $L^2/t$ which is the same as that of the mutual-diffusion coefficient $D$; hence, $\Lambda$ is dimensionless. Since both $\lambda/\rho c_p$ and $D$ are proportional to $T^{1+s}$ (**5**), $\Lambda$ is nearly temperature-independent.

Values of $\Lambda$ can be estimated on the basis of the kinetic theory of gases. For isotope mixtures, the mutual-diffusion coefficient must be nearly equal to the coefficient of self-diffusion of either isotope. Using the self-diffusion formula for Maxwellian molecules and Eucken's formula for thermal conductivity, one obtains $\Lambda = 0{\cdot}9$ for diatomic mixtures. The value of $\Lambda$ for a mixture of $H_2$ and $N_2$ is estimated to be 0·32, using the mutual-diffusion coefficient.

In the case of an isotope mixture, $\alpha$ is usually very small compared with unity. If $a = 1$, a simple formula for the diffusive separation factor for the boundary layer can be obtained, namely

$$\left[\frac{\theta_0}{\theta_\infty}\right]_b = 1+\alpha\, 2^{\alpha-1}[\psi(1-\tfrac{1}{2}\Lambda)-\psi(\tfrac{1}{2}-\tfrac{1}{2}\Lambda)]. \tag{5.6}$$

On the basis of (5.6), one can calculate the enrichment factor $(\theta_0-\theta_\infty)/\theta_\infty$. This is found to be about fourteen times that corresponding to the convection-free case, namely $(T_0/T_\infty)^\alpha-1$, when the value of $\alpha$ lies in the range 0·01 to 0·1.

In view of (5.1), one obtains the total diffusive separation factor

$$\left[\frac{\theta_0}{\theta_\infty}\right] = \left[1+Z\left(1-\left(\frac{m_1}{m_2}\right)^{\frac{1}{2}}\right)\right]\left[\frac{\theta_0}{\theta_\infty}\right]_b. \tag{5.7}$$

## 6. The time to attain the steady state

The time required to attain the steady state will largely determine whether or not this method of separating gas mixtures by suction of the thermal-diffusion boundary layer is convenient and practical. It will be mathematically difficult to determine the time lag of the system by solving the time-dependent equation (4.12). A careful investigation of the problem, however, reveals that most of the concentration change occurs near the wall surface of the boundary layer; hence it may suffice to solve an approximate form of (4.12), valid for the region near the plate. The temperature distribution near the wall surface of the boundary layer can be approximated by

$$T = T_0 \exp(G_0 \zeta), \tag{6.1}$$

where $G_0$ is determined by matching the temperature gradient of (6.1) with that of the exact expression (4.10) at $\zeta = 0$; hence

$$G_0 = [dT/d\zeta]_0/T_0. \tag{6.2}$$

The velocity near the plate is taken as $u = 0$. With these approximations, (4.12) becomes

$$\partial\theta/\partial t = (v_0^2/\nu_0 S)[\partial^2\theta/\partial\zeta^2 - (\alpha G_0 - S)\partial\theta/\partial\zeta], \tag{6.3}$$

provided one assumes that $\mu/\mu_0 = T/T_0$. The boundary conditions are

$$\theta(0,\zeta) = \theta_\infty, \qquad \theta(t,0) = \theta_0, \qquad \theta(t,\delta) = \theta_\delta \approx \theta_\infty. \tag{6.4}$$

The simple transformation

$$\theta = \theta^* \exp[\tfrac{1}{2}(\alpha G_0 - S)\zeta - (\alpha G_0 - S)^2 v_0^2 t/4\nu_0 S] \tag{6.5}$$

applied to (6.3) leads to

$$\partial\theta^*/\partial t = (v_0^2/\nu_0 S)(\partial^2\theta^*/\partial\zeta^2), \tag{6.6}$$

a form of the familiar heat equation. The transformed boundary conditions (6.4) are as follows:

$$\theta^*(0,\zeta) = \theta_\infty \exp[-\tfrac{1}{2}(\alpha G_0 - S)\zeta], \tag{6.7 a}$$

$$\theta^*(t,0) = \theta_0 \exp[(\alpha G_0 - S)^2 v_0^2 t/4\nu_0 S], \tag{6.7 b}$$

$$\theta^*(t,\delta) = \theta \exp[-\tfrac{1}{2}(\alpha G_0 - S)\delta + (\alpha G_0 - S)^2 v_0^2 t/4\nu_0 S]. \tag{6.7 c}$$

The solution to the boundary-value problem of (6.6) with (6.7) can be constructed by the classical method of Laplace transformation or Duhamel's theorem. One may note, however, that the present boundary-value problem is completely analogous to that of heat conduction in a solid bar with initial and boundary conditions prescribed as in (6.7) (14).

Using this mathematical analogy, the concentration near the plate is found to be

$$\theta(t,\zeta) = \theta^* \exp[\tfrac{1}{2}(\alpha G_0 - S)\zeta - (\alpha G_0 - S)^2 v_0^2 t/4\nu_0 S],$$

where

$$\theta^*(t,\zeta) = (2/\delta)\sum_1^\infty \frac{4n\pi\delta\sin(n\pi\zeta/\delta)}{\delta^2(\alpha G_0 - S)^2 + 4n^2\pi^2}[(\theta_\infty - \theta_0)e^{-n^2\pi^2 v_0^2 t/\nu_0 S\delta^2} + \\ + \{\theta_0 - (-1)^n\theta_\infty e^{-(\alpha G_0 - S)\delta/2}\}e^{(\alpha G_0 - S)^2 v_0^2 t/4\nu_0 S}]. \quad (6.8)$$

To determine whether the present system will take an unduly long time to attain the steady state, it is necessary to estimate the relaxation time of the system by taking merely the first eigenvalue $n = 1$ in (6.8). This gives a relaxation time

$$t_1 \sim 4\nu_0 S\delta^2/v_0^2[4\pi^2 + \delta^2(\alpha G_0 - S)^2]. \quad (6.9)$$

It is apparent from (6.9) that with values of $S$ and $\delta$ both of order unity, the governing factor for $t_1$ is $\nu_0/\pi^2 v_0^2$. This is of order 0·1 sec if $v_0$ is 1 cm/sec.

## 7. The stabilization effect of suction on the boundary layer flow

The present analysis is supposedly valid only in the case of a non-turbulent boundary-layer flow, although in the case of turbulent flow a laminar sub-layer along the plate still exists. It is generally known, however, that turbulent motion is the more natural state of fluid motion, whereas laminar motion occurs only when the Reynolds number is so low that deviations from it are liable to be damped out. The transition Reynolds number for an incompressible boundary-layer flow depends upon such factors as the free-stream turbulence, the surface temperature, pressure gradient, and the roughness of the surface, to mention a few (**15**).

Suction reduces the boundary-layer thickness. A thinner boundary layer is less prone to become turbulent; furthermore, it creates a laminar velocity profile which has a higher limit of stability than that without boundary suction.

Experimental investigations with stability analysis (**16**, **17**) appear to confirm the suggestion that above a certain value of $-v_0/u_\infty$, against infinitesimal disturbances, complete stability of the isothermal laminar boundary layer along a flat plate with constant suction may be achieved for all Reynolds numbers. Liepmann and Fila (**18**) provided experimental results of surface temperature on the boundary-layer transition without suction. Although precise information concerning the stabilizing effect by suction on the boundary layer along a heated plate is still lacking, from the expression for the displacement thickness of the boundary layer along such a plate

$$\delta^* = \int_0^\infty \left[1 - \frac{\rho u}{(\rho u)_\infty}\right] dy = \int_0^\infty \frac{\mu}{(\rho v)_0}\left[\frac{\rho u}{(\rho u)_\infty} - 1\right] d\zeta, \quad (7.1)$$

one can glean a suggestion of the stabilizing effect exerted by suction. (This, of course, does not disregard the known fact that, in some cases, surface temperature can have more important effects† on the stabilization of flow.) From (7.1) and the definition of $R_l$, one obtains

$$-\frac{v_0}{u_\infty} = \frac{T_0}{R_l T_\infty} \int_0^\infty \left(\frac{T}{T_\infty} - \frac{u}{u_\infty}\right)\left(\frac{T_\infty}{T}\right)^{1-s} d\zeta. \tag{7.2}$$

After substituting the asymptotic suction profiles (4.9) and (4.10), this can be integrated numerically. In the special case $s = 1$, (7.2) can be integrated in closed form,

$$-\frac{v_0}{u_\infty} = \frac{T_0}{R_l T_\infty}\left[\frac{1}{\sigma}\left(\frac{T_0}{T_\infty} - 1\right) + \frac{\sigma}{2}\frac{(\gamma-1)}{2-\sigma} M_\infty^2 \left(\frac{1}{\sigma} - \frac{1}{2}\right) + 1\right]. \tag{7.3}$$

In the case of isothermal incompressible flow, the suction ratio is

$$-v_0/u_\infty = 1/R_l, \tag{7.4}$$

which is of order $10^{-4}$.

It should be noted that the asymptotic suction profiles, on the existence of which the above calculations are based, develop only after a certain distance from the leading edge (see (4.1)). The velocity and temperature profiles for the intermediate region have lower limits of stability, hence the suction ratio over this region must be larger than (7.3) if laminar flow is to be maintained.

## 8. Conclusion

The case of a flat plate with constant suction and $\theta \ll 1$ is chosen as a model for the purpose of analysis. The solution, simple as it is, preserves the general features of a thermal-diffusion boundary layer with suction. This solution, being exact, serves well to explore the mechanism of the physical phenomenon which is the primary aim of the present paper.

The relaxation of such restrictions as $\theta \ll 1$, $\partial p/\partial x = 0$, and $v_0 =$ constant would involve more laborious, but straightforward, calculations (19).

The radiative heat transfer between the surface and the flowing gases has not been taken into account in the analysis. This would tend to make the present results of diffusive separation appear too high; but the excess is believed to be small unless the surface temperature is much higher than three times the free-stream temperature.

Although the primary function of this discussion is to establish the

† These include the effect of gravitational forces (because of the density differences in the boundary layer) and the effect due to the dependence of the viscosity of a gas on the

principle of separating gas mixtures by suction of the thermal-diffusion boundary layer, it is of interest to suggest a simple scheme of application of this principle. To produce the forced convection of the mixture for separation, one may use a conventional low-turbulence pressure channel (**20**). Unlike the wind tunnel usually designed for aerodynamic tests of models, the pressure channel in question should have at its test section properly-spaced porous plates designed for the production and suction of the thermal-diffusion boundary layers. If the channel is geometrically similar to the Langley two-dimensional low-turbulence pressure channel, and can, for example, displace 5 kg of gas mixture per second at a speed of 30 m per sec at its test section, the power consumed in the channel will be about $\frac{3}{4}$ kW. This does not include the power lost in the drive-unit, nor that used in heating the plates, sucking the boundary layers, and cooling the mixtures in the channel. The power consumption is estimated on the basis of a power factor of 0·32, an average value for tunnels of this type. The above estimation is meant to give the right order of magnitude only. In order to achieve a large change in gas abundance, one needs to use a cascade of these processes.

## Acknowledgement

The present investigation is a part of a broad research programme on upper atmosphere supported by the Meteorological Branch of the U.S. Signal Corps under Contract No. DA–36–039 SC–64659 with the University of Michigan. The author wishes to record his indebtedness to Professor Sydney Chapman for his reading of the manuscript and his critical, illuminating discussions of this work; and to Mr. Howard Jew for the assistance in the numerical computations.

## APPENDIX

## CAPILLARY THEORY OF SEPARATION

In the special case $\theta \ll 1$, the separation efficiency becomes (**12**)

$$Z(\xi_0, \xi_c, E) = \int_{\xi_e}^{\xi_0} \exp(\xi^2)\, d\xi/(\xi_0 - \xi_c)\exp(\xi_0^2), \tag{A.1}$$

where

$$\xi = (128S/9\pi)^{\frac{1}{4}}[1+(9\pi/128)(r/l)]+(9\pi/512)^{\frac{1}{4}}(Sm_2/m_1)^{-\frac{1}{4}},$$
$$E = (128S/9\pi)^{\frac{1}{4}}+(9\pi/512)^{\frac{1}{4}}(Sm_2/m_1)^{-\frac{1}{4}}.$$

## REFERENCES

1. K. Clusius and G. Dickel, *Naturwiss.* **26** (1938) 546.
2. L. Onsager and W. H. Watson, *Phys. Rev.* **56** (1939) 474.
3. R. C. Jones and W. H. Furry, *Rev. Mod. Phys.* **18** (1946) 151.
4. H. Schlichting, *Boundary Layer Theory* (New York, 1955), pp. 229–40.

5. S. CHAPMAN and T. G. COWLING, *The Mathematical Theory of Non-uniform Gases*, 2nd edition (Cambridge, 1952), pp. 244–58.
6. K. E. GREW and T. L. IBBS, *Thermal Diffusion in Gases* (Cambridge, 1952), pp. 128–32.
7. R. IGLISCH, *Schriften d. dt. Akad. d. Luftfahrtforschung*, **8** B (1944), No. 1.
8. V. C. LIU, *On Compressible Laminar Boundary Layer with Suction* (Ph.D. Dissertation, Ann Arbor, Univ. Michigan, 1950).
9. L. HOWARTH, *Modern Developments in Fluid Dynamics, High Speed Flow* (Oxford, 1953), vol. 1, p. 381.
10. A. D. YOUNG, *Quart. J. Mech. Appl. Math.* **1** (1948) 70.
11. E. H. KENNARD, *Kinetic Theory of Gases* (New York, 1938), pp. 291–310.
12. R. D. PRESENT and A. J. DEBETHUNE, *Phys. Rev.* **75** (1949) 1050.
13. W. MAGNUS and F. OBERHETTINGER, *Formulas and Theorems for the Functions of Mathematical Physics* (New York, 1954), pp. 1–8.
14. H. S. CARSLAW and J. C. JAEGER, *Conduction of Heat in Solids* (Oxford, 1947), pp. 85–87.
15. A. M. KUETHE, *J. Aero. Sci.* **23** (1956) 444.
16. J. M. KAY, Aero. Res. Counc. R. and M. 2628 (1948).
17. P. A. LIBBY, L. KAUFMANN, and R. P. HARRINGTON, *J. Aero. Sci.* **19** (1952) 127.
18. H. W. LIEPMANN and G. H. FILA, Nat. Adv. Comm. Aero; Wash. Tech. Rep. 890 (1947).
19. V. C. LIU, *On Diffusive Separation of Gas Mixtures in Flow Fields*, Pts. 1 and 2, Tech. Rep. 2387–29–T. Ann Arbor: Eng. Res. Inst. Univ. Michigan (unpublished).
20. H. L. DRYDEN and I. H. ABBOTT, Nat. Adv. Comm. Aero.; Wash. Tech. Rep. 940 (1949).

# HEAT TRANSFER BY LAMINAR FLOW FROM A ROTATING DISK AT LARGE PRANDTL NUMBERS

*By* D. R. DAVIES (*University of Sheffield*)

[Received 18 December 1957]

SUMMARY

In this paper the approximate method of calculating the distribution of rate of heat transfer by laminar flow from a flat plate, described recently by Davies and Bourne, is extended to the problem of a heated rotating disk for an *arbitrary* radial distribution of surface temperature on the disk. The analysis is applicable if the temperature boundary layer is embedded well within the velocity boundary layer over the disk. By comparing the ensuing numerical results for heat transfer with those calculated from an exact solution, by Millsaps and Pohlhausen in the special case of *constant* surface temperature, we find that very good accuracy is obtained when the Prandtl number is greater than about 6.

## 1. Introduction

Millsaps and Pohlhausen (**1**) have recently obtained an exact solution (including aerodynamic heating) of the equation of forced convection from a rotating plate, when the flow is entirely laminar. This solution was used to compute the distribution of temperature and rate of heat transfer for values of the Prandtl number $\sigma$, between 1 and 10. However, the analysis is only applicable when the surface temperature is independent of radial and angular position on the plate. In order to obtain a solution when the surface temperature of the plate is an *arbitrary* function of radial distance, Morgan and Warner (**2**) have applied in a modified form the approximate technique used first by Lighthill (**3**) in the flat plate case. A linear representation of the velocity profile (valid in the region very near the surface of the disk) was assumed to apply over the whole thickness of the boundary layer. At very large values of $\sigma$ ($\sigma \simeq 10$ for cold water, $\sigma > 100$ for oils) the thickness of the temperature boundary layer is very much smaller than that of the velocity boundary layer, so that the crucial part of the velocity profile for heat flow is that near the surface. Consequently a linear representation is likely to be adequate for large values of $\sigma$. By comparing their numerical results with the exact values given by Millsaps and Pohlhausen, Morgan and Warner find that the error is large at $\sigma = 10$, the highest Prandtl number for which heat transfer rates were computed by Millsaps and Pohlhausen, and they suggest that the smallest value of $\sigma$ for which the linear approximation is suitable is very considerably greater than 10.

Davies and Bourne (**4**) have shown that this form of approximation

can be improved by using a power law representation of the velocity profile and so produced a better approximation over a larger part of the boundary layer thickness than was possible by using the linear (tangent) representation. An application to the disk problem of the power law approximation is therefore likely to yield a very substantial reduction in the minimum value of $\sigma$ at which good accuracy is obtained.

In the problem of the heated disk the radial component of velocity conveys the heat in the air stream outwards and consequently plays the dominant role in the convection of heat. A very good power law representation of this component can be made for the inner one-sixth of the velocity boundary layer. Following Davies and Bourne (4), the basic temperature equation is considerably simplified by using a von Mises transformation with the power law representation. The method of sources is then applied, the heated disk being regarded as an assembly of concentric circular sources. The radial distribution of source strength (or rate of heat transfer) is determined by solving an integral equation, the solution depending on the prescribed *radial* distribution of surface temperature on the disk. In the particular case of *constant* disk temperature the numerical values of rate of heat transfer for values of $\sigma$ greater than about 6 are found to be in very good agreement with the exact results given by Millsaps and Pohlhausen; these numerical values are given and discussed in section 4 of this paper.

The advantage of this method of calculation lies in the comparative simplicity of the numerical evaluation and particularly in its application to cases in which the distribution of disk temperature is an *arbitrary* function of radial distance from the centre of the disk. An additional point of interest lies in the possibility of extending the analysis (as in the flat plate case, 4) to include the important practical problem of convective heat transfer by turbulent flow from a rotating heated disk.

## 2. The basic temperature equation

If $r$ denotes radial distance from the centre of the disk, $z$ normal distance from the surface of the disk, $u_r$ the component velocity in the radial direction, $u_z$ the component velocity perpendicular to the plate, $\nu$ the kinematic viscosity, $\kappa$ the thermal diffusivity, $T$ the temperature, the equation of continuity is

$$\frac{1}{r}\frac{\partial}{\partial r}(ru_r)+\frac{\partial}{\partial z}u_z = 0, \tag{1}$$

and the temperature equation is

$$u_r\frac{\partial T}{\partial r}+u_z\frac{\partial T}{\partial z} = \kappa\left[\frac{1}{r}\frac{\partial}{\partial r}\left(r\frac{\partial T}{\partial r}\right)+\frac{\partial^2 T}{\partial z^2}\right]. \tag{2}$$

The aerodynamic heating term has been neglected in equation (2) but this effect is independent of the distribution of surface temperature; it is dependent only on the velocity distribution and (as shown by Millsaps and Pohlhausen) can be added to the solution of equation (2).

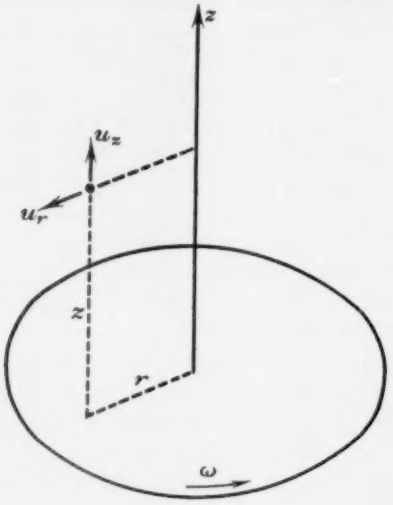


FIG. 1

The distributions of $u_r$ and $u_z$ are required in order to obtain solutions of (2) and these have been computed by Cochran (**5**). The tangential velocity component does not enter the temperature equation, since the problem is axially symmetric and tangential derivatives of temperature vanish.

Following the usual boundary layer approximations, we neglect, on the right-hand side of (2), the terms involving derivatives of $T$ with respect to $r$ in comparison with those involving derivatives with respect to $z$. This is particularly applicable in the case of the disk, as von Kármán (**6**) has shown that the boundary layer thickness in the laminar case is approximately independent of radial distance. Millsaps and Pohlhausen have also shown, by calculation of the exact solution, that in practical cases this approximation is permissible.

The basic temperature equation is then

$$u_r \frac{\partial T}{\partial r} + u_z \frac{\partial T}{\partial z} = \kappa \frac{\partial^2 T}{\partial z^2}. \tag{3}$$

This is further simplified by a von Mises transformation (see, for example, **7**, p. 126), taking $r$ and $\psi$ (the stream function) as independent variables

instead of $r$ and $z$ and using the continuity equation (1). We obtain

$$\frac{\partial T}{\partial r} = \kappa r^2 \frac{\partial}{\partial \psi}\left(u_r \frac{\partial T}{\partial \psi}\right). \tag{4}$$

The radial velocity $u_r$ has been computed by Cochran (5), and is written in the form

$$u_r = \omega r F(\zeta), \tag{5}$$

where $\omega$ is the angular velocity of the disk and $\zeta = (\omega/\nu)^{\frac{1}{2}} z$; a part of the computed function $F(\zeta)$ is shown in Fig. 2.

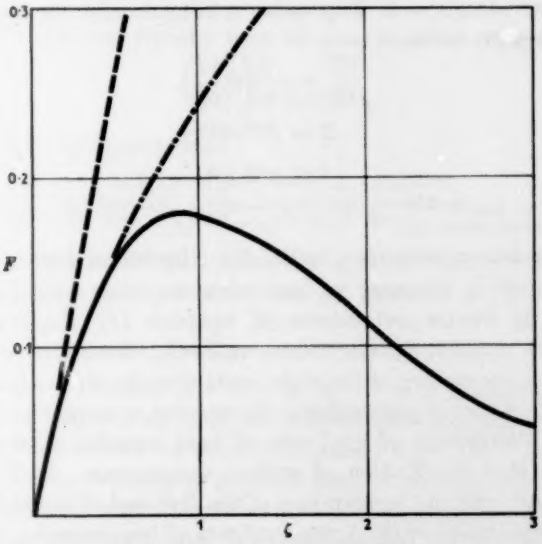


FIG. 2. Calculated values of $F(\zeta) = u_r/(r\omega)$, where $\zeta = (\omega/\nu)^{\frac{1}{2}} z$:
———— exact solution; —·—·—· power law ($F = 0{\cdot}245\zeta^{0{\cdot}67}$);
— — — — linear law ($F = 0{\cdot}51\zeta^{1{\cdot}0}$).

It has not been found possible to apply the method of sources, used previously by Davies and Bourne (4) in the flat plate case, with the exact form of the function $F$. However, in many practical problems $\sigma$ is large, the temperature boundary layer is embedded within the velocity boundary layer and the method used by Davies and Bourne can be applied by choosing a power law representation in the form

$$F = A\zeta^{\alpha} \tag{6}$$

to fit the $u_r$ profile in the inner range of $\zeta$ (i.e. $\zeta < 0{\cdot}7$). A very good representation is found to be possible (4 per cent deviation at most from the exact values in this range of $\zeta$), and the ensuing calculated heat transfer

values are found not to depend critically on the choice of $A$ and $\alpha$; i.e. any pair of values of $A$ and $\alpha$ which yields a good fit to the actual profile for $\zeta < 0{\cdot}7$ leads to calculated heat transfer values in reasonable agreement with each other.

Using power law (6) and the continuity relation expressed in terms of $\psi$, we obtain

$$\frac{\partial \psi}{\partial z} = r u_r = A \omega^{(1+\frac{1}{2}\alpha)} \nu^{-\frac{1}{2}\alpha} r^2 z^{\alpha} \tag{7}$$

and hence

$$\psi = A \omega^{(1+\frac{1}{2}\alpha)} \nu^{-\frac{1}{2}\alpha} (1+\alpha)^{-1} r^2 z^{(1+\alpha)}, \tag{8}$$

taking $\psi = 0$ along $z = 0$. Expressing $u_r$ in terms of $\psi$, the basic temperature equation (4) becomes

$$\frac{\partial T}{\partial R} = c \frac{\partial}{\partial \psi}\left(\psi^t \frac{\partial T}{\partial \psi}\right), \tag{9}$$

where

$$R = r^{2(2+\alpha)/(1+\alpha)},$$

$$t = \alpha/(1+\alpha),$$

and

$$c = \tfrac{1}{2}\kappa \omega^{(\alpha+2)/2(1+\alpha)} \nu^{-\frac{1}{2}\alpha/(1+\alpha)} A^{1/(1+\alpha)} (1+\alpha)^{(1+2\alpha)/(1+\alpha)} \times (2+\alpha)^{-1}.$$

### 3. Solution for an arbitrary radial distribution of disk temperature

Equation (9) is identical in form with the basic equation discussed previously by Davies and Bourne (**4**, equation 11). Suppose now that a continuous uniform circular source, radius $r_0$, concentric with the disk and lying on the surface of the disk, emits $Q$ units of heat per unit time. The analysis of the flat plate solution (**4**) can then be applied and a solution, giving the distribution of local rate of heat transfer, obtained for *any prescribed radial* distribution of surface temperature. If $T_1(r_0)$ and $T_0$ denote respectively the temperature of the disk and of the stationary air, then the distribution of $Q(r_0)$, the local rate of heat transfer, is given by

$$Q(r_0) = \pi^{-1} 2^{-2/s} (1+\alpha)^{2/s} (2+\alpha)^{(2/s-1)} \Gamma(2/s) \sin(2\pi/s) A^{(1-2/s)} k \times$$

$$\times \omega^{\frac{1}{2}} \nu^{-\frac{1}{2}} \sigma^{1/(2+\alpha)} \frac{d}{dr_0} \int_0^{r_0} (r_0^s - R)^{(2/s-1)} [T_1(r_0) - T_0] \, dR, \tag{10}$$

where $s = 2(2+\alpha)/(1+\alpha)$ and $k$ is the thermal conductivity.

This expression necessitates, in general, numerical integration and numerical differentiation, but in many cases the integral in (10) can be expressed in terms of tabulated functions or simple quadratures; e.g. if $T_1 - T_0 = \sum_{n=0}^{\infty} a_n r^n$, the integral can be written, as in the flat plate case discussed by Davies and Bourne (**4**), as a series of beta functions and the temperature distribution expressed in terms of a Pearson $I$ function (**8**) and a series of quadratures (these have been shown recently by D. E.

Bourne, in a private communication, to be expressible as Whittaker functions). Once the distribution of $Q(r_0)$ has been evaluated, the distribution of temperature can of course also be evaluated, as in the flat plate case.

## 4. Solution for constant disk temperature

In the particular case of constant temperature, $T_1$, on the surface of the disk, the expression (10) for $Q$ reduces to

$$Q(r_0) = \pi^{-1}2^{-2/s}(1+\alpha)^{2/s}(2+\alpha)^{2/s-1}\Gamma(2/s)\sin(2\pi/s)A^{1-2/s}k\omega^{\frac{1}{2}}\nu^{-\frac{1}{2}}\sigma^{1/(2+\alpha)}\times \\ \times(T_1-T_0)\,r_0^{(2-s)}.$$

The total rate of heat transfer from an area of radius $r$ is given by

$$E = \int_0^r 2\pi Q(r_0)dr_0,$$

and we find on integration that

$$E[k(T_1-T_0)\omega^{\frac{1}{2}}\nu^{-\frac{1}{2}}r^2]^{-1} = K\sigma^{1/(2+\alpha)}, \tag{11}$$

where $K = 2^{(1-2/s)}(2+\alpha)^{2/s}(1+\alpha)^{(2/s-1)}A^{(1-2/s)}\Gamma(2/s)\sin(2\pi/s)$;

we note that the form of the dependence of $E$ on $r$, $\omega$, and $\nu$ is *independent of* $\alpha$. The corresponding result given by Millsaps and Pohlhausen (**1**, equation 2.29) is

$$E[k(T_1-T_0)\omega^{\frac{1}{2}}\nu^{-\frac{1}{2}}r^2]^{-1} = \pi Q_1'(0), \tag{12}$$

where $Q_1'(0)$ is a function of $\sigma$ (**1**, Fig. 9). It is of interest to note here that for very large values of $\sigma$, the temperature boundary layer is only a very small fraction of the velocity boundary layer; the (tangent) linear approximation to the velocity profile is likely to be adequate, we can then take $\alpha = 1$, and equation (11) shows that the dependence of $E$ on $\sigma$ is given by $\sigma^{\frac{1}{3}}$ as in the flat plate case. We note also that the asymptotic form of the Millsaps–Pohlhausen equation (12), as $\sigma \to \infty$, can easily be shown, using the first term of the series expansion given by Cochran (**5**) for $u_z$ and equation (2.19) of Millsaps and Pohlhausen (**1**), to coincide with formula (11), with $\alpha = 1$ and $A = 0{\cdot}51$; it is given by

$$E[k(T_1-T_0)\omega^{\frac{1}{2}}\nu^{-\frac{1}{2}}r^2]^{-1} = (0{\cdot}51)^{\frac{1}{3}}3^{\frac{2}{3}}\Gamma(\tfrac{2}{3})\sin(\tfrac{1}{3}\pi)\sigma^{\frac{1}{3}}.$$

The numerical results calculated from formulae (11) and (12) are shown in Table 1 for various Prandtl numbers.

The numerical values of rate of heat transfer given in the second column of Table 1 were computed from the exact solution (12), for $\sigma > 10$, using the Millsaps–Pohlhausen expression for $Q_1'(0)$ (**1**, equation 2.19), with the series and numerical values for $u_z$ given by Cochran; in this way the numerical values for $E$, evaluated by Millsaps and Pohlhausen for $1 < \sigma < 10$, are extended from $\sigma = 10$ up to $\sigma = 1{,}000$. These numerical

results show that the approximate formula (11) with a power law representation ($\alpha = 0{\cdot}67$, $A = 0{\cdot}245$) can be applied with very good accuracy for values of $\sigma$ between 6 and 200 (this range will include many cases of practical importance). For values of $\sigma$ less than 6 an effective part of the temperature boundary layer clearly lies outside the inner zone $0 < \zeta < 0{\cdot}7$.

TABLE 1

*Calculated values of rate of heat transfer from a rotating disk using the exact and approximate solutions*

| | *Calculated values of* $E[k(T_1-T_0)r^2\omega^{\frac{1}{2}}\nu^{-\frac{1}{2}}]^{-1}$ *in cm. sec. units* | | | *Percentage over-estimates of the exact values by the approximate formulae* | |
|---|---|---|---|---|---|
| *Prandtl number* | *Using exact formula* (12) | *Using formula* (11) *with* $\alpha = 0{\cdot}67$ *and* $A = 0{\cdot}245$ | *Using formula* (11) *with* $\alpha = 1{\cdot}0$ *and* $A = 0{\cdot}51$ | $\alpha = 0{\cdot}67$ | $\alpha = 1{\cdot}0$ |
| 1 | 1·26 | 1·60 | 1·95 | 27 | 55 |
| 2 | 1·66 | 2·01 | 2·46 | 21 | 48 |
| 4 | 2·36 | 2·59 | 3·09 | 10 | 31 |
| 6 | 2·86 | 3·01 | 3·54 | 5 | 23 |
| 8 | 3·26 | 3·36 | 3·90 | 3 | 20 |
| 10 | 3·53 | 3·65 | 4·20 | 3 | 19 |
| 25 | 5·08 | 5·13 | 5·69 | 1 | 12 |
| 50 | 6·63 | 6·65 | 7·15 | 0 | 8 |
| 100 | 8·51 | 8·60 | 9·01 | 1 | 6 |
| 200 | 10·91 | 11·32 | 11·34 | 4 | 4 |
| 500 | 15·10 | 15·97 | 15·40 | 6 | 2 |
| 1,000 | 19·20 | 20·70 | 19·40 | 8 | 1 |

At $\sigma = 200$ we find that the asymptotic solution leads to the same error (4 per cent) as the approximate power law formula (11). If $\sigma > 200$, however, the error due to the power law formula increases, and the error involved in applying the asymptotic solution of course decreases. The error due to the application of the linear approximation is considerably greater than that due to the power law approximation if $\sigma$ is less than 200, but at higher values of $\sigma$ the linear approximation is more accurate than the power law approximation. However, an application in this range of the simpler asymptotic solution leads to an equally small percentage error. These results show that we can apply the power law formula (11) with good accuracy for values of $\sigma$ between 6 and 200, while the simple asymptotic formula is sufficiently accurate for $\sigma > 200$.

A convenient expression for the temperature distribution is also easily derived, as in the flat plate case. We obtain

$$\frac{T_1-T}{T_1-T_0} = 1-I[2A(1+\alpha)^{-1}(2+\alpha)^{-1}\sigma\zeta^{(2+\alpha)}, -(1+\alpha)(2+\alpha)^{-1}], \quad (13)$$

where $I$ is a Pearson function (8). We again find that, for values of $\sigma$ greater than about 6, the temperature distributions calculated from (13) are in agreement with the exact values calculated by Millsaps and Pohlhausen (1, Fig. 7) but the deviations increase as $\sigma$ decreases below $\sigma = 6$, as in the calculation of heat transfer rates.

We can, therefore, reasonably infer that for values of $\sigma$ greater than 6 this approximate method of calculation is likely to be sufficiently accurate to calculate rates of heat transfer and temperature distributions for an *arbitrary* radial distribution of disk temperature, the associated numerical work in general consisting of the numerical integration and differentiation involved in expression (10).

## REFERENCES

1. K. Millsaps and K. Pohlhausen, *J. Aero. Sci.* **19** (1952) 120.
2. G. W. Morgan and W. H. Warner, ibid. **23** (1956) 937.
3. M. J. Lighthill, *Proc. Roy. Soc.* A **202** (1950) 359.
4. D. R. Davies and D. E. Bourne, *Quart. J. Mech. App. Math.* **9** (1956) 457.
5. W. G. Cochran, *Proc. Camb. Phil. Soc.* **30** (1934) 365.
6. T. von Kármán, *Z. angew. Math. Mech.* **1** (1921) 245.
7. S. Goldstein (Ed.), *Modern Developments in Fluid Dynamics* (Oxford, 1938).
8. K. Pearson, *Tables of the Incomplete Gamma Function* (London, H.M.S.O., 1922).

# VIBRATIONS OF BEAMS

## III. SCREW MODES†

*By* W. A. GREEN (*Atomic Weapons Research Establishment, Aldermaston, Berks.*)‡

[Received 14 November 1957]

SUMMARY

The exact equations of wave propagation in an elastic medium are solved to obtain the dispersion equation for the screw form of vibration of a circular cylinder. Dispersion curves are obtained for the fundamental mode, for a range of values of the Poisson's ratio, in the long and intermediate wavelength region and the cross-overs of these curves and the corresponding curves for the longitudinal form of motion determined.

### Notation

| | |
|---|---|
| $u$, $v$, $w$ | displacements in the directions $r$, $\theta$, $z$ respectively. |
| $u_{ni}$, $v_{ni}$, $w_{ni}$ | functions of $r$, see (1). |
| $A_{ni}$, $B_{ni}$ | arbitrary constants. |
| $\lambda$, $\mu$ | Lamé's constants. |
| $\sigma$ | Poisson's ratio. |
| $c_1 = \left(\frac{\lambda+2\mu}{\rho}\right)^{\frac{1}{2}}$ | velocity of dilatation waves in an infinite medium. |
| $c_2 = \left(\frac{\mu}{\rho}\right)^{\frac{1}{2}}$ | velocity of shear waves in an infinite medium. |
| $c_s$ | velocity of Rayleigh surface waves. |
| $c = \frac{\omega}{k}$ | phase velocity of waves in the bar. |
| $\omega = 2\pi\nu$ | angular frequency. |
| $k = \frac{2\pi}{\Lambda}$ | wave number. |
| $a$ | radius of bar. |

$$\alpha^2 = k^2\left(\frac{c^2}{c_1^2}-1\right).$$

$$\beta^2 = k^2\left(\frac{c^2}{c_2^2}-1\right).$$

$$x = \beta a.$$

$$y = \alpha a.$$

$$z = ka.$$

$$K = 1+\lambda(z^2+y^2)/2\mu y^2.$$

† Part of a thesis submitted to the University of Wales for the degree of Ph.D.

‡ Now at M.E.R.L., East Kilbride, Lanarks.

$$\theta_2 = x\frac{J_2'(x)}{J_2(x)}. \qquad \text{See Hudson (11).}$$

$$\bar{\theta}_2 = y\frac{J_2'(y)}{J_2(y)}.$$

$$\theta_2(s) \approx 2 - \tfrac{1}{6}s^2 \quad (s \ll 1).$$

$$\left.\begin{aligned}\theta_2(s) &\approx s\cot[s - \tfrac{3}{4}\pi], \ s \text{ real} \\ &\approx -is - \tfrac{1}{2}, \ s \text{ imaginary}\end{aligned}\right\} |s| \gg 1.$$

## 1. Introduction

In the previous papers (1 and 2) the perturbation theory developed to determine the dispersion curves for elastic wave propagation in beams of non-circular section was found to break down at certain points in the intermediate wavelength region due to degeneracy between the screw form of vibration (3) of a circular cylinder and, on the one hand, the longitudinal form (1), on the other, the torsional form (2). This cross-over of the dispersion curves for beams possessing fourfold symmetry has been interpreted as implying that in this region the screw becomes the fundamental mode of motion (4), and a further examination of this form of motion was felt to be worth while.

The simplest way of examining wave propagation in elastic beams using the exact equations of motion is by considering beams of circular section where the boundary conditions are such that the different possible forms of motion can arise independently. In this way the longitudinal forms of motion have been considered in the intermediate wavelength region by Bancroft (5), Davies (6), and others (see 7), and in the short wavelength region by Adem (8), McSkimin (9), and Redwood and Lamb (10). In particular Bancroft has obtained the dispersion curves for a range of values of Poisson's ratio for the fundamental mode of propagation in a circular cylinder, Davies obtaining similar solutions for the fundamental mode and first two harmonics for a Poisson's ratio $\sigma = 0{\cdot}29$. The flexural form of motion has been examined in a similar way by Hudson (11) and Abramson (12), the former also obtaining some information about the higher forms of motion in the short wavelength region. In the following the dispersion equation for screw vibrations of a circular cylinder is solved numerically to obtain dispersion curves for the fundamental mode over the intermediate wavelength range for a set of values of the Poisson's ratio analogous to the solutions of Bancroft and Hudson for the longitudinal and flexural vibrations respectively.

## 2. Dispersion equation

The Pochhammer–Chree equations governing the propagation of elastic waves in cylindrical coordinates have solutions, for waves travelling along

the axis of $z$, of the form

$$\begin{aligned} u &= u_{ni}(A_{ni}\cos n\theta + B_{ni}\sin n\theta)\cos(kz-\omega t) \\ v &= v_{ni}(A_{ni}\sin n\theta - B_{ni}\cos n\theta)\cos(kz-\omega t) \quad (i = 1, 2, 3) \\ w &= w_{ni}(A_{ni}\cos n\theta + B_{ni}\sin n\theta)\sin(kz-\omega t) \end{aligned} \tag{2.1}$$

where the $u_{ni}$, $v_{ni}$, $w_{ni}$ are functions of $r$ only and are given elsewhere (**1**) and the $A_{ni}$, $B_{ni}$ are arbitrary constants. The general solution for the displacements consists of linear combinations of these solutions over all values of $n$, but as has previously been pointed out (**1** and **11**) the boundary conditions for free vibrations of an infinitely long circular cylinder are satisfied by displacements involving each value of $n$ separately. In fact for any given value of $n$ the boundary conditions are satisfied by displacements involving only the $A_{ni}$ or only the $B_{ni}$, one set being obtained from the other for all $n > 0$ by a rotation of axes through an angle $\pi/n$.

The screw form of motion is characterized by two nodal planes through the axis of the cylinder, the corresponding displacements being given by (2.1) with $n = 2$. Imposing the boundary conditions leads to the dispersion or frequency equation

$$\begin{vmatrix} \{xJ_2'(x)-J_2(x)\}/x^2 & \frac{1}{2}J_2''(x) & \frac{1}{2}\{J_2''(y)-(K-1)J_2(y)\} \\ \{xJ_2'(x)-(\frac{1}{2}x^2-4)J_2(x)\}/2x^2 & \{J_2(x)-xJ_2'(x)\}/x^2 & \{J_2(y)-yJ_2'(y)\}/y^2 \\ -kaJ_2(x)/2x^2 & -(k^2-\beta^2)J_2'(x)/4k\beta & -kJ_2'(y)/2\alpha \end{vmatrix} = 0 \tag{2.2}$$

or in terms of the $\theta_2$ functions defined by Hudson

$$\begin{vmatrix} 2(\theta_2-1) & 4-x^2-\theta_2 & 4-Ky^2-\bar{\theta}_2 \\ \theta_2-4+\frac{1}{2}x^2 & 2(1-\theta_2) & 2(1-\bar{\theta}_2) \\ 2 & (1-x^2/z^2)\theta_2 & 2\bar{\theta}_2 \end{vmatrix} = 0. \tag{2.3}$$

## 3. Dispersion curves

For any given value of the Poisson's ratio $\sigma$ equation (2.3) may be solved to give the dispersion curve relating the reduced phase velocity $c/c_2$ to the number of wavelengths in the circumference of the bar $ka$. An infinite number of such curves exist for any value of $\sigma$, the solution giving the smallest value of the phase velocity for any $ka$ being termed the fundamental mode of motion, that giving the next value the first harmonic and so on. We consider the solution for the fundamental mode of motion only.

Assuming a solution for which the phase velocity remains finite and bounded as the wavelength is increased indefinitely, both $x$ and $y$ become

small and with the appropriate expansion for the $\theta_2$ function equation (2.3) may be written

$$\frac{x^2}{z^2}(x^2-y^2) = 0 \tag{3.1}$$

correct to second order. This has solutions

$$x \equiv 0, \qquad c = c_2$$

or

$$x \equiv y, \qquad c = 0.$$

Of these, the first satisfies equation (2.3) identically and for this case the displacements are no longer given by (2.1), whilst the second solution is trivial. Thus no solution of the screw dispersion equation exists for which the phase velocity remains finite and bounded at large wavelengths, and the velocity of propagation of the fundamental mode must therefore become infinite as $ka$ tends to zero.

In the intermediate wavelength region the dispersion equation is simplified to a greater or lesser extent at the points $c/c_2 = 1$ ($x = 0$); $c/c_2 = \sqrt{2}$ ($x = z$), and $c = c_1$ ($y = 0$), and solutions were accordingly obtained at these points first, for a Poisson's ratio $\sigma = 0{\cdot}3$. This allowed a sketch curve to be drawn which served to provide initial trial values for the numerical solution of equation (2.3) at any value of $ka$, the solution then proceeding by iteration. The exact curve for $\sigma = 0{\cdot}3$ having been obtained this in turn provides the initial trial values for other values of $\sigma$.

The solution in the short wavelength region has been investigated for the general dispersion equation ($n$) by Hudson (11), who shows that the limiting value for velocities below the shear wave velocity $c_2$ is that of the Rayleigh surface waves $c_s$ in the medium and this has been verified for equation (2.3).

The results for the fundamental mode of screw vibration are given in Table 1 for six values of the Poisson's ratio over the range $ka = 1$ to 5, and the dispersion curve for $\sigma = 0{\cdot}3$ plotted in Fig. 1 together with the corresponding curve for the longitudinal form of motion obtained from Bancroft's results. Of particular interest are the cross-overs between the screw and longitudinal curves in the intermediate wavelength region, and these have been obtained graphically using Bancroft's solutions for the longitudinal curves, extrapolated to $\sigma = 0$ and $\sigma = 0{\cdot}5$, and are given in Table 2.

That these solutions do in fact represent the fundamental screw mode has been verified by examining the cross-over of the curves and the line $c = c_2$. At the shear wave velocity ($x = 0$) equation (2.3) reduces to

$$\theta_2 = \frac{z^4+12z^2+144}{6(z^2+12)}. \tag{3.2}$$

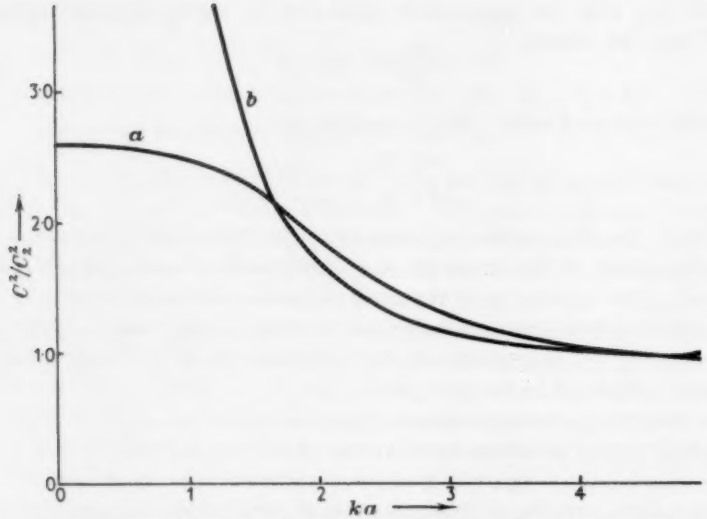


FIG. 1. Dispersion curves for (*a*) longitudinal, (*b*) screw, modes ($\sigma = 0{\cdot}3$).

## TABLE 1

*Phase velocity as a function of wavelength and Poisson's ratio*

$c^2/c_2^2$

| $ka$ | $\sigma = 0$ | $\sigma = 0{\cdot}1$ | $\sigma = 0{\cdot}2$ | $\sigma = 0{\cdot}3$ | $\sigma = 0{\cdot}4$ | $\sigma = 0{\cdot}5$ |
|---|---|---|---|---|---|---|
| 1·00 | 5·234349 | 5·292716 | 5·345614 | 5·393598 | 5·437195 | 5·476901 |
| 1·25 | 3·406852 | 3·458626 | 3·505699 | 3·548470 | 3·587350 | 3·622744 |
| 1·50 | 2·456182 | 2·504674 | 2·548836 | 2·588965 | 2·625403 | 2·658507 |
| 1·75 | 1·910442 | 1·957380 | 1·999938 | 2·038560 | 2·073541 | 2·105215 |
| 2·00 | 1·575260 | 1·620971 | 1·662574 | 1·700237 | 1·734224 | 1·764864 |
| 2·25 | 1·358160 | 1·403277 | 1·444271 | 1·481258 | 1·514483 | 1·544282 |
| 2·50 | 1·211878 | 1·256641 | 1·297221 | 1·333688 | 1·366282 | 1·395345 |
| 2·75 | 1·110054 | 1·154611 | 1·194896 | 1·230942 | 1·262981 | 1·291376 |
| 3·00 | 1·037218 | 1·081662 | 1·121735 | 1·157426 | 1·188969 | 1·216750 |
| 3·25 | 0·983873 | 1·028271 | 1·068190 | 1·103582 | 1·134679 | 1·161896 |
| 3·50 | 0·943975 | 0·988373 | 1·028187 | 1·063326 | 1·094028 | 1·120731 |
| 3·75 | 0·913555 | 0·957988 | 0·997738 | 1·032660 | 1·063023 | 1·089254 |
| 4·00 | 0·889942 | 0·934434 | 0·974157 | 1·008928 | 1·038959 | 1·064748 |
| 4·25 | 0·871299 | 0·915868 | 0·955596 | 0·990251 | 1·020021 | 1·045438 |
| 4·50 | 0·856337 | 0·900995 | 0·940756 | 0·975334 | 1·004908 | 1·030029 |
| 4·75 | 0·844141 | 0·888891 | 0·928711 | 0·963251 | 0·992704 | 1·017619 |
| 5·00 | 0·834048 | 0·878892 | 0·918789 | 0·953326 | 0·982671 | 1·007476 |

## TABLE 2

*Intersections of longitudinal and screw dispersion curves*

| $\sigma$ | 0 | | 0·1 | | 0·2 | | 0·3 | | 0·4 | | 0·5 | |
|---|---|---|---|---|---|---|---|---|---|---|---|---|
| $ka$ | 1·692 | .. | 1·666 | 3·375 | 1·680 | 4·130 | 1·714 | 4·645 | 1·752 | 5·155 | 1·790 | .. |
| $c^2/c_2^2$ | 2·000 | .. | 2·097 | 0·978 | 2·120 | 0·962 | 2·100 | 0·967 | 2·068 | 0·976 | 2·040 | .. |

Considering the equation

$$f(z) = \bar{\theta}_2(y) - \frac{z^4+12z^2+144}{6(z^2+12)} = 0 \tag{3.3}$$

since $y$ is imaginary, $f(z)$ is a regular function of $z$ with the limits

$$f(z) = (1-c_2^2/c_1^2)z^2/6+O(z^4) \quad (z \to 0),$$
$$f(z) = -z^2/6+O(z) \quad (z \to \infty),$$

and there exists at least one real positive root of equation (3.3). Denoting the least real positive root of (3.3) by $z_1$ we must have that

$$\frac{df}{dz_1} = \frac{4-\bar{\theta}_2^2+z_1^2(1-c_2^2/c_1^2)}{z_1} - \frac{z_1^3(z_1^2+24)}{3(z_1^2+12)^2} \leqslant 0$$

which on substituting for $\bar{\theta}_2^2$ from equation (3.3) leads to the condition

$$z_1^6+36z_1^4c_2^2/c_1^2-288z_1^2(1-3c_2^2/c_1^2)-5184(1-c_2^2/c_1^2) \geqslant 0. \tag{3.4}$$

This is satisfied provided $z_1 \geqslant z'$ where $z'$ is the only real positive root of the equation in (3.4). Further if the equality holds then we have

$$\frac{d^2f}{dz_1^2} = -\frac{z_1^2(z_1^6+36z_1^4+288z_1^2+6912)}{18(z_1^2+12)^3} \tag{3.5}$$

and $z_1 = z'$ is a maximum of the function $f(z)$. This is clearly impossible and hence we must have $z_1 > z'$. If $z_2$ is any other real positive root of equation (3.3) then since $z_2 > z_1$ we would again have $df/dz_2 < 0$ showing that no such root $z_2$ exists. Thus there exists one and only one dispersion curve for any given Poisson's ratio which crosses the line $c = c_2$. Since no solution of the dispersion equation exists for which the phase velocity is always less than the shear wave velocity then the curve which crosses the line $c = c_2$ must correspond to the fundamental mode of motion, and this is the solution which we have picked out.

## 4. Discussion

The results given in Table 1 may be interpolated to give the dispersion curve for the fundamental mode of screw vibration of a circular cylinder of a material of any Poisson's ratio in the long and intermediate wavelength region. In the region of short wavelengths and for higher modes an approximate method (13) has been employed to give qualitative and partly quantitative results.

From the solutions of the determinantal equation (2.3) it is possible to obtain the ratios of the $A_{ni}$ or $B_{ni}$ and thus determine the displacements corresponding to this mode of motion. This has not been carried out here but the general behaviour of the displacements may be inferred from equations (2.1) and have been sketched in Fig. 2 over two cross-sections,

half a wavelength apart. This brings out the squeezing or screw character of the motion and the fourfold symmetry involved. It may be seen that the two axial planes which are nodal to the displacements in the longitudinal and radial directions are antinodal to the transverse displacement and vice versa. Displacements of this type would in practice be difficult to excite by the usual quartz crystal driving methods but a suitable means of squeezing together the opposite faces of a square bar might be expected to give rise to this form of vibration.

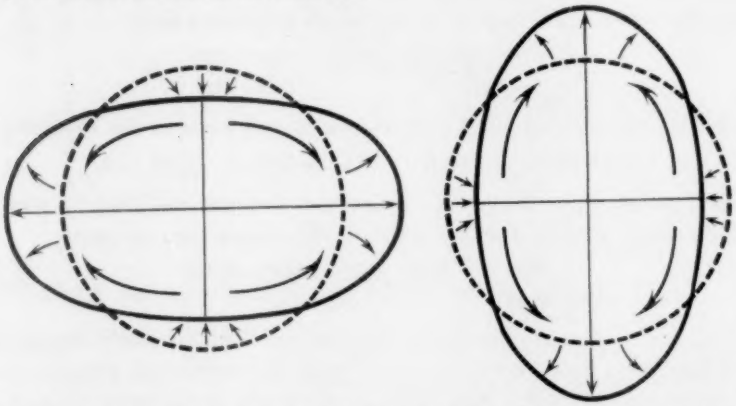

FIG. 2. Screw mode displacements for circular cylinder over two cross-sections half a wavelength apart.

## Acknowledgements

I wish to thank Professor G. J. Kynch for suggesting this problem and his continued interest in the work, and the Department of Scientific and Industrial Research for a maintenance allowance during the period of which part of the work was carried out.

## REFERENCES

1. G. J. KYNCH and W. A. GREEN, *Quart. J. Mech. Appl. Math.* **10** (1957) 63.
2. W. A. GREEN, ibid. 74.
3. G. J. KYNCH, *Nature, London*, **175** (1955) 559.
4. —— *British J. Appl. Physics*, **8** (1957) 64.
5. D. BANCROFT, *Phys. Rev.* **59** (1941) 588.
6. R. M. DAVIES, *Phil. Trans.* A, **240** (1948) 375.
7. —— *Appl. Mech. Rev.* **6** (1953) 1.
8. J. ADEM, *Quart. Appl. Math.* **12** (1954) 261.
9. H. J. MCSKIMIN, *J. Acoust. Soc. Amer.* **28** (1956) 469.
10. M. REDWOOD and J. LAMB, *Proc. Phys. Soc.* B, **70** (1957) 136.
11. G. E. HUDSON, *Phys. Rev.* **63** (1943) 46.
12. H. N. ABRAMSON, *J. Acoust. Soc. Amer.* **29** (1957) 42.
13. W. A. GREEN, Ph.D. Thesis (Wales), 1957.

# THE VIBRATION OF A RECTANGULAR PLATE WITH EDGES ELASTICALLY RESTRAINED AGAINST ROTATION

*By* T. E. CARMICHAEL

(*Research Assistant, Department of Civil Engineering, University of Bristol*)

[Received 18 December 1957]

SUMMARY

By means of the Rayleigh–Ritz method, an analysis is made of the vibration of a rectangular plate whose edges are elastically restrained against rotation. Plate deflexions are represented by a set of functions which define the normal modes of vibration of a beam whose ends are elastically restrained against rotation. Values of various integrals of these functions and their derivatives are established. Frequencies are obtained from a set of linear simultaneous equations which may be solved by a simple iterative process. An approximate frequency equation is also derived and numerical tables for use with this equation are presented.

## 1. Introduction

Exact solutions to the differential equation of transverse vibration of a thin rectangular plate can be obtained only if one pair of opposite edges are simply supported (1, 2). For other boundary conditions approximate methods of solution must be adopted. Reference should be made to Warburton (3) for a comprehensive summary of these methods, as applied to plate vibrations, and to Hearmon (4) who quotes the numerical results of various authorities. However, all solutions, exact and approximate, known to the author, deal with plates under either simply supported, free or clamped boundary conditions, or mixed boundary conditions involving these three types of support.

In the present paper we consider the vibration of a plate whose edges are rigidly supported against displacement, but which are elastically restrained against rotation. Opposite pairs of edges are taken to be restrained to the same degree, although the method can be extended to a plate whose four edges are restrained to differing degrees. The Rayleigh–Ritz energy method is employed, and so the calculated frequencies will be somewhat higher than the exact values. Frequencies and modes of vibration are obtained from a set of linear simultaneous equations, which may be solved by a simple iterative process. An approximate frequency equation is also given, which is considered sufficiently accurate for

practical purposes, and numerical tables for use with this equation are presented.

## 2. Notation

| | |
|---|---|
| $a, b$ | lengths of sides of plate ($b/a \leqslant 1$). |
| $h$ | thickness of plate. |
| $E$ | Young's modulus. |
| $\nu$ | Poisson's ratio. |
| $\rho$ | density of plate material. |
| $D$ | bending stiffness of plate $Eh^3/12(1-\nu^2)$. |
| $g$ | gravitational acceleration. |
| $\omega$ | angular frequency, radians/sec. |
| $Ox$, $Oy$ | rectangular coordinate axes. |
| $w(x, y)$ | amplitude of plate vibration. |
| $V$ | maximum elastic strain energy of plate. |
| $T$ | maximum kinetic energy of plate. |
| $\xi$, $\xi_A$, $\xi_B$ | boundary restraint parameters. |
| $L$ | span of beam. |
| $a_{mn}$ | coefficient in series representation of $w(x, y)$. |
| $F_r$, $F_s$ | characteristic beam functions defined by equation (7). |
| $A_r$, $B_r$, $C_r$ | constants of integration associated with $F_r$. |
| $\alpha_r$ | characteristic value of $F_r$. |
| $X_m$ | a function of $x$ alone. |
| $Y_n$ | a function of $y$ alone. |
| $L_{im}$, $N_{im}$, $H_{im}$<br>$E_{im}$, $M_{kn}$, $P_{kn}$<br>$K_{kn}$, $F_{kn}$ | integrals defined by equations (11). |
| $i, m, p, q$<br>$r, s, k, n$ | positive integers. |
| $\lambda$ | characteristic value $\rho h\omega^2 b^4/gD$. |
| $C_{mn}^{(ik)}$ | typical element of frequency determinant, defined by equations (15). |
| $\delta_{mn}$ | Kronecker delta defined by equations (15). |
| $\phi_{mm}$, $\phi_{nn}$ | parameters defined by equations (17). |
| $\theta_{mn}$ | parameter defined by equation (20). |

## 3. The Rayleigh–Ritz method

In the rectangular plate $OABC$, coordinate axes $Ox$, $Oy$ are taken as shown in Fig. 1. The plate is assumed to be rigidly supported against transverse displacement around the edges $OA$, $AB$, $BC$, $CO$, and these

edges are elastically restrained against rotation. Opposite edges are taken to be restrained to the same degree. If the plate is vibrating harmonically

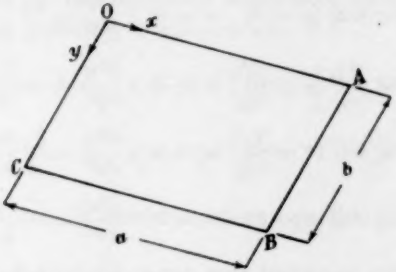


FIG. 1. Details of rectangular plate.

with amplitude $w(x, y)$ and angular frequency $\omega$, the maximum strain energy is given by

$$V = \tfrac{1}{2}D \int_0^a \int_0^b \left[ \left(\frac{\partial^2 w}{\partial x^2}\right)^2 + \left(\frac{\partial^2 w}{\partial y^2}\right)^2 + 2\nu \frac{\partial^2 w}{\partial x^2}\frac{\partial^2 w}{\partial y^2} + 2(1-\nu)\left(\frac{\partial^2 w}{\partial x \partial y}\right)^2 \right] dx dy -$$

$$-\tfrac{1}{2}D\left[ \int_0^a \left(\frac{\partial^2 w}{\partial y^2}\frac{\partial w}{\partial y}\right)_0^b dx + \int_0^b \left(\frac{\partial^2 w}{\partial x^2}\frac{\partial w}{\partial x}\right)_0^a dy \right] \tag{1}$$

and the maximum kinetic energy is

$$T = \frac{1}{2}\frac{\rho h}{g}\omega^2 \int_0^a \int_0^b w^2 \, dx dy. \tag{2}$$

In equation (1) the first term on the right-hand side represents the energy stored in the plate, the second term represents the energy transferred to the surrounding structure due to the edge rotation. From equations (1) and (2)

$$\omega^2 = \frac{V}{(\rho h/2g) \int_0^a \int_0^b w^2 \, dx dy}. \tag{3}$$

The Rayleigh–Ritz method of solution of equation (3) consists of assuming a waveform $w(x, y)$ as a linear series of functions of $x$ and $y$, and adjusting the coefficients in this series so as to minimize equation (3). A set of simultaneous equations is thereby obtained, and may be solved for characteristic values, say $\lambda$, which determine the critical frequencies of the panel. The functions chosen to represent the waveform must satisfy the 'artificial'

boundary conditions of the problem (5) and, for the panel shown in Fig. 1, these boundary conditions may be written†

$$\left.\begin{aligned} &\text{Along } OA\ (y=0) \quad w=0; \quad \frac{\partial^2 w}{\partial y^2} = \frac{\xi_B}{b}\frac{\partial w}{\partial y} \\ &\text{Along } BC\ (y=b) \quad w=0; \quad \frac{\partial^2 w}{\partial y^2} = -\frac{\xi_B}{b}\frac{\partial w}{\partial y} \end{aligned}\right\}. \tag{4a}$$

$$\left.\begin{aligned} &\text{Along } OC\ (x=0) \quad w=0; \quad \frac{\partial^2 w}{\partial x^2} = \frac{\xi_A}{a}\frac{\partial w}{\partial x} \\ &\text{Along } AB\ (x=a) \quad w=0; \quad \frac{\partial^2 w}{\partial x^2} = -\frac{\xi_A}{a}\frac{\partial w}{\partial x} \end{aligned}\right\}. \tag{4b}$$

It will subsequently be shown that a suitable waveform, which satisfies the conditions equations (4), may be taken as

$$w = \sum_{m=1}^{p}\sum_{n=1}^{q} a_{mn} X_m Y_n, \tag{5}$$

where $X_m$, $Y_n$ are the so-called characteristic functions of a beam whose ends are elastically restrained against rotation.

## 4. The characteristic beam function

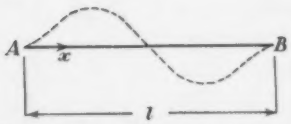


FIG. 2. Details of uniform beam.

Consider the uniform beam $AB$, of span $L$, shown in Fig. 2. The ends $A$ and $B$ of this beam are rigidly supported and elastically restrained against rotation, an equal degree of restraint being applied to both ends. The differential equation of vibration of the beam may be written

$$\frac{d^4 F_r}{dx^4} = \frac{\alpha_r^4}{L^4} F_r \tag{6}$$

from which

$$F_r = A_r \cosh\left(\frac{\alpha_r x}{L}\right) + B_r \sinh\left(\frac{\alpha_r x}{L}\right) + C_r \cos\left(\frac{\alpha_r x}{L}\right) + \sin\left(\frac{\alpha_r x}{L}\right). \tag{7}$$

$F_r$ is a characteristic beam function and represents the waveform of the

† Since $w = 0$ around the rectangular boundary of the panel, then as shown by Leggett (6), the expression in the first bracket on the right-hand side of equation (1), which represents the strain energy stored in the panel, reduces to

$$\tfrac{1}{2}D \int_0^a \int_0^b \left(\frac{\partial^2 w}{\partial x^2} + \frac{\partial^2 w}{\partial y^2}\right)^2 dxdy.$$

In consequence, numerical values for $\lambda$ may be obtained, which are independent of the value of Poisson's ratio for the panel material. This would not be so, for example, if one of the edges of the panel was free.

$r$th mode of vibration of the beam. The constants $A_r, \ldots, C_r$, which define the modal form, and the coefficient $\alpha_r$, which determines the $r$th resonant frequency, depend on the boundary conditions. For the beam under consideration these boundary conditions are

$$\left.\begin{aligned} &\text{At } x = 0; \quad F_r = 0; \quad \frac{d^2F_r}{dx^2} = \frac{\xi}{L}\frac{dF_r}{dx} \\ &\text{At } x = L; \quad F_r = 0; \quad \frac{d^2F_r}{dx^2} = -\frac{\xi}{L}\frac{dF_r}{dx} \end{aligned}\right\}. \tag{8}$$

Substituting for $F_r$ and its derivatives from equation (7) into equation (8), then

$$\left.\begin{aligned} A_r = -C_r = -\cot\tfrac{1}{2}\alpha_r; \quad B_r = \cot\tfrac{1}{2}\alpha_r \tanh\tfrac{1}{2}\alpha_r \\ \alpha_r = -\tfrac{1}{2}\xi(\tan\tfrac{1}{2}\alpha_r + \tanh\tfrac{1}{2}\alpha_r) \end{aligned}\right\} r = 1, 3, \text{ etc.}$$
$$\left.\begin{aligned} A_r = -C_r = \tan\tfrac{1}{2}\alpha_r; \quad B_r = -\tan\tfrac{1}{2}\alpha_r \coth\tfrac{1}{2}\alpha_r \\ \alpha_r = \tfrac{1}{2}\xi(\cot\tfrac{1}{2}\alpha_r - \coth\tfrac{1}{2}\alpha_r) \end{aligned}\right\} r = 2, 4, \text{ etc.} \tag{9}$$

Particular cases of equations (9) arise for a simply supported beam ($\xi = 0$), when, after rearrangement, it may be shown that

$$A_r = B_r = C_r = 0; \quad \sin\alpha_r = 0, \quad \text{i.e.} \quad \alpha_r = r\pi,$$

and for a clamped beam ($\xi = \infty$) when

$$A_r = -C_r = \frac{\sinh\alpha_r - \sin\alpha_r}{\cosh\alpha_r - \cos\alpha_r}; \qquad B_r = -1;$$

$$1 - \cos\alpha_r \cosh\alpha_r = 0.$$

Both of these solutions are well known (7).

Numerical values of $\alpha_r$, $A_r$, and $B_r$ up to the sixth mode, computed from equations (9) for various values of $\xi$ are given in Table 1.

## 5. Application of the Rayleigh–Ritz method

If, in equation (5), $X_m$ and $Y_n$ are taken in the form

$$\left.\begin{aligned} X_m &= A_m\left\{\cosh\left(\frac{\alpha_m x}{a}\right) - \cos\left(\frac{\alpha_m x}{a}\right)\right\} + B_m \sinh\left(\frac{\alpha_m x}{a}\right) + \sin\left(\frac{\alpha_m x}{a}\right) \\ Y_n &= A_n\left\{\cosh\left(\frac{\alpha_n y}{b}\right) - \cos\left(\frac{\alpha_n y}{b}\right)\right\} + B_n \sinh\left(\frac{\alpha_n y}{b}\right) + \sin\left(\frac{\alpha_n y}{b}\right) \end{aligned}\right\}, \tag{10}$$

it is seen that the assumed waveform can be made to satisfy the boundary conditions equations (4) term by term and so may legitimately be used in the Rayleigh–Ritz analysis.

## TABLE 1

*Values of $\alpha$, $A$, $B$, and $\phi$ for the characteristic functions $F_r$ of a uniform beam with ends elastically restrained against rotation*

| | $r=1$ | | | | $r=2$ | | | | $r=3$ | | | $r=4$ | | | $r=5$ | | | $r=6$ | | |
|---|---|---|---|---|---|---|---|---|---|---|---|---|---|---|---|---|---|---|---|---|
| $\xi$ | $\alpha_1$ | $A_1$ | $-B_1$ | $\phi_{11}$ | $\alpha_2$ | $A_2$ | $-B_2$ | $\phi_{22}$ | $\alpha_3$ | $A_3=-B_3$ | $\phi_{23}$ | $\alpha_4$ | $A_4=-B_4$ | $\phi_{44}$ | $\alpha_5$ | $A_5=-B_5$ | $\phi_{55}$ | $\alpha_6$ | $A_6=-B_6$ | $\phi_{66}$ |
| 0 | 3·1416 | 0 | 0 | 9·8697 | 6·2832 | 0 | 0 | 39·479 | 9·4248 | 0 | 88·827 | 12·566 | 0 | 157·91 | 15·708 | 0 | 246·74 | 18·850 | 0 | 355·31 |
| 0·25 | 3·2166 | ·0375 | ·0346 | 9·8710 | 6·3220 | ·0194 | ·0195 | 39·482 | 9·4909 | ·0131 | 88·827 | 12·566 | ·0098 | 157·92 | 15·724 | ·0079 | 246·74 | 18·863 | ·0066 | 355·31 |
| 0·5 | 3·2836 | ·0711 | ·0668 | 9·8750 | 6·3588 | ·0378 | ·0380 | 39·485 | 9·4762 | ·0257 | 88·830 | 12·605 | ·0194 | 157·92 | 15·739 | ·0156 | 246·74 | 18·876 | ·0131 | 355·31 |
| 0·75 | 3·3440 | ·1015 | ·0946 | 9·8806 | 6·3939 | ·0554 | ·0556 | 39·495 | 9·5007 | ·0380 | 88·833 | 12·624 | ·0288 | 157·92 | 15·755 | ·0232 | 246·74 | 18·889 | ·0195 | 355·31 |
| 1 | 3·3988 | ·1293 | ·1210 | 9·8880 | 6·4273 | ·0722 | ·0724 | 39·505 | 9·5245 | ·0499 | 88·839 | 12·642 | ·0380 | 157·92 | 15·769 | ·0307 | 246·74 | 18·901 | ·0258 | 355·31 |
| 1·5 | 3·4949 | ·1785 | ·1680 | 9·9074 | 6·4896 | ·1036 | ·1039 | 39·534 | 9·5699 | ·0727 | 88·853 | 12·678 | ·0558 | 157·93 | 15·799 | ·0454 | 246·75 | 18·926 | ·0381 | 355·32 |
| 2 | 3·5768 | ·2211 | ·2091 | 9·9320 | 6·5466 | ·1325 | ·1328 | 39·572 | 9·6127 | ·0942 | 88·874 | 12·712 | ·0729 | 157·94 | 15·827 | ·0594 | 246·76 | 18·950 | ·0501 | 355·32 |
| 2·5 | 3·6477 | ·2586 | ·2454 | 9·9604 | 6·5989 | ·1592 | ·1596 | 39·614 | 9·6531 | ·1146 | 88·901 | 12·745 | ·0893 | 157·96 | 15·854 | ·0731 | 246·78 | 18·973 | ·0618 | 355·34 |
| 3 | 3·7097 | ·2919 | ·2780 | 9·9908 | 6·6472 | ·1840 | ·1845 | 39·652 | 9·6913 | ·1340 | 88·934 | 12·776 | ·1051 | 157·99 | 15·880 | ·0863 | 246·79 | 18·996 | ·0732 | 355·34 |
| 3·5 | 3·7646 | ·3220 | ·3074 | 10·023 | 6·6918 | ·2072 | ·2077 | 39·718 | 9·7274 | ·1525 | 88·971 | 12·806 | ·1202 | 158·01 | 15·906 | ·0991 | 246·82 | 19·018 | ·0842 | 355·36 |
| 4 | 3·8135 | ·3492 | ·3341 | 10·057 | 6·7332 | ·2289 | ·2294 | 39·775 | 9·7617 | ·1700 | 89·022 | 12·834 | ·1348 | 158·04 | 15·930 | ·1115 | 246·83 | 19·039 | ·0951 | 355·38 |
| 5 | 3·8974 | ·3970 | ·3812 | 10·126 | 6·8077 | ·2684 | ·2690 | 39·900 | 9·8250 | ·2028 | 89·108 | 12·889 | ·1625 | 158·12 | 15·977 | ·1353 | 246·89 | 19·080 | ·1158 | 355·42 |
| 6 | 3·9666 | ·4376 | ·4214 | 10·196 | 6·8728 | ·3037 | ·3043 | 40·028 | 9·8824 | ·2329 | 89·218 | 12·939 | ·1882 | 158·21 | 16·021 | ·1577 | 246·96 | 19·119 | ·1356 | 355·48 |
| 7 | 4·0250 | ·4729 | ·4563 | 10·265 | 6·9303 | ·3353 | ·3360 | 40·162 | 9·9345 | ·2605 | 89·257 | 12·985 | ·2123 | 158·31 | 16·062 | ·1788 | 247·05 | 19·156 | ·1545 | 355·55 |
| 8 | 4·0748 | ·5037 | ·4869 | 10·332 | 6·9814 | ·3640 | ·3647 | 40·297 | 9·9821 | ·2861 | 89·466 | 13·028 | ·2349 | 158·42 | 16·101 | ·1990 | 247·14 | 19·191 | ·1724 | 355·63 |
| 10 | 4·1557 | ·5555 | ·5383 | 10·459 | 7·0683 | ·4140 | ·4147 | 40·564 | 10·066 | ·3322 | 89·729 | 13·105 | ·2762 | 158·84 | 16·172 | ·2362 | 247·36 | 19·256 | ·2061 | 355·81 |
| 12 | 4·2185 | ·5973 | ·5800 | 10·573 | 7·1394 | ·4563 | ·4570 | 40·819 | 10·137 | ·3718 | 90·021 | 13·173 | ·3129 | 158·94 | 16·235 | ·2698 | 247·61 | 19·315 | ·2370 | 356·04 |
| 15 | 4·2905 | ·6472 | ·6297 | 10·726 | 7·2248 | ·5090 | ·5097 | 41·176 | 10·225 | ·4231 | 90·447 | 13·260 | ·3613 | 159·38 | 16·318 | ·3149 | 248·02 | 19·394 | ·2789 | 356·41 |
| 20 | 4·3737 | ·7080 | ·6924 | 10·932 | 7·3293 | ·5766 | ·5774 | 41·695 | 10·339 | ·4917 | 91·123 | 13·375 | ·4278 | 160·12 | 16·431 | ·3783 | 248·77 | 19·503 | ·3393 | 357·15 |
| 25 | 4·4304 | ·7514 | ·7337 | 11·095 | 7·4040 | ·6275 | ·6283 | 42·097 | 10·423 | ·5453 | 91·735 | 13·464 | ·4814 | 160·84 | 16·521 | ·4307 | 249·54 | 19·592 | ·3895 | 357·91 |
| 30 | 4·4714 | ·7840 | ·7663 | 11·223 | 7·4601 | ·6673 | ·6681 | 42·486 | 10·489 | ·5885 | 92·358 | 13·534 | ·5257 | 161·51 | 16·595 | ·4748 | 250·28 | 19·666 | ·4327 | 358·68 |
| 45 | 4·5467 | ·8467 | ·8289 | 11·487 | 7·5673 | ·7477 | ·7485 | 43·268 | 10·618 | ·6794 | 93·539 | 13·679 | ·6219 | 163·17 | 16·749 | ·5733 | 252·25 | 19·827 | ·5316 | 360·86 |
| 60 | 4·5880 | ·8828 | ·8650 | 11·648 | 7·6286 | ·7966 | ·7974 | 43·775 | 10·695 | ·7372 | 94·418 | 13·768 | ·6854 | 164·41 | 16·847 | ·6404 | 253·80 | 19·932 | ·6008 | 362·68 |
| 80 | 4·6208 | ·9124 | ·8946 | 11·785 | 7·6735 | ·8460 | ·8467 | 44·185 | 10·760 | ·7880 | 95·233 | 13·844 | ·7428 | 165·62 | 16·933 | ·7026 | 255·38 | 20·025 | ·6664 | 364·61 |
| 100 | 4·6413 | ·9313 | ·9135 | 11·875 | 7·7103 | ·8657 | ·8665 | 44·523 | 10·801 | ·8224 | 95·802 | 13·894 | ·7825 | 166·48 | 16·990 | ·7464 | 256·55 | 20·089 | ·7134 | 366·08 |
| 150 | 4·6697 | ·9582 | ·9404 | 12·005 | 7·7550 | ·9056 | ·9064 | 44·970 | 10·861 | ·8735 | 96·671 | 13·967 | ·8430 | 167·85 | 17·075 | ·8145 | 258·47 | 20·184 | ·7880 | 368·55 |
| 200 | 4·6843 | ·9723 | ·9544 | 12·074 | 7·7784 | ·9271 | ·9279 | 45·214 | 10·892 | ·9184 | 97·092 | 14·007 | ·8771 | 168·65 | 17·121 | ·8538 | 259·10 | 20·237 | ·8317 | 370·07 |
| 300 | 4·6992 | ·9869 | ·9691 | 12·146 | 7·8025 | ·9498 | ·9506 | 45·475 | 10·925 | ·9320 | 97·693 | 14·048 | ·9144 | 169·53 | 17·171 | ·8973 | 260·89 | 20·294 | ·8808 | 371·84 |
| 500 | 4·7114 | ·9990 | ·9812 | 12·207 | 7·8224 | ·9689 | ·9697 | 45·696 | 10·953 | ·9581 | 98·152 | 14·082 | ·9476 | 170·29 | 17·212 | ·9356 | 262·04 | 20·342 | ·9248 | 373·40 |
| 1,000 | 4·7207 | 1·0083 | ·9905 | 12·254 | 7·8377 | ·9838 | ·9846 | 45·870 | 10·974 | ·9785 | 98·515 | 14·109 | ·9726 | 170·92 | 17·245 | ·9667 | 262·98 | 20·380 | ·9608 | 374·71 |
| ∞ | 4·7300 | 1·0178 | 1·0000 | 12·302 | 7·8532 | ·9992 | 1·0000 | 46·050 | 10·996 | 1·0000 | 98·905 | 14·137 | 1·0000 | 171·59 | 17·279 | 1·0000 | 264·00 | 20·240 | 1·0000 | 376·15 |

It is now convenient to introduce the following notation:

$$\left.\begin{aligned}
&\frac{1}{a}\int_0^a X_i X_m\,dx = L_{im}; \qquad \frac{1}{b}\int_0^b Y_k Y_n\,dy = M_{kn},\\
&a\int_0^a \frac{dX_i}{dx}\frac{dX_m}{dx}\,dx = H_{im}; \qquad b\int_0^b \frac{dY_k}{dy}\frac{dY_n}{dy}\,dy = K_{kn},\\
&a\int_0^a X_i\frac{d^2X_m}{dx^2}\,dx = E_{im}; \qquad b\int_0^b Y_k\frac{d^2Y_n}{dy^2}\,dy = F_{kn},\\
&\frac{1}{a}\int_0^a \frac{d^2X_i}{dx^2}\frac{d^2X_m}{dx^2}\,dx = N_{im}+\frac{1}{a}\left[\frac{dX_i}{dx}\frac{d^2X_m}{dx^2}\right]_0^a;\\
&\frac{1}{b}\int_0^b \frac{d^2Y_k}{dy^2}\frac{d^2Y_n}{dy^2}\,dy = P_{kn}+\frac{1}{b}\left[\frac{dY_k}{dy}\frac{d^2Y_n}{dy^2}\right]_0^b.
\end{aligned}\right\} \tag{11}$$

As shown in the Appendix, these integrals have the following numerical values:

$$\left.\begin{aligned}
L_{im} &= \frac{a^4}{\alpha_m^4}N_{im} = \tfrac{1}{2}[2A_m^2-B_m^2+1]+\frac{A_m}{\alpha_m}[B_m+1],\ \text{if } i=m\\
&= 0,\ \text{if } i\neq m
\end{aligned}\right\}, \tag{12a}$$

$$\left.\begin{aligned}
E_{im} = E_{mi} &= -H_{im} = \tfrac{1}{2}\alpha_m^2[B_m^2+1]+\frac{A_m}{\alpha_m}[B_m-1],\ \text{if } i=m\\
&= \frac{4\alpha_i^2\alpha_m^2}{\alpha_i^4-\alpha_m^4}[A_i(B_m-1)\alpha_m-A_m(B_i-1)\alpha_i],\ \text{if } i\neq m;\\
&\qquad\qquad m\,\frac{\text{odd}}{\text{even}};\ i\,\frac{\text{odd}}{\text{even}}\\
&= 0,\ \text{if } i\neq m;\ m\,\frac{\text{odd}}{\text{even}};\ i\,\frac{\text{even}}{\text{odd}}.
\end{aligned}\right\} \tag{12b}$$

Similar expressions may be obtained for $M_{kn}$, $P_{kn}$, $K_{kn}$, and $F_{kn}$ by changing the subscripts $k$ for $i$, $n$ for $m$ in equations (12). It is to be noted that there is a particular reason why the terms

$$\frac{1}{a}\left[\frac{dX_i}{dx}\frac{d^2X_m}{dx^2}\right]_0^a; \qquad \frac{1}{b}\left[\frac{dY_k}{dy}\frac{d^2Y_n}{dx^2}\right]_0^b$$

have been retained in the last of equations (11) and have not been incorporated directly into $N_{im}$ and $P_{kn}$ respectively. These terms cancel with similar terms arising in the expression for the energy stored in the structure surrounding the plate and do not, in fact, appear in the final solution.

Substituting for $w(x, y)$ from equation (5) into equation (3), and using the notation of equations (11), we get

$$\frac{Da}{2b^3}\sum_{i,m=1}^{p}\sum_{k,n=1}^{q} a_{ik}a_{mn}\left[b^4(N_{im}M_{kn}+L_{im}P_{kn})+2\left(\frac{b}{a}\right)^2 H_{im}K_{kn}\right]- \\ -\frac{\rho hab\omega^2}{2g}\sum_{i,m=1}^{p}\sum_{k,n=1}^{q} a_{ik}a_{mn}L_{im}M_{kn}=0. \quad (13)$$

Differentiating equation (13) with respect to $a_{ik}$, the resulting equation may be expressed in the form

$$\sum_{m=1}^{p}\sum_{n=1}^{q}[C_{mn}^{(ik)}-\lambda\delta_{mn}]a_{mn}=0, \quad (14)$$

where

$$\left.\begin{aligned} \lambda &= \frac{\rho h\omega^2 b^4}{gD} \\ \delta_{mn} &= L_{mm}M_{nn}, \quad \text{if } ik=mn \\ &= 0, \quad \text{if } ik\neq mn \\ C_{mn}^{(ik)} &= 2\left(\frac{b}{a}\right)^2 H_{im}K_{kn}, \quad \text{if } ik\neq mn \\ C_{mn}^{(mn)} &= \left[\left(\frac{b}{a}\right)^4\alpha_m^4+\alpha_n^4\right]L_{mm}M_{nn}+2\left(\frac{b}{a}\right)^2 H_{mm}K_{nn}, \quad \text{if } ik=mn \end{aligned}\right\}. \quad (15)$$

Equation (14) represents a set of linear simultaneous equations: there will be one equation for each of the $pq$ combinations of $mn$. These equations divide into four independent groups as follows:

($a$) those in which $i$, $m$, $k$, $n$ are all odd,

($b$) those in which $i$, $m$, $k$, $n$ are all even,

($c$) those in which $i$, $m$ are odd and $k$, $n$ are even,

($d$) those in which $i$, $m$ are even and $k$, $n$ are odd,

and each of these groups is associated with one of the four possible combinations of symmetrical and antisymmetrical modes in the coordinate directions.

For a square plate, with all edges restrained to the same degree, groups ($c$) and ($d$) are essentially the same and lead to identical frequencies. Groups ($a$) and ($b$), however, can be rearranged to form two subgroups, which give independent solutions. The first subgroup includes solutions for which $a_{mn}=a_{nm}$, whilst the second subgroup includes solutions for which $a_{mn}=-a_{nm}$. The existence of these modes in a square plate clamped at all edges is discussed by Warburton (3).

## 6. Solution of equations

The characteristic values $\lambda$ of the equations (14) may be found from the condition that the determinant of the system is zero. However, the labour involved in expanding this determinant will generally be prohibitive. By using characteristic beam functions for $X_m$ and $Y_n$ in equation (5), it is found that the diagonal terms in the resulting determinant are much greater than the off-diagonal terms. The characteristic values $\lambda$ can therefore be determined by the iterative process developed by Ritz (8) and explained in detail by Young (9).

## 7. Approximate frequency equation

As the diagonal terms of the frequency determinant are much greater than all other terms, an approximate solution is suggested by representing the $mn$th mode by the $mn$th term only in the series equation (5). Proceeding with the energy solution, the $mn$th resonant frequency may then be written

$$\omega_{mn} = \frac{1}{b^2}\sqrt{\left(\frac{Dg}{\rho h}\right)\left[\left(\frac{b}{a}\right)^4 \alpha_m^4 + \alpha_n^4 + 2\left(\frac{b}{a}\right)^2 \phi_{mm}\phi_{nn}\right]^{\frac{1}{2}}}, \tag{16}$$

where

$$\left.\begin{aligned} \phi_{mm} &= \frac{H_{mm}}{L_{mm}} = \frac{\alpha_m^2[\alpha_m(B_m^2+1)+2A_m(B_m-1)]}{\alpha_m(2A_m^2-B_m^2+1)+2A_m(B_m+1)} \\ \phi_{nn} &= \frac{K_{nn}}{M_{nn}} = \frac{\alpha_n^2[\alpha_n(B_n^2+1)+2A_n(B_n-1)]}{\alpha_n(2A_n^2-B_n^2+1)+2A_n(B_n+1)} \end{aligned}\right\}. \tag{17}$$

For any values of the boundary restraints $\xi_A$, $\xi_B$, appropriate numerical values of $\alpha_m$, $\alpha_n$, $\phi_{mm}$, $\phi_{nn}$ may be obtained from Table 1.

It should be noted that, for a simply supported panel, equation (16) reduces to the well known exact solution (1)

$$\omega_{mn} = \frac{\pi^2}{b^2}\sqrt{\left(\frac{Dg}{\rho h}\right)\left[m^2\left(\frac{b}{a}\right)^2 + n^2\right]}. \tag{18}$$

For a square plate, under equal restraint on all edges, as already stated, there exist modes in which $a_{mn} = a_{nm}$ and $a_{mn} = -a_{nm}$, and these occur when $m$ is odd/even; $n$ is odd/even, and $m \neq n$. The corresponding approximate frequency equations may be written

$$\left.\begin{aligned} \omega_{(mn-nm)} &= \frac{1}{b^2}\sqrt{\left(\frac{Dg}{\rho h}\right)[\alpha_m^4 + \alpha_n^4 + 2(\phi_{mm}\phi_{nn} - \theta_{mn})]^{\frac{1}{2}}} \\ \omega_{(mn+nm)} &= \frac{1}{b^2}\sqrt{\left(\frac{Dg}{\rho h}\right)[\alpha_m^4 + \alpha_n^4 + 2(\phi_{mm}\phi_{nn} + \theta_{mn})]^{\frac{1}{2}}} \end{aligned}\right\}, \tag{19}$$

where

$$\theta_{mn} = \frac{H_{mn}K_{nm}}{L_{mm}M_{nn}}. \tag{20}$$

## TABLE 2

*Characteristic values $\sqrt{\lambda}$ for square and for rectangular plates*

| | | *The mode number* | | | | | |
|---|---|---|---|---|---|---|---|
| *b/a* | $\xi$ | 1 | 2 | 3 | 4 | 5 | 6 |
| 1·0 | 0 | 19·74 | 49·35 | 78·96 | 98·70 | 98·70 | 128·3 |
| | 20 | 31·09 | 64·31 | 95·85 | 117·3 | 116·8 | 147·6 |
| | | (31·16) | (64·52) | (96·17) | (117·8) | (116·9) | (148·0) |
| | ∞ | 35·99 | 73·41 | 108·3 | 131·6 | 132·3 | 165·2 |
| | | (36·11) | (73·74) | (108·9) | (131·7) | (132·4) | (165·4) |
| | |  |  |  |  |  |  |
| 0·9 | 0 | 17·86 | 41·85 | 47·47 | 71·46 | 81·82 | 111·4 |
| | 20 | 28·21 | 54·57 | 61·97 | 86·85 | 97·03 | 123·0 |
| | | (28·28) | (54·77) | (62·17) | (87·15) | (97·34) | (123·3) |
| | ∞ | 32·67 | 62·29 | 70·76 | 98·14 | 109·4 | 143·5 |
| | | (32·78) | (62·71) | (71·06) | (98·66) | (109·8) | (144·1) |
| | | 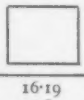 |  |  | 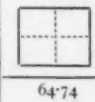 | 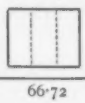 |  |
| 0·8 | 0 | 16·19 | 35·14 | 45·79 | 64·74 | 66·72 | 96·33 |
| | 20 | 25·80 | 46·02 | 59·98 | 79·06 | 79·24 | 111·2 |
| | | (25·86) | (46·17) | (60·16) | (79·32) | (79·50) | (111·5) |
| | ∞ | 29·08 | 52·52 | 68·52 | 89·40 | 89·29 | 124·5 |
| | | (29·18) | (52·76) | (68·80) | (89·86) | (89·69) | (125·0) |
| | |  |  | 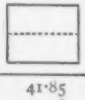 |  | 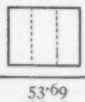 |  |
| 0·6 | 0 | 13·42 | 24·08 | 41·85 | 43·03 | 53·69 | |
| | 20 | 22·30 | 32·58 | 50·48 | 56·97 | 66·96 | |
| | | (22·34) | (32·68) | (50·63) | (57·11) | (67·17) | |
| | ∞ | 25·90 | 37·28 | 56·93 | 65·18 | 75·94 | |
| | | (25·97) | (37·43) | (57·20) | (65·39) | (76·31) | |
| | | 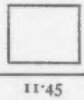 |  |  |  |  | |
| 0·4 | 0 | 11·45 | 16·19 | 24·08 | | | |
| | 20 | 20·30 | 24·15 | 31·20 | | | |
| | | (20·33) | (24·20) | (31·26) | | | |
| | ∞ | 23·65 | 27·81 | 35·45 | | | |
| | | (23·70) | (27·91) | (35·56) | | | |
| | |  |  |  | | | |
| 0·2 | 0 | 10·26 | 11·45 | 13·42 | | | |
| | 20 | 19·38 | 20·15 | 21·52 | | | |
| | | (19·39) | (20·17) | (21·54) | | | |
| | ∞ | 22·64 | 23·45 | 24·89 | | | |
| | | (22·66) | (23·49) | (24·92) | | | |
| | |  |  |  | | | |

## 8. Accuracy of solution

In discussing the accuracy of the present method it is first necessary to compare the approximate frequency equation with the more exact series solution. For this purpose characteristic values $\sqrt{\lambda}$ have been calculated by series solution for plates of side ratios $b/a = 1{\cdot}0$, $0{\cdot}9$, $0{\cdot}8$, $0{\cdot}6$, $0{\cdot}4$, and $0{\cdot}2$, under equal restraint on all four edges ($\xi_A = \xi_B = \xi$) and for values of $\xi = 20$ and $\infty$. Calculations were based on a 36-term series taking both $m$ and $n = 1, 2, 3, 4, 5, 6$. The results are presented in Table 2. Corresponding values of $\sqrt{\lambda}$ obtained from the approximate frequency equation are given in brackets. For comparison, the exact values of $\sqrt{\lambda}$ for a simply supported panel ($\xi = 0$) are also included. It is seen that the approximate solution nowhere differs from the series solution by more than 0·7 per cent.

The series solution overestimates the exact numerical solution to a degree which is in general unknown. However, in the case of a square plate clamped at all edges Aronszajn (**10**) has determined lower limits to the first ten modes, using a method originated by Weinstein (**11**). Aronszajn actually calculated the value of $\lambda/\pi^4$ but, converting accordingly, his values for the first six modes of a square clamped plate are $\sqrt{\lambda} = 35{\cdot}98$, $73{\cdot}37$, $108{\cdot}2$, $131{\cdot}6$, $131{\cdot}8$, $164{\cdot}4$, which differ by only 0·03–0·48 per cent from the corresponding upper limits given in Table 2.

## Acknowledgements

The author is indebted to Professor Sir Alfred Pugsley for his advice and guidance during the course of this work. He also wishes to record his gratitude to Mrs. E. Tilley, whose assistance with the numerical work has been invaluable.

## APPENDIX

### Evaluation of integrals of characteristic functions

1. *The integrals*

$$\frac{1}{L}\int_0^L F_r^2\,dx; \qquad \frac{1}{L}\int_0^L F_r'^2\,dx; \qquad \frac{1}{L}\int_0^L F_r' F_r'''\,dx.$$

Now
$$\int_0^L F_r^2\,dx = \frac{L^4}{\alpha_r^4}\int_0^L F_r^{iv} F_r\,dx = \frac{L^4}{\alpha_r^4}\left[[F_r''' F_r]_0^L - \int_0^L F_r' F_r'''\,dx\right].$$

But $F_r = 0$ at $x = 0$ and $x = L$, whence

$$\int_0^L F_r^2\,dx = -\frac{L^4}{\alpha_r^4}\int_0^L F_r' F_r'''\,dx, \tag{21}$$

$$\int_0^L F_r''^2\,dx = [F_r'' F_r']_0^L - \int_0^L F_r''' F_r'\,dx,$$

and hence
$$\int_0^L F_r''^2\,dx = \frac{\alpha_r^4}{L^4}\int_0^L F_r^2\,dx + [F_r' F_r'']_0^L. \tag{22}$$

It may be shown that
$$F_r^2 + \frac{L^4}{\alpha_m^4}F_r''^2 - \frac{2L^4}{\alpha_r^4}F_r' F_r''' = 2(2A_r^2 - B_r^2 + 1).$$

Thus by integration
$$\int_0^L F_r^2\,dx + \frac{L^4}{\alpha_r^4}\int_0^L F_r''^2\,dx - \frac{2L^4}{\alpha_r^4}\int_0^L F_r' F_r'''\,dx = 2L(2A_r^2 - B_r^2 + 1).$$

By substitution from equations (21) and (22)
$$\frac{1}{L}\int_0^L F_r^2\,dx = \tfrac{1}{2}(2A_r^2 - B_r^2 + 1) - \frac{L^3}{4\alpha_r^4}[F_r' F_r'']_0^L. \tag{23}$$

If opposite ends of the beam are restrained to the same degree then, by symmetry
$$[F_r F_r'']_{x=0} = -[F_r' F_r'']_{x=L} = \frac{2\alpha_r^2}{L^3}A_r(B_r + 1).$$

Thus equation (23) becomes
$$\frac{1}{L}\int_0^L F_r^2\,dx = \tfrac{1}{2}(2A_r^2 - B_r^2 + 1) + \frac{A_r}{\alpha_r}(B_r + 1). \tag{24}$$

2. *The integrals*
$$L\int_0^L F_r F_r''\,dx; \qquad L\int_0^L F_r'^2\,dx; \qquad L\int_0^L F_r''^2\,dx.$$

We have
$$\int_0^L F_r F_r''\,dx = [F_r F_r']_0^L - \int_0^L F_r'^2\,dx.$$

But $F_r = 0$ at $x = 0$ and $x = L$
$$\int_0^L F_r F_r''\,dx = -\int_0^L F_r'^2\,dx. \tag{25}$$

Also,
$$\int_0^L F_r F_r''\,dx = \frac{L^4}{\alpha_r^4}\int_0^L F_r'' F_r^{IV}\,dx = \frac{L^4}{\alpha_r^4}\left[[F_r'' F_r''']_0^L - \int_0^L F_r'''^2\,dx\right].$$

Hence
$$\int_0^L F_r'''^2\,dx = [F_r'' F_r''']_0^L - \frac{\alpha_r^4}{L^4}\int_0^L F_r F_r''\,dx. \tag{26}$$

It may be shown that
$$\frac{L^4}{\alpha_r^4}F_r'''^2 + F_r'^2 - 2F_r F_r'' = \frac{2\alpha_r^2}{L^2}(B_r^2 + 1).$$

Thus by integration
$$\frac{L^4}{\alpha_r^4}\int_0^L F_r'''^2\,dx + \int_0^L F_r'^2\,dx - 2\int_0^L F_r F_r''\,dx = \frac{2\alpha_r^2}{L}(B_r^2 + 1).$$

By substitution from equations (25) and (26)
$$L\int_0^L F_r'^2\,dx = -L\int_0^L F_r F_r''\,dx = \frac{\alpha_r^2}{2}(B_r^2 + 1) - \frac{L^3}{4\alpha_r^4}[F_r'' F_r''']_0^L. \tag{27}$$

If opposite ends of the beam are restrained to the same degree, then, by symmetry

$$(F_r'' F_r''')_{x=0} = -(F_r'' F_r''')_{x=L} = 2\frac{\alpha_r^5}{L^5} A_r(B_r-1).$$

Thus equation (27) becomes

$$L\int_0^L F_r'^2\,dx = -L\int_0^L F_r F_r''\,dx = \frac{\alpha_r^2}{2}(B_r^2+1)+\alpha_r A_r(B_r-1). \tag{28}$$

**3.** *The integrals*

$$\frac{1}{L}\int_0^L F_r F_s\,dx; \qquad \frac{1}{L}\int_0^L F_r' F_s'''\,dx; \qquad \frac{1}{L}\int_0^L F_r'' F_s''\,dx \quad (r \neq s).$$

Now $$(\alpha_r^4-\alpha_s^4)F_r F_s = \frac{d}{dx}(F_s F_r'''-F_r F_s'''-F_s' F_r''+F_r' F_s'').$$

By integration

$$(\alpha_r^4-\alpha_s^4)\int_0^L F_r F_s\,dx = [F_s F_r'''-F_r F_s'''-F_s' F_r''+F_r' F_s'']_0^L.$$

But

$$F_{r(s)} = 0; \qquad F_{r(s)}'' = \frac{\xi}{L}F_{r(s)}' \quad \text{at } x = 0,$$

$$F_{r(s)} = 0; \qquad F_{r(s)}'' = -\frac{\xi}{L}F_{r(s)}' \quad \text{at } x = L.$$

Therefore

$$\int_0^L F_r F_s\,dx = 0. \tag{29}$$

$$\int_0^L F_r F_s\,dx = \frac{L^4}{\alpha_r^4}\int_0^L F_r^{iv} F_s\,dx = \frac{L^4}{\alpha_r^4}\left[[F_r''' F_s]_0^L - \int_0^L F_r''' F_s'\,dx\right].$$

But $F_s = 0$ at $x = 0$ and $x = L$. Therefore

$$\int_0^L F_r''' F_s'\,dx = \int_0^L F_r' F_s'''\,dx = 0. \tag{30}$$

$$\int_0^L F_r''' F_s'\,dx = [F_r'' F_s']_0^L - \int_0^L F_r'' F_s''\,dx = 0.$$

Thus

$$\frac{1}{L}\int_0^L F_r'' F_s''\,dx = \frac{1}{L}[F_r'' F_s']_0^L = \frac{1}{L}[F_r' F_s'']_0^L. \tag{31}$$

**4.** *The integrals*

$$L\int_0^L F_r F_s''\,dx; \qquad L\int_0^L F_r' F_s'\,dx.$$

We have

$$\int_0^L F_r F_s''\,dx = [F_r F_s']_0^L - \int_0^L F_r' F_s'\,dx \quad (r \neq s).$$

But $F_r = 0$ at $x = 0$ and $x = L$; hence

$$\int_0^L F_r F_s''\,dx = \int_0^L F_r'' F_s\,dx = -\int_0^L F_r' F_s'\,dx. \tag{32}$$

$$\int_0^L F_r F_s'' \, dx = \frac{L^4}{\alpha_r^4} \int_0^L F_r^{IV} F_s'' \, dx = \frac{L^4}{\alpha_r^4} \left[ [F_r''' F_s'']_0^L - \int_0^L F_r''' F_s''' \, dx \right]$$

$$= \frac{L^4}{\alpha_r^4} \left[ [F_r''' F_s'']_0^L - [F_r'' F_s''']_0^L + \int_0^L F_r'' F_s^{IV} \, dx \right],$$

hence

$$\frac{\alpha_r^4}{L^4} \int_0^L F_r F_s'' \, dx = [F_r''' F_s'' - F'' F_s''']_0^L + \frac{\alpha_s^4}{L^4} \int_0^L F_r'' F_s \, dx.$$

Substituting from equation (32),

$$L \int_0^L F_r F_s'' \, dx = L \int_0^L F_r'' F_s \, dx = -L \int_0^L F_r' F_s' \, dx = \frac{L^5 [F_r''' F_s'' - F_r'' F_s''']_0^L}{\alpha_r^4 - \alpha_s^4}. \quad (33)$$

If opposite ends of the beam are restrained to the same degree, then, by symmetry

$$\left.\begin{aligned} F''_{r(s)x=0} &= F''_{r(s)x=L} \\ F'''_{r(s)x=0} &= -F'''_{r(s)x=L} \end{aligned}\right\} r = 1, 3, 5, \text{ etc.}$$

$$\left.\begin{aligned} F''_{r(s)x=0} &= -F''_{r(s)x=L} \\ F'''_{r(s)x=0} &= F'''_{r(s)x=L} \end{aligned}\right\} r = 2, 4, 6, \text{ etc.}$$

Thus

$$L \int_0^L F_r F_s'' \, dx = L \int_0^L F_r'' F_s \, dx = -L \int_0^L F_r' F_s' \, dx = 0 \quad \text{if } r \text{ is } \frac{\text{odd}}{\text{even}}; \; s \text{ is } \frac{\text{even}}{\text{odd}},$$

and

$$= \frac{-4\alpha_r^2 \alpha_s^2 [\alpha_r (B_r - 1) A_s + \alpha_s (B_s - 1) A_r]}{\alpha_r^4 - \alpha_s^4} \quad \text{if } r \text{ is } \frac{\text{odd}}{\text{even}}; \; s \text{ is } \frac{\text{odd}}{\text{even}}. \quad (34)$$

## REFERENCES


1. S. Timoshenko, *Vibration Problems in Engineering*, 2nd edition (New York, 1937).
2. W. Voigt, *Bemerkung zu dem Problem der transversalen Schwingungen rechteckiger Platten* (Göttinger Nachrichten, 1893), p. 225.
3. G. B. Warburton, 'The vibration of rectangular plates', *Proc. Inst. Mech. Eng.* **168** (1954) 371.
4. R. F. S. Hearmon, 'The frequency of vibration of rectangular isotropic plates', *J. Appl. Mech.* **19** (1952) 402.
5. R. Courant, *Advanced Methods in Applied Mathematics* (New York, 1941).
6. D. M. A. Leggett, *The Buckling of a Square Panel under Shear, when one Pair of Edges is Clamped and the Other Pair is Simply Supported*, Aeronautical Research Council, Reports and Memoranda No. 1991, 1941.
7. C. E. Inglis, 'The determination of critical speeds, natural frequencies and modes of vibration by means of basic functions', *N.E.C. Inst.*, **61**, 1944.
8. W. Ritz, 'Theorie der Transversalschwingungen einer quadratischen Platten mit freien Rändern', *Annalen der Physik, Vierte Folge*, **28** (1909) 737.
9. D. Young, 'Vibration of rectangular plates by the Ritz method', *J. Appl. Mech.* **17** (1950) 448.
10. N. Aronszajn, *The Rayleigh–Ritz and the Weinstein Methods of Approximation of Eigenvalues. III*, Technical Report No. 3, Project NR 041,090 (Oklahoma A. and M. College, Stillwater, Oklahoma, 1950).
11. *Alexander Weinstein Memorial des Sciences Mathématiques*, No. 88, 1937.

# TRANSVERSE ELASTIC WAVES IN AN INTERNAL STRATUM

*By* V. T. BUCHWALD

(*College of Science and Technology, Manchester*)

[Received 5 December 1957]

SUMMARY

This paper is concerned with the propagation of Love waves in a stratum bounded by infinite media with different elastic properties. The symmetrical case is considered first and it is shown that there are an infinite number of modes of vibration. The properties of the dispersion curves in each mode are derived. These properties are illustrated by graphs obtained from numerical computation. It is found that the general case is very similar to the case of symmetry, and corresponding results are given. The limits between which the phase and group velocities must lie are found in each case, and cut-off frequencies and wavelengths are also determined for each mode.

## 1. Introduction

STONELEY (1) has shown that under certain conditions it is possible for transverse waves to be transmitted in a stratum of uniform thickness, bounded on both sides by infinitely deep materials with different elastic properties, without a significant penetration of these waves into the infinite materials. Stoneley obtained the secular equations for waves of this sort, but his investigation did not yield much further information. In this paper it is first assumed that the infinite bounding materials have the same elastic properties and with this simplification it is possible to obtain results which give us a greater insight into the propagation of these waves. In fact, the properties of the phase and group velocities of the waves are found to be very similar to transverse waves in a surface layer, which were first investigated by Love (2). Once these results have been obtained it is not too difficult to extend the investigation to the case where the bounding materials possess different elastic properties.

## 2. Fundamental equations

We shall assume that the stratum, consisting of a material labelled 2 in which the velocity of rotational waves is $c_2$, and the modulus of rigidity is $\mu_2$, occupies the space between the planes $z = \mp h$, of a system of rectangular cartesian coordinates $x$, $y$, $z$. Materials 1 and 3 extend respectively from $z = h$ and $z = -h$ to infinity, the corresponding elastic constants being $c_1$, $\mu_1$, $c_3$, $\mu_3$. If $u$, $v$, $w$ are the displacements in the

directions $x$, $y$, $z$, then for the propagation of a plane transverse wave in the positive $x$-direction, we may take $u = w = 0$, and $v$ in the form

$$v_i = \psi_i e^{i(px - \quad t)} \tag{2.1}$$

where $\psi_i$ is a function of $z$ only. The suffix $i = 1, 2, 3$ refers to the material in which the displacement takes place. The equation to be satisfied by the $v_i$ is

$$c_i^2 \nabla^2 v_i = \partial^2 v_i / \partial t^2. \tag{2.2}$$

Thus $\psi_i$ must satisfy the equation

$$d^2\psi_i/dz^2 - (p^2 - n^2/c_i^2)\psi_i = 0, \tag{2.3}$$

the solutions of which are circular or hyperbolic functions. We may construct the following solution of (2.3),

$$\psi_1 = Ae^{-s_1 z}, \quad \psi_2 = B\cos s_2 z + C\sin s_2 z, \quad \text{and} \quad \psi_3 = De^{s_3 z}, \tag{2.4}$$

where $A$, $B$, $C$, $D$ are constants, and $s_1$, $s_2$, $s_3$ are given by

$$s_1^2 = p^2 - n^2/c_1^2, \quad s_2^2 = n^2/c_2^2 - p^2, \quad \text{and} \quad s_3^2 = p^2 - n^2/c_3^2. \tag{2.5}$$

Equations (2.4) represent a wave which does not penetrate very deeply into the bounding media provided that $s_1$ and $s_3$ are real and positive. Stoneley has shown that if $s_2$ is imaginary it is impossible to satisfy the boundary conditions. There is no loss of generality in assuming that $s_2$ is positive and that $c_1 \geqslant c_3$. From (2.5), if $c$ $(= n/p)$ is the phase velocity, then

$$c_1 \geqslant c_3 \geqslant c \geqslant c_2, \tag{2.6}$$

whilst $s_3 \leqslant s_1$. We assume that the tangential displacements and tractions are continuous across the planes $z = \mp h$. Thus, when $z = h$, $v_1 = v_2$, and $\mu_1 \dfrac{\partial v_1}{\partial z} = \mu_2 \dfrac{\partial v_2}{\partial z}$, and when $z = -h$, $v_2 = v_3$, and $\mu_2 \dfrac{\partial v_2}{\partial z} = \mu_3 \dfrac{\partial v_3}{\partial z}$. Substituting the expressions (2.4) in the boundary conditions and eliminating $A$, $B$, $C$, $D$ we obtain the secular equation

$$s_2(\tau_1 s_1 + \tau_3 s_3)t^2 + 2(s_2^2 - \tau_1\tau_3 s_1 s_3)t - s_2(\tau_1 s_1 + \tau_3 s_3) = 0, \tag{2.7}$$

where $t = \tan hs_2$, and $\tau_1$, $\tau_3$ are the ratios $\mu_1/\mu_2$, $\mu_3/\mu_2$ respectively. This is essentially the same as the equation obtained by Stoneley, which is

$$(s_2^2 - \tau_1\tau_3 s_1 s_3)T = s_2(\tau_1 s_1 + \tau_3 s_3), \tag{2.8}$$

where $T = \tan 2hs_2$.

## 3. The symmetrical case

In this section we shall assume that the media 1 and 3 possess the same elastic properties, so that $c_3 = c_1$ and $\mu_3 = \mu_1$. The equation (2.7) now reduces to

$$(s_2 t - \tau_1 s_1)(\tau_1 s_1 t + s_2) = 0, \tag{3.1}$$

which means that either

$$\text{(i)} \quad \tau_1 s_1 = s_2 \tan hs_2, \tag{3.2}$$

or

$$\text{(ii)} \quad \tau_1 s_1 = -s_2 \cot hs_2. \tag{3.3}$$

The equations (2.7) are now incompatible unless either (i) $C = 0$ and $A = D$, in which case we arrive at the equation (3.2), or (ii) $B = 0$ and $A = -D$, when we arrive at the equation (3.3). We may therefore separate the waves into two kinds, waves (i) which consist of displacements which are symmetrical about the plane $z = 0$, and for which the secular equation is (3.2), and waves (ii) for which the secular equation is (3.3) and which consist of displacements antisymmetrical about the plane $z = 0$. The equation (3.2) is the same as the secular equation for Love waves in a surface layer (**2**), (**3**).

The equations (2.5) now reduce to

$$\begin{aligned} s_1^2 &= p^2 - n^2/c_1^2, \\ s_2^2 &= n^2/c_2^2 - p^2. \end{aligned} \tag{3.4}$$

The phase velocity $c$, $p$, and $n$ may be obtained from (3.4) in the form

$$\begin{aligned} n^2 &= \nu_1(s_1^2+s_2^2)c_2^2/(\nu_1-1), \\ p^2 &= (\nu_1 s_1^2+s_2^2)/(\nu_1-1), \end{aligned} \tag{3.5}$$

whilst

$$c^2 = \nu_1(s_1^2+s_2^2)c_2^2/(\nu_1 s_1^2+s_2^2), \tag{3.6}$$

where $\nu_1 = c_1^2/c_2^2$. By differentiating either (3.2) or (3.3) it can be shown that the group velocity $V$ $(dn/dp)$ can be written as

$$V = \frac{\nu_1[(s_1^2+s_2^2)\tau_1+hs_1(s_2^2+\tau_1^2 s_1^2)]c_2^2}{[(\nu_1 s_1^2+s_2^2)\tau_1+hs_1(s_2^2+\tau_2^2 s_1^2)]c}. \tag{3.7}$$

This expression for the group velocity holds for both the symmetrical and antisymmetrical cases.

An examination of equation (3.2) shows that if we take a fixed value of $s_1$ there is a single solution for $s_2$ in each interval of the type $m\pi \leqslant hs_2 \leqslant (m+\frac{1}{2})\pi$, where $m$ is a positive integer, whence corresponding values of $p$, $n$, $c$, and $V$ may be found. Thus $c$ and $V$ as functions of $p$ depend on the branch of the solution of (3.2) taken, and every branch corresponds to a separate mode of vibration. In the same way there exists a separate solution of (3.3) in each interval of the type

$$(m+\tfrac{1}{2})\pi \leqslant hs_2 \leqslant (m+1)\pi.$$

Thus each interval $\frac{1}{2}(m-1)\pi \leqslant hs_2 \leqslant \frac{1}{2}m\pi$ corresponds to a separate mode of vibration, where $m = 1, 2, 3,...$ and so on. The modes in which $m$ is odd consist of symmetric displacements, whilst even $m$ correspond to antisymmetric displacements.

Before examining any mode in detail there are a number of general conclusions that can be drawn.

(*a*) When $hs_2$ tends to the lower limit in each mode, $s_1$ tends to zero, so that from (3.5) we see that there exist in each mode minimum values of $p$ and $n$ given by

$$p^2 \geqslant s_0^2/(\nu_1-1),$$

and

$$n^2 \geqslant \nu_1(s_0c)^2/(\nu_1-1), \tag{3.8}$$

where $hs_0 = \frac{1}{2}(m-1)\pi$. Hence the higher modes consist of comparatively short waves of high frequency. In particular, if $\lambda$, the wavelength, is greater than $2h/(\nu_1-1)^{\frac{1}{2}}$ then this wavelength only occurs in the first two modes, whilst only the first (symmetrical) mode can produce a wavelength greater than $4h/(\nu_1-1)^{\frac{1}{2}}$.

(*b*) Let us consider the behaviour of the phase and group velocities when $hs_2$ tends to the lower limit $\frac{1}{2}(m-1)\pi$ in each mode. From (3.2) or (3.3), whichever applies, we can see that $s_1$ tends to zero in each case, and is very small compared to $s_2$. With the exception of the first mode, which is a special case, if we allow $s_1$ to become very small in (3.6) then

$$c = c_1[1-(\nu_1-1)s_1^2/s_2^2+O(s_1^4)], \tag{3.9}$$

whilst from (3.7) and (3.9),

$$V = c_1[1-(\nu_1-1)hs_1/\tau_1+O(s_1^2)]. \tag{3.10}$$

In the first mode, from (3.2),

$$s_1 = hs_2^2+O(s_2^4),$$

whence

$$c = c_1[1-(\nu_1-1)h^2s_2^2/2\tau_1^2+O(s_2^4)], \tag{3.11}$$

and

$$V = c_1[1-3(\nu_1-1)h^2s_2^2/2\tau_1^2+O(s_2^4)]. \tag{3.12}$$

The conclusion to be drawn from (3.9) to (3.12) is that in each mode both $c$ and $V$ are equal to $c_1$, when $p$ and $n$ are at their minimum values, and that $c$ and $V$ decrease from $c_1$ as $p$ increases.

(*c*) If $hs_2$ tends to the upper limit $\frac{1}{2}m\pi$ in each mode then we see from (3.2) or (3.3) that $s_1$ tends to infinity and consequently, from (3.5) that both $p$ and $n$ tend to infinity, corresponding to very short waves of very high frequency. From (3.6), if $s_1$ is very large,

$$c = c_2[1+(\nu_1-1)s_2^2/\nu_1s_1^2+O(s_1^{-4})], \tag{3.13}$$

whilst from (3.7) and (3.13),

$$V = c_2[1-(\nu_1-1)s_2^2/\nu_1s_1^2+O(s_1^{-4})]. \tag{3.14}$$

Remembering our assumption that $\nu_1 > 1$, it is clear from (3.13) and (3.14) that as $p$ tends to infinity, $c$ tends to the lower limit $c_2$ from above, while $V$ tends to $c_2$ from below. Since in any one mode both $c$ and $V$ are continuous functions of $p$, $V$ must possess a minimum which is less than $c_2$.

(*d*) From (3.7) we see that $V \geqslant c_2^2/c$, so that on no account can $V$ be less than $c_2^2/c_1$. If we fix a value $s_2^0$ in the first mode, and examine $c$ and $V$ in the other modes for $s_2 = s_2^0 + \frac{1}{2}m\pi$, then $t$ remains unaltered, as will the ratio $s_1/s_2$. This means that $c$ is independent of $m$, $V$ decreases steadily from its value in the first mode to the limit $c_2^2/c$. In the limit, if $m$ is very large, $V = c_2^2/c$, except in the immediate neighbourhood of $s_1 = 0$. Thus

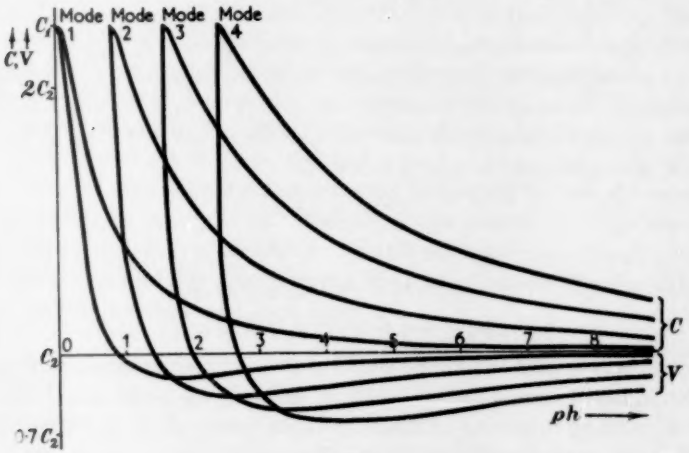


FIG. 1

the minimum value of $V$ approaches $c_2^2/c_1$ as $m$ becomes very large, and the position of this minimum will approach the smallest value of $p$ occurring in the mode.

Fig. 1 illustrates the dispersion curves of the first four modes, with $\nu_1$ and $\tau_1$ being taken as 5 and 2 respectively. The graphs, drawn from values obtained by numerical computation, illustrate points (*a*) to (*d*) very well.

Jeffreys (4) has shown that when there is a stationary value of the group velocity then the dispersion is comparatively small for that particular value of $p$. Thus we conclude that though the first signal of transverse waves will travel with a velocity of $c_1$, and will consist chiefly of longer waves, the main part of the vibration will follow, the slowest waves travelling with a velocity of $c_2^2/c_1$. In addition, certain frequencies and wavelengths, corresponding to the minima of the group velocity, will suffer less dispersion, and will predominate at a large distance from the disturbance. Further, these predominating waves will travel with velocities between $c_2$ and $c_2^2/c_1$, and the important frequencies will be located at intervals of roughly $c_2/4h(\nu_1-1)^{\frac{1}{2}}$.

## 4. The general case

Here we merely assume that $c_1 > c_3 > c_2$, so that $s_1 > s_3$. In theory it is possible to express $n$ in terms of $p$ from the equations (2.5) and (2.7), but this is not possible in practice. It is best to eliminate $n$ and $p$ from the equations (2.5) to obtain

$$\nu_1(\nu_3-1)s_1^2 = \nu_3(\nu_1-1)s_3^2+(\nu_1-\nu_3)s_2^2, \tag{4.1}$$

where $\nu_3 = c_3^2/c_2^2$ and $\nu_1 > \nu_3 > 1$. We can now proceed by choosing a value of $s_2$ and determining the corresponding values of $s_3$, $s_1$, $p$, $n$, $c$, and $V$. Before attempting to find particular numerical solutions it is advisable to separate the modes of vibration and to try to find some general properties of the dispersion curves. The secular equation (2.7) can be considered as a quadratic in $t$, with solutions

$$\text{(i)} \quad t = \alpha+\beta, \tag{4.2}$$

or

$$\text{(ii)} \quad t = \alpha-\beta, \tag{4.3}$$

where

$$\alpha = (\tau_1\tau_3 s_1 s_3 - s_2^2)/s_2(\tau_1 s_1+\tau_3 s_3), \tag{4.4}$$

and

$$\beta = (s_2^4+\tau_1^2 s_2^2 s_1^2+\tau_3^2 s_2^2 s_3^2+\tau_1^2\tau_3^2 s_1^2 s_3^2)^{\frac{1}{2}}/(\tau_1 s_1+\tau_3 s_3)s_2. \tag{4.5}$$

A glance at (4.4) and (4.5) shows that $\beta$ is always greater than $|\alpha|$, and therefore if $hs_2$ lies in an interval $m\pi \leqslant hs_2 \leqslant (m+\frac{1}{2})\pi$, $t$ is positive and the solution (i), given by equation (4.2) has to be taken, whilst if $(m-\frac{1}{2})\pi \leqslant hs_2 \leqslant m\pi$, $t$ is negative so that solution (ii), given by equation (4.3), applies. This suggests that there exists a mode of vibration in each interval of $\frac{1}{2}\pi$, although the modes can no longer be separated into symmetrical and antisymmetrical ones. We have yet to show that while $hs_2$ lies in such an interval there exists not more than one solution for $s_1$, $s_2$, and $s_3$; this will be done in an appendix at the end of this section and for the remainder of this section we shall assume that each interval corresponds to a separate mode.

When $s_2$ tends to the upper limit in each mode, $2hs_2$ tends to $m\pi$ from below, so that, from (2.8), $T$ tends to zero through negative values. This can only occur if both $s_1$ and $s_3$ tend to infinity. From (4.1) we see that for large $s_3$,

$$s_1 = \omega s_3+O(s_3^{-1}), \tag{4.6}$$

where $\omega$ is the constant $[\nu_3(\nu_1-1)/\nu_1(\nu_3-1)]^{\frac{1}{2}}$. Using this result and the equation (2.8) we find that

$$T = -\Omega s_2/s_3+O(s_3^{-3}), \tag{4.7}$$

where $\Omega = (\tau_1\omega+\tau_3)/\tau_1\tau_3\omega$. From (2.5) the phase velocity may be written in the form

$$c^2 = \nu_3 c_2^2(s_2^2+s_3^2)/(\nu_3 s_3^2+s_2^2), \tag{4.8}$$

and, if $s_3$ is large,

$$c = c_2[1+(\nu_3-1)s_2^2/2\nu_3 s_3^2+O(s_3^{-4})]. \tag{4.9}$$

The group velocity may be obtained in the form

$$V = \nu_3(s_3 s_3'+s_2)c_2^2/(\nu_3 s_3 s_3'+s_2)c, \tag{4.10}$$

where $s_3'$ means $ds_3/ds_2$. If we differentiate (4.7) we find that $s_3' = O(s_3^2)$, and, using this result, together with (4.9) and (4.10) we find that if $s_3$ is large,

$$V = c_2[1-(\nu_3-1)s_2^2/2\nu_3 s_3^2+O(s_3^{-3})]. \tag{4.11}$$

Thus, when $s_3$, and consequently $p$ and $n$ are large, the phase velocity approaches the limit $c_2$ from above, whilst the group velocity approaches it from below—a result corresponding to the previous section.

If, as in the previous section, we attempt to make $s_2$ tend to the lower limit in each mode we find from (2.8) that if $m \neq 0$, both $s_1$ and $s_3$ tend to zero as $hs_2$ decreases to $\frac{1}{2}m\pi$, whilst if $m = 0$, both $s_1$ and $s_3$ are of $O(s_2^2)$ as $s_2$ tends to zero. These conclusions are incompatible with the equation (4.1), except in case $\nu_1 = \nu_3$. Excepting this special case, we conclude that there is no solution of our equations at the lower end of each interval. We now try to find out what happens if we let $s_3$ become very small on its own. In this case (4.1) can be reduced to

$$\tau_1 s_1 = ks_2+O(s_3^2), \tag{4.12}$$

where

$$k = \tau_1[(\nu_1-\nu_3)/\nu_1(\nu_3-1)]^{\frac{1}{2}}, \tag{4.13}$$

so that from (2.8),

$$T = k+(1+k^2)\tau_3 s_3/s_2+O(s_3^2). \tag{4.14}$$

We may rewrite (2.8) in the form

$$s_3 = s_2(Ts_2-\tau_1 s_1)/\tau_3(s_2+T\tau_1 s_1). \tag{4.15}$$

Since $s_3$ is always positive it follows that if $T > 0$, $T \geqslant \tau_1 s_1/s_2$, and from (4.12) it is clear that $\tau_1 s_1 \geqslant ks_2$. Hence we see that for all values of $s_3$, either $T < 0$, or $T \geqslant k$. This means that in the $m$th mode,

$$hs_2 \geqslant \tfrac{1}{2}[\tan^{-1}k+(m-1)\pi]. \tag{4.16}$$

If, from (2.5), we write $n$ and $p$ in terms of $s_2$ and $s_3$, we find that in the $m$th mode the minimum cut-off frequency is given by

$$n \geqslant \nu_3^{\frac{1}{2}}\{\tan^{-1}k+\pi(m-1)\}/2h(\nu_3-1)^{\frac{1}{2}}, \tag{4.17}$$

with a similar expression for $p$. In particular, the longest possible wavelength that can occur is given by

$$\lambda \geqslant 4h\pi/[(\nu_3-1)^{\frac{1}{2}}\tan^{-1}k]. \tag{4.18}$$

If, in (4.8), we make $s_3$ small then we find that

$$c = c_3[1-\tfrac{1}{2}(\nu_3-1)s^2+O(s^4)], \tag{4.19}$$

where $s = s_3/s_2$. By differentiating (4.14) we obtain

$$s_3'(1+k) = 2hs_2(1+T^2)+T-k+O(s). \tag{4.20}$$

It has been shown that $T \geqslant k$ in the neighbourhood of $s_3 = 0$, so that in this neighbourhood $s_3'$ must be positive and of $O(1)$. From (4.19), (4.20), and (4.10) we find that

$$V = c_3[1 - s s_3'(\nu_3 - 1) + O(s^2)]. \tag{4.21}$$

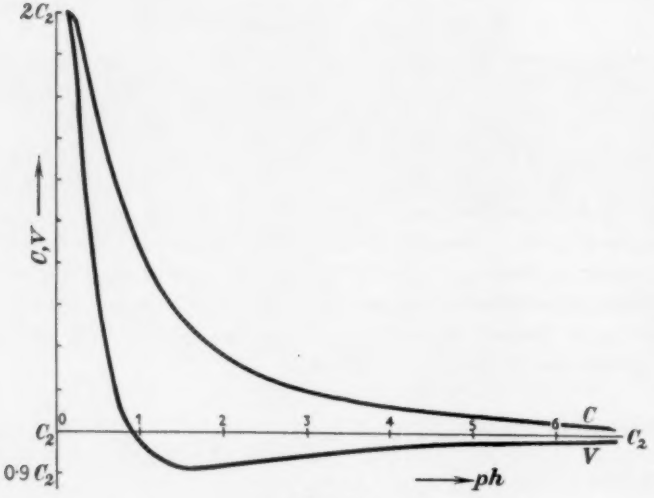


FIG. 2

Thus, when $s_3$ increases from zero, both $s_2$ and $s_1$, as well as $p$ and $n$, will increase from their minimum values in each mode, whilst $c$ and $V$ will decrease from their maximum value $c_3$, $V$ decreasing much more rapidly than $c$.

If we differentiate the last two equations in (2.5) with respect to $p$ and eliminate $V$ and $n$, we find that

$$\nu_3 s_3 \frac{ds_3}{dp} + s_2 \frac{ds_2}{dp} = (\nu_3 - 1)p > 0. \tag{4.22}$$

Thus $\nu_3 s_3 s_3' + s_2 > 0$, which from (4.10) means that

$$V \geqslant c_2^2/c \geqslant c_2^2/c_3. \tag{4.23}$$

From the results in this section it appears that the dispersion curves for any one mode look rather like Fig. 2. In fact, the graphs in Fig. 2 have been obtained by numerical computation, with $\nu_1$, $\nu_3$, $\tau_1$, and $\tau_3$ having the assigned values 5, 4, 3, and 2 respectively, in the first mode. In this particular case, $c_3 = 2c_2$, $k = 0{\cdot}77460$, $\tan^{-1}k = 0{\cdot}66$, and $p_{\min}$ approximately $0{\cdot}19/h$. The numerical work was done assuming values of $s_2 h$ at regular intervals between $0{\cdot}33$ and $\pi$, and then eliminating $s_1$ from the

equations (4.1) and (2.8). The resulting quartic was solved by Newton's method. Throughout this paper the numerical work has been done by means of autocode programmes for the Manchester University digital computer.

In view of the similarity between the results in this section and the previous, we can conclude that provided the condition $\nu_1 \geqslant \nu_3 > 1$ is observed, Love waves may be transmitted in a stratum and that at a large distance from the disturbance we would expect certain discrete frequencies and wavelengths to predominate, corresponding to minima in the group velocity. These predominant waves will travel with velocities of between $c_2$ and $c_2^2/c_3$, although we have shown that the maximum velocity with which Love waves can travel is $c_3$.

## APPENDIX

There remains the question whether we are justified in assuming that there is at most one solution of equations (4.1) and (2.8) in every interval

$$\tfrac{1}{2}(m-1)\pi \leqslant hs_2 \leqslant \tfrac{1}{2}m\pi.$$

If we take
$$R = (s_2^2-\tau_1\tau_2 s_1 s_3)/s_2(\tau_1 s_1+\tau_3 s_3), \tag{i}$$

and we assume that $s_3$ is fixed, then

$$s_2^2(\tau_1 s_1+\tau_3 s_3)^2\frac{dR}{ds_2} = (s_2^2+\tau_1\tau_3 s_1 s_3)(\tau_1 s_1+\tau_2 s_3)-s_1(\tau_3^2 s_2^2+s_3^2)s_1', \tag{ii}$$

where $s_1' = ds_1/ds_2$. A similar expression for $dR/ds_2$ in terms of $s_2'$ may be obtained by assuming $s_1$ fixed. From (4.1) we find that $s_1' \leqslant s_1/s_2$, so that, from (ii), if $s_3$ is fixed

$$\frac{dR}{ds_2} \geqslant \tau_3 s_3(\tau_1^2 s_1^2+s_2^2)/s_2^2(\tau_1 s_1+\tau_3 s_3)^2 > 0. \tag{iii}$$

$R$ is a continuous function of $s_2$ in the region $s_2 > 0$, and when $s_2$ is small and positive, $R$ is very large and negative. We conclude that the graphs of $\cot 2hs_2$ and of $R$ must intersect once in every interval $\frac{1}{2}(m-1)\pi \leqslant hs_2 \leqslant \frac{1}{2}m\pi$, whence (4.1) and (2.8) will have at most one solution in such an interval. Similarly, if we fix $s_1$ we find from (4.1) that $s_2' \leqslant 0$, whence $dR/ds_2 > 0$, with much the same result as above. Finally the question arises as to what happens if we assign a fixed value to $s_2$. From (2.8) we may express $s_1$ as a function of $s_3$ in the form

$$\tau_1 s_1 = s_2(Ts_2-\tau_3 s_3)/(s_2+T\tau_3 s_3). \tag{iv}$$

If we draw the graph of this function, and the function given by (4.1) with $s_2$ constant, we find that there will be just one intersection for positive $s_3$ and $s_1$, provided that either $T < 0$, or $T > k$, whilst if $0 \leqslant T < k$ there will be no such intersection.

## REFERENCES

1. R. Stoneley, *Proc. Roy. Soc.* **A 106** (1924) 424.
2. A. E. H. Love, *Some Problems of Geodynamics* (Cambridge, 1911), p. 160.
3. V. T. Buchwald, *Quart. J. Mech. App. Math.* 11 (1958) 506.
4. H. Jeffreys and B. Jeffreys, *Methods of Mathematical Physics* (Cambridge, 1956), pp. 511–15.

# THE QUASI-STATIC EXPANSION OF A SPHERICAL CAVITY IN METALS AND IDEAL SOILS

*By* P. CHADWICK

(*Atomic Weapons Research Establishment, Aldermaston, Berkshire*)

[Received 31 October 1957]

SUMMARY

An infinite medium of ideal soil contains a single spherical cavity within which a slowly increasing pressure is applied. The analysis of stress in the resulting plastic-elastic system, in conjunction with the flow rule associated with the Coulomb law of failure, leads to an expression for the radial displacement of the soil. It is found, in particular, that the radius of the cavity increases indefinitely as the applied pressure approaches a finite limiting value. Since the work done at the cavity wall also increases without bound this pressure cannot be attained physically.

When the angle of shearing resistance of the soil is zero the Coulomb law and flow rule are, under conditions of radial symmetry, formally identical to the yield criteria of Tresca and von Mises and their associated flow rules. A special case of the analysis is hence appropriate to the expansion of a spherical cavity in a non-hardening metal. Calculations have been carried out for copper and a comparison is made with numerical results obtained from an alternative solution due to Hill (**1**). It is shown that the inclusion of work-hardening does not alter the behaviour of the medium qualitatively.

If, on the completion of loading, the pressure exceeds a certain limit further plastic flow takes place round the cavity on unloading. Equations are obtained from which can be calculated the residual stresses and displacement at any stage of the unloading process.

## 1. Introduction

A MEDIUM of ideal soil, unbounded in all directions, contains a single spherical cavity. Initially the radius of the cavity is $a_0$ and a hydrostatic pressure $p_0$ acts throughout the soil which is assumed to be homogeneous. An additional pressure $p$ is then applied inside the cavity and increased sufficiently slowly for dynamical effects to be negligible. This paper is concerned with the distribution of stress and displacement in the soil as $p$ increases from zero and when unloading subsequently takes place.

An ideal soil is, by definition, an isotropic elastic–rigid plastic material in which the yield condition is obtained from Coulomb's law of failure. When the principal stress components satisfy the inequalities $\sigma_i \leqslant \sigma_j \leqslant \sigma_k$, Shield (**2**) has shown that the Coulomb law takes the form

$$\sigma_k - \sigma_i = 2c\cos\phi - (\sigma_k + \sigma_i)\sin\phi, \tag{1}$$

where $c$ is the cohesion and $\phi$ the angle of shearing resistance of the soil.

Putting $$\alpha = \frac{2\sin\phi}{1-\sin\phi}, \quad Y = \frac{2c\cos\phi}{1-\sin\phi},$$

equation (1) becomes $$(1+\alpha)\sigma_k - \sigma_i = Y. \tag{2}$$

The permutations of the suffixes in equation (2) define six planes in principal stress space forming a right hexagonal pyramid. This yield surface has also been discussed by Shield.

When $\phi = 0$, then $\alpha = 0$ and equation (2) reduces to the yield criterion of Tresca. This is a special case of some importance as saturated soils display no internal friction when deformed in such a way as to preserve their natural water content. In the case of radial symmetry the yield criteria of Tresca and von Mises and the associated flow rules are formally identical. The theory of the expansion of a spherical cavity in Tresca and Reuss materials therefore emerges as a special case of the analysis which follows.

The properties of an ideal soil are very much simpler than those of natural soils and attempts have been made to put the theory of soil plasticity on a more realistic basis. Drucker, Gibson, and Henkel (**3**), for instance, have suggested that soils should be treated as work-hardening materials. These ideas have not yet been stated in a mathematical form, however, and in this paper the resistance of the medium to deformation is therefore simply expressed (in equation (1)) in terms of the cohesive forces between the constituent particles and the frictional forces set up at inter-particle contacts. In the absence of detailed experimental data on the behaviour of soils under the conditions envisaged a more elaborate description is hardly justified.

The quasi-static expansion of a spherical cavity in a Reuss material has been studied by Hill (**1**, pp. 103–4). This solution has been applied to the determination of bearing capacities by Meyerhof (**4**), and Skempton, Yassin, and Gibson (**5**) have produced an analysis which incorporates the shearing resistance characteristic of ideal soils. The more comprehensive treatment presented here is based entirely upon the theory of ideal plastic solids and in that respect differs from the earlier work of Skempton *et al.*

The initial position of a particle of soil is specified by the spherical polar coordinates $(r_0, \theta, \psi)$ measured about the centre of the cavity. Since the system has radial symmetry the particle retains the same angular coordinates throughout the deformation and its current position is given by $(r, \theta, \psi)$. The principal components of stress and strain everywhere act in the directions of $r$, $\theta$, $\psi$ increasing. Denoting them by $\sigma_r$, $\sigma_\theta$, $\sigma_\psi$; $\epsilon_r$, $\epsilon_\theta$, $\epsilon_\psi$ respectively, then

$$\sigma_\theta \equiv \sigma_\psi, \qquad \epsilon_\theta \equiv \epsilon_\psi. \tag{3}$$

At the cavity wall, $$\sigma_r(a) = -p - p_0, \tag{4}$$

$a$ being the current radius of the cavity. The other external boundary condition is

$$\sigma_r(\infty) = -p_0. \tag{5}$$

The displacement $u\ (= r-r_0)$ is purely radial and the elastic properties of the soil are described by Young's modulus $E$, and Poisson's ratio $\nu$.

## 2. The elastic solution

As $p$ increases from zero the deformation of the soil is at first entirely elastic. Under conditions of radial symmetry the equations connecting stress, strain, and displacement are

$$\epsilon_r = \frac{du}{dr} = \frac{1}{E}[\sigma_r - 2\nu\sigma_\theta],$$

$$\epsilon_\theta = \frac{u}{r} = \frac{1}{E}[-\nu\sigma_r + (1-\nu)\sigma_\theta], \tag{6}$$

and the elastic equilibrium equations reduce to the single relation

$$r\frac{d\sigma_r}{dr} + 2(\sigma_r - \sigma_\theta) = 0. \tag{7}$$

The solution of equations (6), (7) subject to the boundary conditions (4), (5) is

$$\sigma_r = -p_0 - p\left(\frac{a}{r}\right)^3, \qquad \sigma_\theta = -p_0 + \tfrac{1}{2}p\left(\frac{a}{r}\right)^3, \tag{8}$$

$$u = \tfrac{1}{2}p\frac{1+\nu}{E}\left(\frac{a}{r}\right)^3 r. \tag{9}$$

From equations (3), (8) it follows that $\sigma_r < \sigma_\theta = \sigma_\psi$. Plastic yielding thus commences when the state of stress is represented by a point on the edge of the yield pyramid given by

$$(1+\alpha)\sigma_\theta - \sigma_r = Y, \qquad \sigma_\theta = \sigma_\psi. \tag{10}$$

Since $(1+\alpha)\sigma_\theta - \sigma_r = -\alpha p_0 + \frac{1}{2}(3+\alpha)p(a/r)^3$ takes its greatest value at $r = a$, yielding starts at the cavity wall when the applied pressure reaches the value

$$p_1 = \frac{2(Y+\alpha p_0)}{3+\alpha}. \tag{11}$$

Both strain components are of greatest magnitude at the cavity wall and when $p = p_1$,

$$\epsilon_r(a) = -\frac{2(1+\nu)(Y+\alpha p_0)}{(3+\alpha)E}, \qquad \epsilon_\theta(a) = \frac{(1+\nu)(Y+\alpha p_0)}{(3+\alpha)E}. \tag{12}$$

Soils, like metals, are characterized by the strong inequality $Y \ll E$. Provided that $p_0 \ll E$ the use of the infinitesimal strain theory throughout the initial phase of elastic deformation is therefore justified.

### 3. The plastic–elastic solution

When $p > p_1$ a plastic zone is formed around the cavity. Considerations of symmetry require the outer boundary of this region to be spherical and the current value of its radius is denoted by $b$.

The stress components in the plastic zone $a \leqslant r \leqslant b$ satisfy the yield condition (10) and the equilibrium equation (7). The solution of these equations is easily shown to be

$$\sigma_r = \frac{Y}{\alpha} + Ar^{-2\alpha/(1+\alpha)}, \qquad \sigma_\theta = \frac{Y}{\alpha} + \frac{A}{1+\alpha} r^{-2\alpha/(1+\alpha)}, \tag{13}$$

where $A$ is the constant of integration.

From equations (5) to (7) the stress components in the elastic region $r \geqslant b$ are

$$\sigma_r = -p_0 - Br^{-3}, \qquad \sigma_\theta = -p_0 + \tfrac{1}{2}Br^{-3}, \tag{14}$$

$B$ being a second constant.

At the junction of the plastic and elastic regions the radial stress component $\sigma_r$ must be continuous in order to preserve equilibrium and the material on the elastic side of the interface must be about to yield. These two internal boundary conditions together imply the continuity of $\sigma_r$ and $\sigma_\theta$ at $r = b$ and determine the constants $A$, $B$ in the form

$$A = -\frac{3(1+\alpha)(Y+\alpha p_0)}{\alpha(3+\alpha)} b^{2\alpha/(1+\alpha)}, \qquad B = \frac{2(Y+\alpha p_0)}{3+\alpha} b^3. \tag{15}$$

The radial stress component in the elastic region already satisfies the boundary condition at infinity (5). The other external boundary condition, equation (4), gives the relation

$$\frac{b}{a} = \left[\frac{(3+\alpha)(Y+\alpha p+\alpha p_0)}{3(1+\alpha)(Y+\alpha p_0)}\right]^{(1+\alpha)/2\alpha}. \tag{16}$$

It may readily be verified that $b \geqslant a$ if and only if $p \geqslant p_1$.

From equations (15), $A < 0$, $B > 0$, and it follows from (13), (14) that $\sigma_\theta > \sigma_r$ throughout the soil. In the elastic region, moreover,

$$(1+\alpha)\sigma_\theta - \sigma_r \leqslant Y \quad \text{for} \quad r \geqslant b,$$

the signs of equality holding together. These inequalities establish the validity of the solution.

### 4. Evaluation of the displacement

On substituting from equations (14), (15) into (6) the displacement in the elastic region, $r \geqslant b$, is found to be

$$u = \frac{(1+\nu)(Y+\alpha p_0)}{(3+\alpha)E}\left(\frac{b}{r}\right)^3 r. \tag{17}$$

The strain components in this region, obtained from equations (6), decrease in magnitude as $r$ increases and attain their greatest absolute values at $r = b$. These maxima are given by the right-hand sides of equations (12) so that the strain components at the inner boundary of the elastic region remain constant from the initiation of plastic flow in the soil until the completion of the loading process. It follows that if $p_0 \ll E$ the strains in the elastic region are always small enough to warrant the neglect of their products and higher powers.

In the plastic zone indices $e$, $p$ are used to distinguish the elastic and plastic components of the total strains. The plastic strain increments are given by the flow rule associated with Coulomb's law of failure. At all points in the plastic zone the state of stress corresponds to a singular point on the yield surface. The appropriate form of the plastic potential is therefore

$$f = \gamma[(1+\alpha)\sigma_\theta - \sigma_r] + (1-\gamma)[(1+\alpha)\sigma_\psi - \sigma_r],$$

where $0 < \gamma < 1$. Differentiation with respect to the stress components yields the plastic strain increments

$$d\epsilon_r^p = -d\lambda, \qquad d\epsilon_\theta^p = (1+\alpha)\gamma\, d\lambda, \qquad d\epsilon_\psi^p = (1+\alpha)(1-\gamma)\, d\lambda, \tag{18}$$

$\lambda$ being a non-negative function of $r$. In general $\gamma$ also depends upon $r$, but the second of the identities (3) requires in the present case that $\epsilon_\theta^p \equiv \epsilon_\psi^p$, and hence $\gamma = \frac{1}{2}$.

Adding to equations (18) the elastic strain increments obtained from equations (6), we get

$$\begin{aligned} d\epsilon_r &= E^{-1}[d\sigma_r - 2\nu\, d\sigma_\theta] - d\lambda, \\ d\epsilon_\theta &= E^{-1}[-\nu\, d\sigma_r + (1-\nu)\, d\sigma_\theta] + \tfrac{1}{2}(1+\alpha)\, d\lambda. \end{aligned} \tag{19}$$

These equations are exact. Eliminating $d\lambda$, we find

$$(1+\alpha)\, d\epsilon_r + 2 d\epsilon_\theta = E^{-1}[(1-2\nu+\alpha)\, d\sigma_r + 2(1-2\nu-\alpha\nu)\, d\sigma_\theta]. \tag{20}$$

The distributions of stress and strain in the soil at the commencement of plastic yielding are obtained from equations (6), (8), (9) by putting $p = p_1$. The integral of equation (20) subject to these initial conditions is

$$(1+\alpha)\epsilon_r + 2\epsilon_\theta = E^{-1}[(1-2\nu+\alpha)\sigma_r + 2(1-2\nu-\alpha\nu)\sigma_\theta + (3+\alpha)(1-2\nu)p_0]. \tag{21}$$

For all $a \leqslant r \leqslant b$ the plastic strain increments define a normal to the yield surface with the direction ratios $-2 : 1+\alpha : 1+\alpha$. As these ratios are independent of $r$ the effect of further deformation is to translate a given normal along the edge of the yield pyramid without rotation. The expression of the stress-strain relation of the plastic zone in total form is a direct consequence of this property.

As $r \to b$, $\epsilon_r^p$ and $\epsilon_\theta^p$ become vanishingly small and, from continuity considerations, the elastic strains are also small. In the inner part of the plastic zone, however, the total strains become large as $p$ increases and the stress-displacement relations (6) cease to be applicable. In order to use the stress-strain relation in its total form (21) some definition of finite strain must be adopted. The most satisfactory choice is the natural (or logarithmic) strain which, in the case of radial symmetry, leads to the expressions

$$\epsilon_r = \ln\left(\frac{dr}{dr_0}\right) = \frac{du}{dr} + \frac{1}{2}\left(\frac{du}{dr}\right)^2 + \ldots,$$

$$\epsilon_\theta = \ln\left(\frac{r}{r_0}\right) = \frac{u}{r} + \frac{1}{2}\left(\frac{u}{r}\right)^2 + \ldots. \tag{22}$$

Combining equations (13), (15), (22) with equation (21) there follows

$$\ln\left[\left(\frac{r}{r_0}\right)^{2(1+\alpha)} \frac{dr}{dr_0}\right] = \ln\beta - \omega\left(\frac{b}{r}\right)^{2\alpha/(1+\alpha)}, \tag{23}$$

where

$$\beta = \exp\left(\frac{(3+\alpha)(1-2\nu)(Y+\alpha p_0)}{\alpha(1+\alpha)E}\right), \qquad \omega = \frac{3\{(3+2\alpha)(1-2\nu)+\alpha^2\}(Y+\alpha p_0)}{\alpha(1+\alpha)(3+\alpha)E}.$$

Since the displacement is continuous at the interface $r = b$ the solution of equation (23) must satisfy the condition

$$r_{p_0} = b_0 = \left[1 - \frac{(1+\nu)(Y+\alpha p_0)}{(3+\alpha)E}\right] b \quad \text{when } r = b$$

(see equation (17)). By means of the transformation

$$\xi = \left(\frac{r_0}{b}\right)^{(3+\alpha)/(1+\alpha)}, \qquad \eta = \omega\left(\frac{b}{r}\right)^{2\alpha/(1+\alpha)},$$

the solution is found to be

$$\frac{2\alpha\beta}{3+\alpha}\omega^{-(3+\alpha)/2\alpha}\left[\left\{1 - \frac{(1+\nu)(Y+\alpha p_0)}{(3+\alpha)E}\right\}^{(3+\alpha)/(1+\alpha)} - \left(\frac{r_0}{b}\right)^{(3+\alpha)/(1+\alpha)}\right] = \int_{\omega}^{\omega(b/r)^{2\alpha/(1+\alpha)}} \eta^{-3(1+\alpha)/2\alpha} e^{\eta}\, d\eta. \tag{24}$$

Putting $r_0 = a_0$, $r = a$, and making use of equation (16),

$$\frac{2\alpha\beta}{3+\alpha}\left[\omega^{-(3+\alpha)/2\alpha}\left\{1 - \frac{(1+\nu)(Y+\alpha p_0)}{(3+\alpha)E}\right\}^{(3+\alpha)/(1+\alpha)} - \Omega^{-(3+\alpha)/2\alpha}\left(\frac{a_0}{a}\right)^{(3+\alpha)/(1+\alpha)}\right] = \int_{\omega}^{\Omega} \eta^{-3(1+\alpha)/2\alpha} e^{\eta}\, d\eta, \tag{25}$$

where

$$\Omega = \frac{\{(3+2\alpha)(1-2\nu)+\alpha^2\}(Y+\alpha p+\alpha p_0)}{\alpha(1+\alpha)^2 E}.$$

Equation (25) gives the value of the current cavity radius, $a_0$ being known. The value of $b$ follows from equation (16). The displacement $r-r_0$ at any radius in the plastic zone can then be determined from equation (24). In these calculations the definite integrals must be evaluated numerically.

If the maximum value of $p$ is sufficiently small for the squares and higher powers of $du/dr$ and $u/r$ to be negligible throughout the plastic zone the displacement can be expressed in the explicit form

$$u = \frac{(1-2\nu)(Y+\alpha p_0)}{\alpha E}r - \frac{3\{(3+2\alpha)(1-2\nu)+\alpha^2\}(Y+\alpha p_0)}{\alpha(9-\alpha^2)E}\left(\frac{b}{r}\right)^{2\alpha/(1+\alpha)}r + \\ + \frac{3(1-\nu)(Y+\alpha p_0)}{(3-\alpha)E}\left(\frac{b}{r}\right)^{2/(1+\alpha)}b.$$

When the displacement has been evaluated it is necessary to verify that $\lambda(r)$ is non-negative in the range $a \leqslant r \leqslant b$. This is the condition that an increase in the applied pressure $p$ shall, at no point in the plastic zone, result in the performance of a negative amount of plastic work. The differential relations (19) can be integrated subject to the conditions prevailing when $p = p_1$, and since $\lambda(r)$ is then identically zero the integral of the second relation is

$$\tfrac{1}{2}(1+\alpha)\lambda = \epsilon_\theta - \frac{(1-2\nu)(Y+\alpha p_0)}{\alpha E}\left[1 - \frac{3(1-2\nu-\alpha\nu)}{(3+\alpha)(1-2\nu)}\left(\frac{b}{r}\right)^{2\alpha/(1+\alpha)}\right]. \quad (26)$$

The value of $\epsilon_\theta$ at $r = b$ is given by the second of equations (12) and it follows that $\lambda(b) = 0$ as required. Differentiating equation (26) with respect to $r$,

$$\tfrac{1}{2}(1+\alpha)r\frac{d\lambda}{dr} = r\frac{d\epsilon_\theta}{dr} - \frac{6(1-2\nu-\alpha\nu)(Y+\alpha p_0)}{(1+\alpha)(3+\alpha)E}\left(\frac{b}{r}\right)^{2\alpha/(1+\alpha)}.$$

If $\alpha \leqslant (1-2\nu)/\nu$ then $d\lambda/dr < 0$ and $\lambda$ is non-negative in the plastic zone. If $\alpha > (1-2\nu)/\nu$ it must be verified by direct calculation from equation (26) that $\lambda(r) \geqslant 0$ for $a \leqslant r \leqslant b$.

## 5. Application of the theory of loading to metals

In the limit $\alpha \to 0$ the equations derived in the preceding sections describe the response of a Tresca (or Reuss) material, initially at uniform hydrostatic pressure $p_0$, to internal static loading at the face of a spherical cavity. The treatment of this special case is simplified by defining the constants

$$\delta = 2(1-2\nu)Y/E, \qquad \epsilon = \tfrac{1}{3}(1+\nu)Y/E. \quad (27)$$

For most metals these numbers are of order $10^{-3}$.

Plastic flow commences when the applied pressure reaches the value $\frac{2}{3}Y$, where $Y$ is the yield stress of the material in uniaxial compression or

tension. When $p$ exceeds this value the components of stress in the plastic zone $a \leqslant r \leqslant b$ are

$$\sigma_r = -p_0 - \tfrac{2}{3}Y + 2Y\ln(r/b), \qquad \sigma_\theta = -p_0 + \tfrac{1}{3}Y + 2Y\ln(r/b),$$

and the radii $a$, $b$ satisfy the relation

$$\frac{b}{a} = \exp\left(\frac{p}{2Y} - \frac{1}{3}\right). \tag{28}$$

Using the method of section 4 to evaluate the displacement in the plastic zone the differential equation corresponding to (23) is found to be

$$\ln\left[\left(\frac{r}{r_0}\right)^2 \frac{dr}{dr_0}\right] = 3\delta \ln\frac{r}{b}. \tag{29}$$

The continuity requirement on the displacement at the interface $r = b$ is, from equation (17),

$$r_0 = b_0 = (1-\epsilon)b \quad \text{when } r = b,$$

and the solution of equation (29) subject to this condition is

$$\left(\frac{r}{b}\right)^{3(1-\delta)} - 1 = (1-\delta)\left[\left(\frac{r_0}{b}\right)^3 - (1-\epsilon)^3\right]. \tag{30}$$

At the cavity wall, $r = a$ when $r_0 = a_0$ and, making use of equation (28),

$$\exp\left[(1-\delta)\left(1 - \frac{3p}{2Y}\right)\right] - 1 = (1-\delta)\left[\left(\frac{a_0}{a}\right)^3 \exp\left(1 - \frac{3p}{2Y}\right) - (1-\epsilon)^3\right]. \tag{31}$$

The quotient $a/a_0$ is easily determined from this equation as a function of $p$. The value of $b$ is then given by equation (28) and $r_0$ may finally be calculated from equation (30) when $r$ is specified.

It will be seen from (31) that $a/a_0$ is infinite at a finite pressure $p_\infty$ given by

$$p_\infty = \tfrac{2}{3}Y[1 - (1-\delta)^{-1}\ln\{1 - (1-\delta)(1-\epsilon)^3\}]. \tag{32}$$

This behaviour is properly understood in terms of the integral

$$W = \tfrac{4}{3}\pi \int_{p_1}^{p} p\, da^3,$$

which represents the total work done in raising the pressure on the cavity wall from $p_1$ to $p$. Substituting for $a^3$ from equation (31) it is not difficult to prove that $W \to \infty$ as $p \to p_\infty$. The limiting pressure $p_\infty$ is hence physically unattainable.

Values of $p_\infty/Y$ for various combinations of $Y/E$ and $\nu$ are contained in Table 1. These results indicate that neither metals nor soils can, in equilibrium, support internal pressures of more than a few times the compressive yield stress. They also show that $p_\infty$ varies only slightly as the value of Poisson's ratio changes. All the other calculations presented in

this paper refer to the expansion of a cavity in a medium of heavily cold-worked copper. It is assumed that no further work-hardening occurs. The appropriate constants, $Y/E = 2{\cdot}19 \times 10^{-3}$, $\nu = 0{\cdot}34$, are taken from a paper by Bishop, Hill, and Mott (**6**). The variation of $a/a_0$ with $p/Y$ for

TABLE 1

*The variation of $p_\infty/Y$ with $Y/E$ and $\nu$ ($\alpha = 0$)*

| $Y/E$ \ $\nu$ | 0·3 | 0·4 | 0·5 |
|---|---|---|---|
| $10^{-2}$ | 3·268 | 3·360 | 3·470 |
| $10^{-3}$ | 4·781 | 4·882 | 5·002 |
| $10^{-4}$ | 6·313 | 6·415 | 6·537 |
| $10^{-5}$ | 7·851 | 7·950 | 8·072 |

copper is given in the first two columns of Table 2 and represented graphically in Fig. 1. It is seen that $a/a_0$ increases extremely sharply as $p$ approaches the limiting value $p_\infty$. On repeating these calculations under the assumption of incompressibility (i.e. $\nu = \frac{1}{2}$) no substantial differences were found. The values of $a/a_0$ are somewhat smaller, as would be expected, and the limit $p_\infty/Y$ is raised to 4·480.

TABLE 2

*The variation of $a/a_0$ and $b/a$ with $p/Y$ for cold-worked copper*

| | $a/a_0$ | | |
|---|---|---|---|
| $p/Y$ | *Present solution* | *Hill's solution* | $b/a$ |
| $\frac{2}{3}$ | 1·0010 | 1·0010 | 1·000 |
| 1·0 | 1·0017 | 1·0017 | 1·181 |
| 1·5 | 1·0040 | 1·0040 | 1·517 |
| 2·0 | 1·0094 | 1·0095 | 1·948 |
| 2·5 | 1·0217 | 1·0218 | 2·501 |
| 3·0 | 1·0504 | 1·0506 | 3·211 |
| 3·5 | 1·1242 | 1·1250 | 4·123 |
| 4·0 | 1·3983 | 1·4036 | 5·294 |
| $p_\infty/Y$ | 4·301 | 4·296 | .. |

As mentioned in section 1, an alternative treatment of the expansion of a spherical cavity in a metallic medium has been given by Hill (**1**, pp. 103–4). An earlier analysis by Bishop, Hill, and Mott (**6**) neglects the compressibility of the material, but is then able to include the effects of work-hardening in an approximate way. The availability of these related investigations prompts the interesting question of the extent to which the behaviour of the medium depends upon the particular mathematical methods and physical approximations employed in the analysis. In the

remainder of this section the results of Hill *et al.* which bear upon this question are briefly recapitulated and somewhat extended.

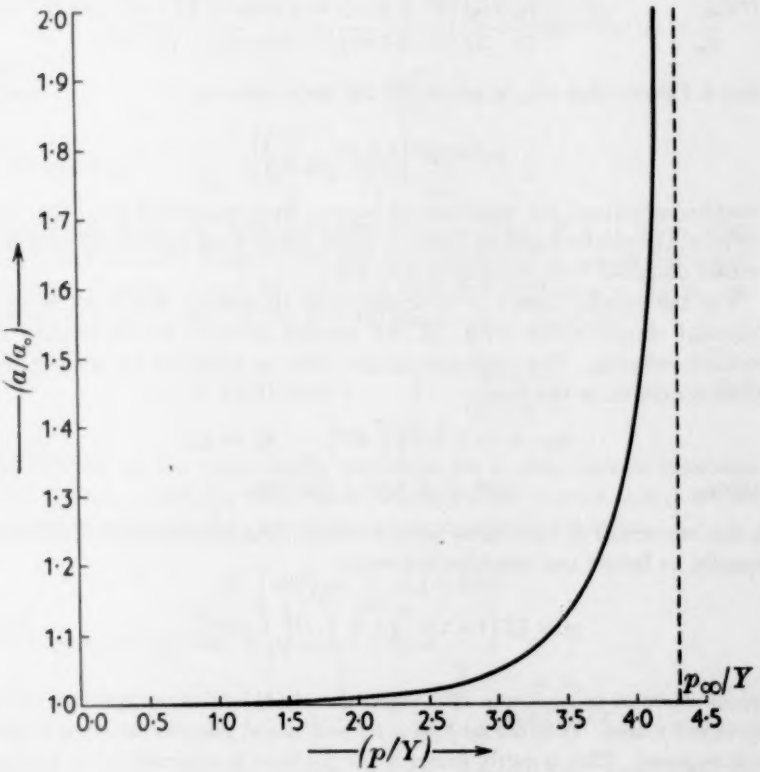


FIG. 1

The mathematical method of Hill differs from that used here in its treatment of the displacement in the plastic zone. Retaining the incremental form of the stress-strain relation and then evaluating each increment following the motion, by using the interface radius $b$ as a measure of the progress of the deformation, Hill arrives at the differential equation (in the present notation)

$$\frac{da}{db} = (\delta+3\epsilon)\left(\frac{b}{a}\right)^2 - \delta\left(\frac{a}{b}\right). \tag{33}$$

At the commencement of plastic-elastic deformation,

$$a = b = a_0(1-\epsilon)^{-1},$$

(from equations (9), (11)). The solution of equation (33) subject to this condition is

$$\frac{a}{a_0} = (1-\epsilon)^{-1}\exp\left(\frac{1}{3}-\frac{p}{2Y}\right)\left[\frac{1-3\epsilon}{(1+\delta)\exp\{1-(3p/2Y)\}-(\delta+3\epsilon)}\right]^{\frac{1}{3}(1+\delta)^{-1}}, \tag{34}$$

and it follows that $a/a_0$ is infinite at the finite pressure

$$p_\infty = \tfrac{2}{3}Y\left[1+\ln\left(\frac{1+\delta}{\delta+3\epsilon}\right)\right]. \tag{35}$$

Results calculated for cold-worked copper from equations (34), (35) are given in the final column of Table 2. They are in good agreement with the values obtained from equations (31), (32).

For the special case $\alpha = 0$, appropriate to metals, the most serious physical simplification made in the present analysis is the neglect of strain-hardening. The inclusion of this effect is achieved by writing the yield condition in the form

$$\sigma_\theta - \sigma_r = Y + H\Big(\int d\bar{\epsilon}^p\Big), \qquad \sigma_\theta = \sigma_\psi,$$

where

$$d\bar{\epsilon}^p = [\tfrac{2}{3}(d\epsilon_r^p)^2 + \tfrac{4}{3}(d\epsilon_\theta^p)^2]^{\frac{1}{2}}$$

is the increment of equivalent plastic strain. The stress analysis proceeds exactly as before and provides the result

$$p = \tfrac{2}{3}Y\left(1+3\ln\frac{b}{a}\right) + 2\int_a^b H\Big(\int d\bar{\epsilon}^p\Big)\frac{dr}{r}, \tag{36}$$

which reduces to equation (28) when the work-hardening function $H$ is identically zero. In order to find $a$ an additional relation between $b$ and $a$ is required. This is easily found if the medium is assumed to be incompressible. The condition of mass conservation then takes the form

$$r^3 - r_0^3 = a^3 - a_0^3 = b^3 - b_0^3 = \tau b^3, \tag{37}$$

where

$$\tau = 1-\left(1-\frac{Y}{2E}\right)^3 = 1-(1-\epsilon)^3,$$

the last equality following from equation (17) with $\alpha = 0$, $\nu = \frac{1}{2}$. As stated above, the neglect of compressibility does not by itself produce wide deviations from the exact solution. By means of the result

$$\int d\bar{\epsilon}^p = 2|\epsilon_\theta|,$$

which may readily be shown to follow from the assumption that the plastic strain components are much larger than the corresponding elastic strains,

equations (36), (37) can be combined in the form

$$p = \tfrac{2}{3}Y(1+\ln\mu-\ln\tau)+\tfrac{2}{3}\int_{\tau}^{\mu} H\left[\tfrac{2}{3}\ln\left(\frac{1}{1-\xi}\right)\right]\frac{d\xi}{\xi}, \tag{38}$$

where $$\mu = 1-\left(\frac{a_0}{a}\right)^3.$$

It follows that $$\frac{d\mu}{dp} = \tfrac{3}{2}\mu\left[Y+H\left(2\ln\frac{a}{a_0}\right)\right]^{-1} > 0,$$

whence $a/a_0$ increases monotonically with $p$. Thus if $p$ is finite when $\mu = 1$ the behaviour illustrated in Fig. 1 is reproduced in a work-hardening medium. Putting $\mu = 1$ in equation (38) and replacing $p$ by $p_\infty$, an obvious transformation of the integral leads to the equation

$$p_\infty = \tfrac{2}{3}Y(1-\ln\tau)+\int_{-2\ln(1-\epsilon)}^{\infty}\frac{H(\eta)\,d\eta}{\exp(\frac{2}{3}\eta)-1}. \tag{39}$$

The integral on the right clearly converges for a wide class of functions $H(\eta)$. In actual fact the work-hardening properties of most metals can be accurately represented by a polynomial expression of the type

$$H\Big(\int d\bar{\epsilon}^p\Big) = \sum_{n=1}^{N} H_n\Big(\int d\bar{\epsilon}^p\Big)^n.$$

The corresponding form of equation (39) is

$$p_\infty = \tfrac{2}{3}Y(1-\ln\tau)+\sum_{n=1}^{N} H_n\int_{-2\ln(1-\epsilon)}^{\infty}\frac{\eta^n\,d\eta}{\exp(\frac{2}{3}\eta)-1},$$

and since $\tau \ll 1$, the lower limit of each integral can, with sufficient accuracy, be replaced by zero. It then follows (see (7), pp. 265–6) that

$$p_\infty = \tfrac{2}{3}Y(1-\ln\tau)+\sum_{n=1}^{N}(\tfrac{2}{3})^{n+1}n!\,\zeta(n+1), \tag{40}$$

$\zeta$ being the Riemann zeta function. In the case of linear work-hardening, $N = 1$ and since $\zeta(2) = \frac{1}{6}\pi^2$,

$$p_\infty = \tfrac{2}{3}Y(1-\ln\tau)+\tfrac{2}{27}\pi^2 H_1,$$

a result due to Bishop, Hill, and Mott (6). From these results it can safely be concluded that non-hardening and work-hardening media respond in qualitatively the same way to pressure applied in an internal cavity.

## 6. Unloading

Returning to the case of an ideal soil and assuming that the pressure in the cavity has been raised monotonically to the value $p$ ($< p_\infty$), consider now the effect on the components of stress and displacement of a monotonic unloading to the pressure $(1-x)p$ $(0 \leqslant x \leqslant 1)$. The configuration of the system on the completion of loading is used as a reference state from which the variables of the unloading process are measured. Deviations from this state are denoted by a single prime and absolute quantities in a partially unloaded state by a double prime. Thus

$$\sigma_r'' = \sigma_r + \sigma_r', \qquad \sigma_\theta'' = \sigma_\theta + \sigma_\theta', \qquad u'' = u + u'. \tag{41}$$

Consistency with the notation used in previous sections is achieved by using unprimed symbols to describe the reference state.

The work expended on plastic deformation during the enlargement of the cavity is not recoverable on unloading. Thus when the pressure is reduced from its peak value $p$ the medium unloads elastically and

$$\sigma_r' = xp\left(\frac{a''}{r''}\right)^3, \qquad \sigma_\theta' = -\tfrac{1}{2}xp\left(\frac{a''}{r''}\right)^3,$$

$$u' = r - r'' = \tfrac{1}{2}xp\,\frac{1+\nu}{E}\left(\frac{a''}{r''}\right)^3 r'', \tag{42}$$

these quantities being the elastic components of stress and displacement produced by the application of an additional pressure $-xp$ at the cavity wall $r'' = a''$. Had no plastic deformation occurred during loading (i.e. if $p \leqslant p_1$), the residual stresses and displacement would be obtained by adding these expressions to equations (8), (9). When completely unloaded (i.e. when $x = 1$) the system would then have reverted to its initial state. If $p \geqslant p_1$, however, the residual stresses are, in the plastic zone $a'' \leqslant r'' \leqslant b''$,

$$\sigma_r'' = \frac{Y}{\alpha} - \frac{3(1+\alpha)(Y+\alpha p_0)}{\alpha(3+\alpha)}\left(\frac{b}{r}\right)^{2\alpha/(1+\alpha)} + xp\left(\frac{a''}{r''}\right)^3,$$

$$\sigma_\theta'' = \frac{Y}{\alpha} - \frac{3(Y+\alpha p_0)}{\alpha(3+\alpha)}\left(\frac{b}{r}\right)^{2\alpha/(1+\alpha)} - \tfrac{1}{2}xp\left(\frac{a''}{r''}\right)^3, \tag{43}$$

and, in the elastic region $r'' \geqslant b''$,

$$\sigma_r'' = -p_0 - \frac{2(Y+\alpha p_0)}{3+\alpha}\left(\frac{b}{r}\right)^3 + xp\left(\frac{a''}{r''}\right)^3,$$

$$\sigma_\theta'' = -p_0 + \frac{Y+\alpha p_0}{3+\alpha}\left(\frac{b}{r}\right)^3 - \tfrac{1}{2}xp\left(\frac{a''}{r''}\right)^3. \tag{44}$$

As $x$ increases $\sigma_r''$ increases and $\sigma''$ decreases. Thus $(1+\alpha)\sigma_\theta'' - \sigma_r'' < Y$

throughout the soil, but if $p$ is sufficiently large $\sigma_r''$ may eventually exceed $\sigma_\theta''$. It is then necessary to examine the possibility that the yield condition

$$(1+\alpha)\sigma_r''-\sigma_\theta'' = Y \tag{45}$$

is satisfied at some level in the soil before the completion of unloading. Expressing equations (43) in terms of $r''$ and $a''$ by means of equations (16) and (42), there follows

$$(1+\alpha)\sigma_r''-\sigma_\theta'' = Y+\left(\frac{a''}{r''}\right)^3\left[\left[\tfrac{1}{2}xp(3+2\alpha)-\frac{2+\alpha}{1+\alpha}(Y+\alpha p+\alpha p_0)\left(\frac{r''}{a''}\right)^{(3+\alpha)(1+\alpha)}\times\right.\right.$$
$$\left.\left.\times\left[\left(1+\tfrac{1}{2}xp\frac{1+\nu}{E}\right)\left\{1+\tfrac{1}{2}xp\frac{1+\nu}{E}\left(\frac{a''}{r''}\right)^3\right\}^{-1}\right]^{2\alpha/(1+\alpha)}\right]\right]$$

for $a'' \leqslant r'' \leqslant b''$. As the expression on the right is a decreasing function of $r''$, yielding recommences at the cavity wall when $x$ reaches the value

$$x_2 = \frac{2(2+\alpha)(Y+\alpha p+\alpha p_0)}{(1+\alpha)(3+2\alpha)p}. \tag{46}$$

It can easily be verified, by means of equations (44) together with (16) and (42), that the yield criterion (45) cannot be satisfied at any level in the elastic region when $x \leqslant x_2$. If $p > p_2$, where

$$p_2 = \frac{2(2+\alpha)(Y+\alpha p_0)}{3+\alpha}, \tag{47}$$

then $0 < x_2 < 1$, and a secondary plastic zone must be formed round the cavity during the course of unloading. If $p_1 \leqslant p \leqslant p_2$, then the medium can be completely unloaded without the occurrence of further plastic flow. For values of $p$ within this range the residual stresses are given by equations (43), (44) for $0 \leqslant x \leqslant 1$, and the residual displacement $r''-r_0$ is found by combining equations (24), (25), and (17) with (42).

Consider now the situation when $p > p_2$ and $x > x_2$. Let $c''$ be the outer radius of the secondary plastic zone and assume, for the present, that $c'' < b''$. In the range $a'' \leqslant r'' \leqslant c''$ the residual stress components $\sigma_r''$, $\sigma_\theta''$ satisfy the equilibrium equation (7) and the yield criterion (45). The general solution of these equations is

$$\sigma_r'' = \frac{Y}{\alpha}+A''r''^{2\alpha}, \qquad \sigma_\theta'' = \frac{Y}{\alpha}+A''(1+\alpha)r''^{2\alpha}. \tag{48}$$

Since the remainder of the soil has unloaded elastically,

$$\sigma_r' = B''r''^{-3}, \qquad \sigma_\theta' = -\tfrac{1}{2}B''r''^{-3} \tag{49}$$

for $r'' \geqslant c''$. The conditions of equilibrium and incipient yielding at $r'' = c''$ imply that $\sigma_r''$ and $\sigma_\theta''$ are continuous across this interface. These conditions

determine the two disposable constants $A''$, $B''$ in the form

$$A'' = -\frac{3(Y+\alpha p_0)}{\alpha(3+2\alpha)}\left(\frac{b}{c}\right)^{2\alpha/(1+\alpha)} c''^{-2\alpha}, \qquad B'' = \frac{6(2+\alpha)(Y+\alpha p_0)}{(3+\alpha)(3+2\alpha)}\left(\frac{b}{c}\right)^{2\alpha/(1+\alpha)} c''^{3}. \tag{50}$$

The condition at the cavity wall,

$$\sigma_r''(a'') = -p_0-(1-x)p, \tag{51}$$

provides the additional relation

$$\left(\frac{a''}{c''}\right)^{2\alpha}\left(\frac{a}{c}\right)^{2\alpha/(1+\alpha)} = \frac{(1+\alpha)(3+2\alpha)\{Y+\alpha p(1-x)+\alpha p_0\}}{(3+\alpha)(Y+\alpha p+\alpha p_0)}. \tag{52}$$

The unloading displacement in the region $r'' \geqslant c''$ is

$$u' = -\frac{B''(1+\nu)}{2Er''^2} = -\frac{3(2+\alpha)(1+\nu)(Y+\alpha p_0)}{(3+\alpha)(3+2\alpha)E}\left(\frac{b}{c}\right)^{2\alpha/(1+\alpha)}\left(\frac{c''}{r''}\right)^{3} r'', \tag{53}$$

and, in particular,

$$c = c''-u'(c'') = c''\left[1+\frac{3(2+\alpha)(1+\nu)(Y+\alpha p_0)}{(3+\alpha)(3+2\alpha)E}\left(\frac{b}{c}\right)^{2\alpha/(1+\alpha)}\right]. \tag{54}$$

The right-hand side of equation (52) is less than unity if and only if $x > x_2$ and since $x$ is known to satisfy this inequality,

$$\left(\frac{a''}{c''}\right)^{2\alpha}\left(\frac{a}{c}\right)^{2\alpha/(1+\alpha)} < 1.$$

As $a'' < c''$ if and only if $a < c$, it follows that $a'' < c''$. Due to the occurrence of secondary flow at the cavity wall the value of $u'(a'') = a-a''$ exceeds the elastic unloading displacement at $r'' = a''$ which would be given by equation (53). Hence $a/c > a''/c''$ and, using equations (16), (52),

$$\left(\frac{a}{c}\right)^{2\alpha}\left(\frac{b}{c}\right)^{2\alpha/(1+\alpha)} > \left(\frac{a''}{c''}\right)^{2\alpha}\left(\frac{b}{c}\right)^{2\alpha/(1+\alpha)} = \frac{(3+2\alpha)\{Y+\alpha p(1-x)+\alpha p_0\}}{3(Y+\alpha p_0)} \geqslant 1.$$

Hence $b > c$ and $a'' < c'' < b''$. These inequalities confirm that a self-consistent solution for the stresses follows from the assumption that $c'' < b''$ made earlier.

There remains the evaluation of the displacement in the secondary plastic zone. The plastic potential associated with the yield condition (45),

$$f'' = \gamma''[(1+\alpha)\sigma_r''-\sigma_\theta'']+(1-\gamma'')[(1+\alpha)\sigma_r''-\sigma_\psi''],$$

generates the plastic strain increments

$$d\epsilon_r''^{p} = (1+\alpha)\,d\lambda'', \qquad d\epsilon_\theta''^{p} = -\gamma''\,d\lambda'', \qquad d\epsilon_\psi''^{p} = -(1-\gamma'')\,d\lambda''.$$

Applying the symmetry requirement that $\gamma'' = \frac{1}{2}$ and adding the elastic strain increments,

$$\begin{aligned} d\epsilon_r'' &= E^{-1}[d\sigma_r''-2\nu\,d\sigma_\theta'']+(1+\alpha)\,d\lambda'', \\ d\epsilon_\theta'' &= E^{-1}[-\nu\,d\sigma_r''+(1-\nu)\,d\sigma_\theta'']-\tfrac{1}{2}\,d\lambda''. \end{aligned} \tag{55}$$

Eliminating $d\lambda''$,

$$d\epsilon_r''+2(1+\alpha)\,d\epsilon_\theta''=E^{-1}[\{1-2\nu(1+\alpha)\}d\sigma_r''+2\{(1-2\nu)+\alpha(1-\nu)\}d\sigma_\theta''].\tag{56}$$

The differential relations (55), (56) are exact and can be integrated subject to the conditions attending the commencement of secondary plastic flow. The latter are obtained from equations (42), (43) by setting $x=x_2$ and the total stress-strain relation is found to be

$$\epsilon_r'+2(1+\alpha)\epsilon_\theta'=\frac{1}{E}\Bigg[\{1-2\nu(1+\alpha)\}\sigma_r''+2\{(1-2\nu)+\alpha(1-\nu)\}\sigma_\theta''-$$

$$-\frac{(3+2\alpha)(1-2\nu)Y}{\alpha}+\frac{3\{3(1+\alpha)(1-2\nu)-2\alpha^2\nu\}(Y+\alpha p_0)}{\alpha(3+\alpha)}\left(\frac{b}{r}\right)^{2\alpha/(1+\alpha)}\Bigg].\tag{57}$$

The logarithmic strain components measured from the fully loaded state are

$$\epsilon_r'=\ln\left(\frac{dr''}{dr}\right),\qquad \epsilon_\theta'=\ln\left(\frac{r''}{r}\right).\tag{58}$$

Entering these expressions into equation (57) and substituting for $\sigma_r''$, $\sigma_\theta''$ from equations (48), (50) there follows the differential equation

$$\ln\left[\left(\frac{r''}{r}\right)^{2(1+\alpha)}\frac{dr''}{dr}\right]=-\frac{3\{(3+4\alpha)(1-2\nu)+2\alpha^2(1-\nu)\}(Y+\alpha p_0)}{\alpha(3+2\alpha)E}\left(\frac{b}{c}\right)^{2\alpha/(1+\alpha)}\left(\frac{r''}{c''}\right)^{2\alpha}+$$

$$+\frac{3\{3(1+\alpha)(1-2\nu)-2\alpha^2\nu\}(Y+\alpha p_0)}{\alpha(3+\alpha)E}\left(\frac{b}{r}\right)^{2\alpha/(1+\alpha)}.\tag{59}$$

This is to be integrated under the boundary condition, $r''=c''$ when $r=c$; $c$, $c''$ being connected by equation (54). By means of the transformation

$$x=\kappa\left(\frac{c}{r}\right)^{2\alpha/(1+\alpha)},\qquad y=\chi\left(\frac{r''}{c''}\right)^{2\alpha},$$

where

$$\kappa=\frac{3\{3(1+\alpha)(1-2\nu)-2\alpha^2\nu\}(Y+\alpha p_0)}{\alpha(3+\alpha)E}\left(\frac{b}{c}\right)^{2\alpha/(1+\alpha)},$$

$$\chi=\frac{3\{(3+4\alpha)(1-2\nu)+2\alpha^2(1-\nu)\}(Y+\alpha p_0)}{\alpha(3+2\alpha)E}\left(\frac{b}{c}\right)^{2\alpha/(1+\alpha)},$$

the solution is obtained in the form

$$(1+\alpha)\int_{\kappa}^{\kappa(c/r)^{2\alpha/(1+\alpha)}}\xi^{-(3+\alpha)(1+2\alpha)/2\alpha}e^{\xi}\,d\xi+$$

$$+\left(\frac{c''}{c}\right)^{3+2\alpha}\kappa^{-(1+\alpha)(3+2\alpha)/2\alpha}\chi^{-(3+2\alpha)/2\alpha}\int_{\chi}^{\chi(r''/c'')^{2\alpha}}\xi^{3/2\alpha}e^{\xi}\,d\xi=0.\tag{60}$$

Putting $r=a$, $r''=a''$ and making use of equations (16), (52), and (54) an equation for $b/c$ is obtained. Since the value of $b$ is known from the

loading solution this equation specifies $c$, and $c''$ follows from equation (54) so that $r''$ can then be determined as a function of $r$ from equation (60).

After evaluating the displacement it must be verified that $\lambda''$ is non-negative in the range $a'' \leqslant r'' \leqslant c''$. The second of the differential relations (55) has the integral

$$\tfrac{1}{2}\lambda'' = -\epsilon'_\theta + \frac{3(Y+\alpha p_0)}{\alpha E} \times \times \left[\frac{1-2\nu-\alpha\nu}{3+\alpha}\left(\frac{b}{r}\right)^{2\alpha/(1+\alpha)} - \frac{(1-2\nu)+\alpha(1-\nu)}{3+2\alpha}\left(\frac{b}{c}\right)^{2\alpha/(1+\alpha)}\left(\frac{r''}{c''}\right)^{2\alpha}\right]. \quad (61)$$

Since the tangential strain component at $r'' = c''$ is $u'(c'')/c''$ it follows from equation (53) that $\lambda''(c'') = 0$. Differentiating equation (61) with respect to $r''$, we obtain

$$\tfrac{1}{2}r''\frac{d\lambda''}{dr''} = -r''\frac{d\epsilon'_\theta}{dr''} - \frac{6(Y+\alpha p_0)}{E} \times \times \left[\frac{1-2\nu-\alpha\nu}{(1+\alpha)(3+\alpha)}\left(\frac{b}{r}\right)^{2\alpha/(1+\alpha)}\frac{r''}{r}\frac{dr}{dr''} + \frac{(1-2\nu)+\alpha(1-\nu)}{3+2\alpha}\left(\frac{b}{c}\right)^{2\alpha/(1+\alpha)}\left(\frac{r''}{c''}\right)^{2\alpha}\right].$$

Since $-\epsilon'_\theta$ is a decreasing function of $r''$, the condition $\alpha \leqslant (1-2\nu)/\nu$ is sufficient for $\lambda''$ to be non-negative in the secondary plastic zone. If $\alpha > (1-2\nu)/\nu$ the necessary verification must be carried out numerically by means of equation (61).

## 7. Application of the theory of unloading to metals

For the case of a metal (i.e. when $\alpha = 0$), plastic flow occurs during unloading when $x > 4Y/3p$. The stress components in the secondary plastic zone $a'' \leqslant r'' \leqslant b''$ are then

$$\sigma''_r = -p_0 + \tfrac{2}{3}Y - 2Y\ln\left(\frac{br''}{cc''}\right), \qquad \sigma''_\theta = -p_0 - \tfrac{1}{3}Y - 2Y\ln\left(\frac{br''}{cc''}\right),$$

where $a''$, $c''$ satisfy the relation

$$\frac{aa''}{cc''} = \exp\left(\frac{2}{3} - \frac{xp}{2Y}\right). \quad (62)$$

The method used in section 6 to evaluate the displacement in the secondary plastic zone leads in this case to the differential equation

$$\ln\left[\left(\frac{r''}{r}\right)^2\frac{dr''}{dr}\right] = -3\delta\ln\left(\frac{rr''}{cc''}\right), \quad (63)$$

use being made in this section of the definitions (27).

The solution which satisfies the condition $r'' = c''$ when $r = c$, is

$$(1-\delta)\left(\frac{c''}{c}\right)^3\left[\left(\frac{r''}{c''}\right)^{3(1+\delta)} - 1\right] = (1+\delta)\left[\left(\frac{r}{c}\right)^{3(1-\delta)} - 1\right], \quad (64)$$

where, from equation (54),

$$\frac{c}{c''} = 1+2\epsilon. \tag{65}$$

Putting $r'' = a'', r = a$ in (64) and making use of equations (62), (65), there follows

$$\exp\left[(1+\delta)\left(2-\frac{3xp}{2Y}\right)\right]\left(\frac{c}{a}\right)^{3(1+\delta)} - 1 = (1+2\epsilon)^3\frac{1+\delta}{1-\delta}\left[\left(\frac{a}{c}\right)^{3(1-\delta)} - 1\right]. \tag{66}$$

Having determined $c$ from this result, $a$ being known from the loading solution, the values of $c''$ and $a''$ follow from equations (62) and (65). $r''$ can then be evaluated from equation (64) when $r$ is specified. The displacement in the region $r'' \geqslant c''$ is obtained from equation (53) with

TABLE 3

*The variation of $a''/a$ and $c''/a''$ with $p/Y$ for cold-worked copper after complete unloading*

| $p/Y$ | $a''/a$ | $c''/a''$ |
|---|---|---|
| $\frac{4}{3}$ | 0·9980 | 1·000 |
| 1·5 | 0·9978 | 1·043 |
| 2·0 | 0·9966 | 1·182 |
| 2·5 | 0·9948 | 1·341 |
| 3·0 | 0·9920 | 1·521 |
| 3·5 | 0·9879 | 1·728 |
| 4·0 | 0·9817 | 1·964 |

TABLE 4

*The variation of $r/r_0$ with $r/a$ in cold-worked copper after loading to $p/Y = 4$ and the corresponding values of $r''/r_0$ and $r''/a''$ after complete unloading*

| *After loading* | | | *After complete unloading* | | |
|---|---|---|---|---|---|
| *Description of material* | $r/a$ | $r/r_0$ | $r''/a''$ | $r''/r_0$ | *Description of material* |
| Cavity wall $r = a$ | 1·00 | 1·3983 | 1·00 | 1·3727 | Cavity wall $r'' = a''$ |
| Plastic | 1·25 | 1·1381 | 1·25 | 1·1333 | Secondary plastic |
| ,, | 1·50 | 1·0700 | 1·50 | 1·0684 | ,, ,, |
| ,, | 1·75 | 1·0411 | 1·75 | 1·0404 | ,, ,, |
| | | | 1·964 | 1·0275 | Interface $r'' = c''$ |
| ,, | 2·0 | 1·0263 | 2·0 | 1·0259 | Plastic |
| ,, | 3·0 | 1·0068 | 3·0 | 1·0066 | ,, |
| ,, | 4·0 | 1·0025 | 4·0 | 1·0024 | ,, |
| ,, | 5·0 | 1·0012 | 5·0 | 1·0011 | ,, |
| Interface $r = b$ | 5·294 | 1·00098 | 5·393 | 1·00088 | Interface $r'' = b''$ |
| Elastic | 6·0 | 1·00067 | 6·0 | 1·00064 | Elastic |
| ,, | 7·0 | 1·00042 | 7·0 | 1·00040 | ,, |
| ,, | 8·0 | 1·00028 | 8·0 | 1·00027 | ,, |
| ,, | 9·0 | 1·00020 | 9·0 | 1·00019 | ,, |
| ,, | 10·0 | 1·00015 | 10·0 | 1·00014 | ,, |

$\alpha = 0$. When $r''$ is known as a function of $r$ throughout the medium appeal to the loading solution gives the residual displacement in terms of $r_0$.

Some further calculations for a medium of heavily cold-worked copper with the properties listed in section 5 are presented in Tables 3 and 4. Table 3 gives values of $a''/a$ and $c''/a''$ after complete unloading from a number of peak pressures in the range $\frac{4}{3}Y \leqslant p \leqslant 4Y$. These results

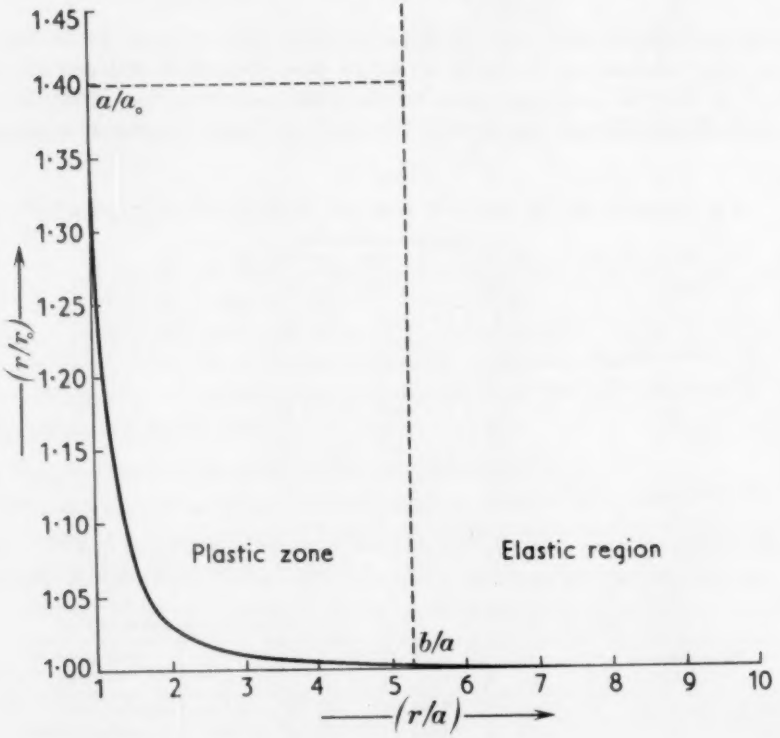


FIG. 2

demonstrate the very small extent to which the cavity radius is reduced when the pressure is returned to its initial value. Table 4 contains values of $r/r_0$ at distances between 1 and 10 cavity radii after loading to a peak pressure of $4Y$ together with the corresponding values of $r''/r_0$ after complete unloading. The distribution of $r/r_0$ on the completion of loading is shown graphically in Fig. 2. The displacement is seen to decrease extremely rapidly near the cavity wall and this implies that finite strains are produced only within the innermost half of the plastic zone.

**Acknowledgements**

I am grateful to Mr. D. R. Bland, Dr. R. E. Gibson, and Mr. H. G. Hopkins for helpful discussions and to the Director of the Atomic Weapons Research Establishment for permission to publish this paper.

## REFERENCES

1. R. Hill, *Mathematical Theory of Plasticity* (Oxford, 1950).
2. R. T. Shield, *J. Mech. Phys. Solids*, **4** (1955) 10–16.
3. D. C. Drucker, R. E. Gibson, and D. J. Henkel, *Proc. Amer. Soc. Civil Eng.* **81** (1955), paper No. 798.
4. G. G. Meyerhof, *Géotechnique*, **2** (1951) 301–32.
5. A. W. Skempton, A. A. Yassin, and R. E. Gibson, *J. de Méchanique des sols* (1953).
6. R. F. Bishop, R. Hill, and N. F. Mott, *Proc. Phys. Soc.* **57** (1945) 147–59.
7. E. T. Whittaker and G. N. Watson, *Modern Analysis*, 4th edn. (Cambridge, 1927).

# SOME MIXED BOUNDARY-VALUE PROBLEMS OF AEOLOTROPIC THIN PLATE THEORY

*By* G. M. L. GLADWELL

(*Department of Math., University College, London*)

[Received 10 October 1957]

SUMMARY

This paper applies the theory of sectionally holomorphic functions, developed by N. I. Muskhelishvili and others, to some mixed boundary-value problems of aeolotropic thin plate theory. The mixed boundary conditions are derived from plates having boundaries which are partly clamped, and partly free or subjected to specified bending moment and shear. Each problem is reduced to the solution of a series of equations relating the boundary values of sectionally holomorphic functions on opposite sides of one or more arcs; these are problems solved in (**2**). Details of the solution are given for the problem of a plate in the form of the upper half-plane, subjected to constant bending moment and shear on a segment of the real axis, and clamped along the remainder.

## 1. Introduction

In a previous paper (**1**) the author considered some mixed boundary-value problems in isotropic thin plate theory; in this paper some of the corresponding problems are studied for aeolotropic plates. It is shown that the mixed boundary-value problems may be reduced to the solution of two non-homogeneous Hilbert problems ((**2**), part IV) whose general solutions are known, and that in this case the solutions of special problems may be also simplified by using contour integration. In the greater part of this paper the plates are considered to have the most general type of digonal symmetry (i.e. elastic symmetry about the midplane of the plate) but even so the complex variable analysis leads to a solution reasonable free from burdensome algebra.

The plates considered occupy one of the following regions:

(i) the upper half plane;

(ii) the infinite region bounded internally by a circle;

(iii) the infinite region bounded internally by an ellipse.

(Note that the boundary-value problem for an aeolotropic circular disk is similar to the problem of an isotropic elliptic disk, and cannot be dealt with by the present method.) The plates are clamped along a part $L_1$ of their boundary $L$ and are free, or have specified bending moment and shear, on $L_2$, the remainder of $L$. There are two main types of mixed boundary-value problems, namely,

(*a*) $L_2$ free and the plate subjected to an isolated normal load at an interior point;

(*b*) $L_2$ subjected to specified bending moment and shear.

## 2. Fundamental equations

Consider first the case when the material has the most general type of digonal elastic symmetry, the stress-strain relations containing thirteen elastic constants ((**3**), 158). Referred to rectangular cartesian axes $O(x, y, Z)$ with the origin in the mid-plane of the plate (bounded by $Z = \pm h$), the transverse displacement $w$ of the mid-plane satisfies the fourth order differential equation

$$a_3\frac{\partial^4 w}{\partial z^4}+2a_2\frac{\partial^4 w}{\partial z^3\partial\bar{z}}+(2a_1+a_4)\frac{\partial^4 w}{\partial z^2\partial\bar{z}^2}+2\bar{a}_2\frac{\partial^4 w}{\partial z\partial\bar{z}^3}+\bar{a}_3\frac{\partial^4 w}{\partial\bar{z}^4}=-\frac{3p}{32h^3}, \quad (2.1)$$

where $a_1$ and $a_4$ are real constants, $a_2$ and $a_3$ are complex constants, $z = x+iy$, and $p$ is obtained from the boundary conditions over the faces of the plate, viz.

$$\widehat{xz} = 0 = \widehat{yz} = \widehat{zz} \text{ over } Z = -h, \qquad \widehat{xz} = 0 = \widehat{yz},\ \widehat{zz} = -p \text{ over } Z = h. \quad (2.2)$$

Equation (2.1) is given in a different notation by Green and Zerna (**3**): it may be noted that when the plate is orthotropic the constants $a_2$ and $a_3$ are real. If the equation

$$a_3+2a_2\gamma+(2a_1+a_4)\gamma^2+2\bar{a}_2\gamma^3+\bar{a}_3\gamma^4=0 \quad (2.3)$$

has distinct roots $\gamma_1$, $\gamma_2$ satisfying $|\gamma_1| < 1$, $|\gamma_2| < 1$, then the general solution of (2.1) is

$$w = w_0+\Omega_1(z_1)+\overline{\Omega_1(z_1)}+\Omega_2(z_2)+\overline{\Omega_2(z_2)}, \quad (2.4)$$

where $z_j = z+\gamma_j\bar{z}$ $(j = 1, 2)$, $\Omega_j(z_j)$ is an analytic function of $z_j$ in the region of the $z_j$-plane which corresponds to the region of the $z$-plane occupied by elastic material, and $w_0$ is a particular solution of (2.1). If (2.3) has a repeated root $\gamma$ satisfying $0 < |\gamma| < 1$, then the general solution of (2.1) is

$$w = w_0+\bar{z}_1\Omega(z_1)+z_1\overline{\Omega(z_1)}+\omega(z_1)+\overline{\omega(z_1)} \quad (2.5)$$

where $z_1 = z+\gamma\bar{z}$ and $\Omega(z_1)$, $\omega(z_1)$ are analytic functions of $z_1$. It may be shown (Gladwell (**4**)) that, in all the problems treated for the general type of aeolotropy, the solution of the problem for this special type may be obtained by a simple modification of the method used in the isotropic case.

## 3. Boundary conditions

The boundary conditions along $L_1$, the clamped part of the boundary, are

$$w = 0 = \partial w/\partial n \quad \text{on } L_1, \quad (3.1)$$

which may be written

$$w = 0 = \partial w/\partial z \quad \text{on } L_1. \tag{3.2}$$

Using the notation of Stevenson (**5**), the boundary conditions on $L_2$ are

$$\tilde{n}s = M, \qquad \tilde{n}z - \partial\tilde{n}\tilde{n}/\partial s = S \quad \text{on } L_2, \tag{3.3}$$

where $M \equiv 0 \equiv S$ when $L_2$ is free.

Equation (2.4) allows the boundary conditions (3.2) to be written in terms of the complex potentials; it is desired to transform (3.3) in the same way. If $F$ and $K$ are respectively the resultant shearing force along an arc of $L$ and the complex moment about the origin of the stresses along that arc, both measured as per unit thickness of the plate, then it is shown in (**1**) that (3.3) is equivalent to

$$\mathrm{re}\,\frac{d}{dz}(K+izF) = \tilde{n}s = M \quad \text{on } L_2, \tag{3.4}$$

$$\mathrm{im}\,\frac{\partial}{\partial s}\frac{d}{dz}(K+izF) = \tilde{n}z - \frac{\partial\tilde{n}\tilde{n}}{\partial s} = S \quad \text{on } L_2. \tag{3.5}$$

These equations show that specification of bending moment and shear along an arc enables the determination there of $K+izF$ apart from an arbitrary combination of the form $iCz+\epsilon$, where $C$ is a real constant and $\epsilon$ is an imaginary constant. In particular the boundary condition for a free boundary may be written

$$K+izF = iCz+\epsilon \quad \text{on } L_2. \tag{3.6}$$

It may easily be shown ((**4**) cf. (**3**), 252) that

$$K+izF = \frac{8h^2}{3}\{\lambda_1\Omega_1'(z_1)+\mu_1\overline{\Omega_1'(z_1)}+\lambda_2\Omega_2'(z_2)+\mu_2\overline{\Omega_2'(z_2)}\}, \tag{3.7}$$

where

$$\lambda_j = (a_1\gamma_j^2+a_2\gamma_j+a_3)/\gamma_j, \qquad \mu_j = a_1+a_2\bar{\gamma}_j+a_3\bar{\gamma}_j^2 \quad (j=1,2). \tag{3.8}$$

By using (2.4) and (3.7), the boundary conditions (3.1) and (3.3) may now be written

$$\Omega_1(z_1)+\overline{\Omega_1(z_1)}+\Omega_2(z_2)+\overline{\Omega_2(z_2)} = 0 \quad \text{on } L_1, \tag{3.9}$$

$$\Omega_1'(z_1)+\bar{\gamma}_1\overline{\Omega_1'(z_1)}+\Omega_2'(z_2)+\bar{\gamma}_2\overline{\Omega_2'(z_2)} = 0 \quad \text{on } L_1, \tag{3.10}$$

$$\lambda_1\Omega_1'(z_1)+\mu_1\overline{\Omega_1'(z_1)}+\lambda_2\Omega_2'(z_2)+\mu_2\overline{\Omega_2'(z_2)} = M(z,\bar{z})+iCz+\epsilon \quad \text{on } L_2, \tag{3.11}$$

where $M(z,\bar{z})$ satisfies the equations

$$\frac{8h^2}{3}\mathrm{re}\left(\frac{d}{dz}M(z,\bar{z})\right) = M \quad \text{on } L_2, \tag{3.12}$$

$$\frac{8h^2}{3}\mathrm{im}\left(\frac{\partial}{\partial s}\frac{d}{dz}M(z,\bar{z})\right) = S \quad \text{on } L_2. \tag{3.13}$$

In particular, if $L_2$ is free (case ($a$)) and $\Omega_j^*(z_j)$ is the complex potential

for the corresponding problem when the plate is clamped along the whole of $L$, then writing

$$\Omega_j(z_j) = \Omega_j^*(z_j)+\Omega_j^0(z_j) \quad (j = 1, 2), \tag{3.14}$$

the boundary conditions become

$$\Omega_1^{0\prime}(z_1)+\bar{\gamma}_1\overline{\Omega_1^{0\prime}(z_1)}+\Omega_2^{0\prime}(z_2)+\bar{\gamma}_2\overline{\Omega_2^{0\prime}(z_2)} = 0 \quad \text{on } L_1, \tag{3.15}$$

$$\lambda_1\Omega_1^{0\prime}(z_1)+\mu_1\overline{\Omega_1^{0\prime}(z_1)}+\lambda_2\Omega_2^{0\prime}(z_2)+\mu_2\overline{\Omega_2^{0\prime}(z_2)} = M(z,\bar{z})+iCz+\epsilon \quad \text{on } L_2, \tag{3.16}$$

where

$$\Omega_1^{*\prime}(z_1)+\bar{\gamma}_1\overline{\Omega_1^{*\prime}(z_1)}+\Omega_2^{*\prime}(z_2)+\bar{\gamma}_2\overline{\Omega_2^{*\prime}(z_2)} = 0 \quad \text{on } L, \tag{3.17}$$

$$\lambda_1\Omega_1^{*\prime}(z_1)+\mu_1\overline{\Omega_1^{*\prime}(z_1)}+\lambda_2\Omega_2^{*\prime}(z_2)+\mu_2\overline{\Omega_2^{*\prime}(z_2)} = -M(z,\bar{z}) \quad \text{on } L_2. \tag{3.18}$$

As in the isotropic case, it is assumed here also that the displacement $w$ is at most $O(|z|)$ at infinity, and inspection of (2.4) shows that this implies that

$$\Omega_j(z_j) = iH_jz_j^2+O(z_j), \tag{3.19}$$

where the $H_j$ satisfy

$$H_1-\bar{H}_1\bar{\gamma}_1^2+H_2-\bar{H}_2\bar{\gamma}_2^2 = 0 = H_1\gamma_1-\bar{H}_1\bar{\gamma}_1+H_2\gamma_2-\bar{H}_2\bar{\gamma}_2. \tag{3.20}$$

Since in case ($a$) it may be shown that the (known) $\Omega_j^*(z_j)$ satisfy such a condition, it follows that the $\Omega_j^0(z_j)$ also satisfy the condition.

Further, it is easy to show that if

$$A_1-\overline{A_1\gamma_1}+A_2-\overline{A_2\gamma_2} = 0 = B_1-\bar{B}_1+B_2-\bar{B}_2, \tag{3.21}$$

then the complex potentials

$$\Omega_j(z_j) = i\{H_jz_j^2+A_jz_j+B_j\} \tag{3.22}$$

give

$$w \equiv 0, \qquad K+izF = \frac{8h^2}{3}(iCz+\epsilon) \tag{3.23}$$

for some real $C$ and complex $\epsilon$. For these reasons the terms $iCz+\epsilon$ in (3.11) and (3.16) may be neglected, and the functions $\Omega_j^{0\prime}(z_j)$ in case ($a$), and $\Omega_j'(z_j)$ in case ($b$), may be taken to be holomorphic functions of $z_j$ in the region occupied by the material, including the point at infinity.

## 4. Mapping of the regions

Denote by $T^+$ the region occupied by the material in the $z$-plane, and let $T^-$ be the complement of $T^++L$. The mapping functions $z_j = z+\gamma_j\bar{z}$ ($j = 1, 2$) transform $T^+$, $T^-$, and $L$ in the $z$-plane into $T_j^+$, $T_j^-$, and $\Lambda_j$ respectively, in the $z_j$-planes. It is desirable to consider boundary conditions along these new boundaries $\Lambda_j$. In order to effect this, the regions $T_j^+$ are mapped on to either the upper half planes (in case (i)) or the exteriors of circles (in cases (ii) and (iii)) in $\zeta_j$-planes. Let $t_j$ represent an

admissible parameter on the boundary in the $\zeta_j$-plane; identical values $t$ of $t_1$ and $t_2$ can be made to correspond to the same value of the parameter $z$ on $L$ by a proper choice of the mapping functions $z_j(\zeta_j)$. The $\zeta_j$-planes may thus be considered as superimposed, and the regions corresponding to $T_j^+$, $T_j^-$, and $\Lambda_j$ may be denoted by $S^+$, $S^-$, and $C$ respectively: $C_1$ and $C_2$ are used to denote the parts of the boundary $C$ which correspond to $L_1$ and $L_2$.

The mapping functions are now given for the three cases:

(i) $L$ is the real axis, and the mapping function is ((3), 332)

$$z_j(\zeta_j) = z+\gamma_j\bar{z} = (1+\gamma_j)\zeta_j. \tag{4.1}$$

It is seen that if $z = x+iy$ then

$$\zeta_j = x+\left(\frac{1-\gamma_j}{1+\gamma_j}\right)iy \tag{4.2}$$

and therefore, on the real axis $\zeta_1 = \zeta_2 = x$.

(ii) If $L$ is the circle $|z| = a$ then ((3), 348)

$$z_j(\zeta_j) = z+\gamma_j\bar{z} = \zeta_j+\gamma_j a^2/\zeta_j. \tag{4.3}$$

Since $|\gamma_j| < 1$, the transformation has no singularities (i.e. points at which $z_j'(\zeta_j) = 0$) in $|\zeta_j| \geqslant a$.

(iii) If $L$ is the ellipse which is given parametrically by ((3), 364)

$$z_j(\zeta_j) = ce^{it}+de^{-it}, \tag{4.4}$$

where $c$ and $d$ are complex and $|c| > |d|$, then

$$z_j(\zeta_j) = (c+\gamma_j\bar{d})\zeta_j+(d+\gamma_j\bar{c})/\zeta_j \tag{4.5}$$

is the required mapping function, having no singularities in $|\zeta_j| \geqslant 1$. By using these mapping functions and writing

$$\Omega_j^{0\prime}(z_j) = f_j^0(\zeta_j), \qquad \Omega_j^{*\prime}(z_j) = f_j^*(\zeta_j), \tag{4.6}$$

the equations (3.15)–(3.18) may be written

$$f_1^0(t)+\bar{\gamma}_1\overline{f_1^0(t)}+f_2^0(t)+\bar{\gamma}_2\overline{f_2^0(t)} = 0 \quad \text{on } C_1, \tag{4.7}$$

$$\lambda_1 f_1^0(t)+\mu_1\overline{f_1^0(t)}+\lambda_2 f_2^0(t)+\mu_2\overline{f_2^0(t)} = M(t) \quad \text{on } C_2, \tag{4.8}$$

$$f_1^*(t)+\bar{\gamma}_1\overline{f_1^*(t)}+f_2^*(t)+\bar{\gamma}_2\overline{f_2^*(t)} = 0 \quad \text{on } C_1, \tag{4.9}$$

$$\lambda_1 f_1^*(t)+\mu_1\overline{f_1^*(t)}+\lambda_2 f_2^*(t)+\mu_2\overline{f_2^*(t)} = -M(t) \quad \text{on } C_2, \tag{4.10}$$

where $M(t) = M(t,\bar{t})$: equations (3.10) and (3.11) may be written in a similar way.

The complex potentials $\Omega_j^*(z_j)$ which correspond to an isolated normal load at an interior point of a plate with fully clamped boundary, may be obtained by a method similar to that used by Green and Zerna (3) in the corresponding problems in plane strain or generalized plane stress. Thus

in case (i), if the force is of magnitude $Q$ and acts at the point $z = c$, and if

$$c_j = c+\gamma_j\bar{c} = z_j(\epsilon_j) = (1+\gamma_j)\epsilon_j, \tag{4.11}$$

then

$$\Omega_1^*(\zeta_1) = \left(\frac{1+\gamma_1}{1-\gamma_1}\right)\left\{\left(\frac{1-\gamma_1\gamma_2}{1+\bar{\gamma}_1}\right)\bar{H}_1\{\bar{z}_1(\zeta_1)-\bar{c}_1\}^2\log(\zeta_1-\bar{\epsilon}_1)+\right.$$

$$\left.+\left(\frac{1-\gamma_2\bar{\gamma}_2}{1+\bar{\gamma}_2}\right)\bar{H}_2\{\bar{z}_2(\zeta_1)-\bar{c}_2\}^2\log(\zeta_1-\bar{\epsilon}_2)\right\}+H_1\{z_1(\zeta_1)-c_1\}^2\log(\zeta_1-\epsilon_1), \tag{4.12}$$

and $\Omega_2^*(\zeta_2)$ is obtained by interchanging suffixes 1 and 2 in (4.12). The constants $H_1$ and $H_2$ satisfy (3.20) and the equation

$$Q = \frac{64\pi h^2 a_3}{3}\left\{\frac{H_1}{\gamma_1}-\bar{H}_1\bar{\gamma}_1^3+\frac{H_2}{\gamma_2}-\bar{H}_2\bar{\gamma}_2^3\right\}. \tag{4.13}$$

These equations, and the corresponding ones for plates with clamped circular and elliptic holes, are derived in (**4**).

## 5. The mixed boundary-value problem for the half-plane

Consideration is here given to equations (4.7) and (4.8), in which $C$ is now the real axis and the functions $f_j^0(\zeta)$ are holomorphic in $S^+$ (the upper half plane).

Define two functions $\Phi(\zeta)$, $\Psi(\zeta)$ sectionally holomorphic throughout the whole plane including the point at infinity, by the relations

$$\Phi(\zeta) = \begin{cases} f_1^0(\zeta)+f_2^0(\zeta), & \zeta \text{ in } S^+ \\ -\bar{\gamma}_1\bar{f}_1^0(\zeta)-\bar{\gamma}_2\bar{f}_2^0(\zeta), & \zeta \text{ in } S^- \end{cases}, \tag{5.1}$$

$$\Psi(\zeta) = \begin{cases} \gamma_1 f_1^0(\zeta)+\gamma_2 f_2^0(\zeta), & \zeta \text{ in } S^+ \\ -\bar{f}_1^0(\zeta)-\bar{f}_2^0(\zeta), & \zeta \text{ in } S^- \end{cases}, \tag{5.2}$$

then

$$\overline{\Phi}(\zeta) = -\Psi(\zeta), \tag{5.3}$$

and (4.7) shows that

$$\Phi^+(t)-\Phi^-(t) = 0 = \Psi^+(t)-\Psi^-(t) \quad \text{on } C_1. \tag{5.4}$$

In order to satisfy (4.8), the left-hand side of that equation is rewritten using $\Phi(\zeta)$ and $\Psi(\zeta)$. The expressions for $f_1^0(\zeta)$ and $f_2^0(\zeta)$ are

$$(\gamma_1-\gamma_2)f_1^0(\zeta) = \Psi(\zeta)-\gamma_2\Phi(\zeta), \quad \zeta \text{ in } S^+, \tag{5.5}$$

$$(\gamma_2-\gamma_1)f_2^0(\zeta) = \Psi(\zeta)-\gamma_1\Phi(\zeta), \quad \zeta \text{ in } S^+. \tag{5.6}$$

By using these equations and the relations obtained from (5.3), namely,

$$\overline{\Phi^+(t)} = -\Psi^-(t), \qquad \overline{\Phi^-(t)} = -\Psi^+(t) \quad \text{on } C, \tag{5.7}$$

equation (4.8) becomes

$$\frac{1}{\gamma_1-\gamma_2}\{\lambda_1(\Psi^+(t)-\gamma_2\Phi^+(t))-\lambda_2(\Psi^+(t)-\gamma_1\Phi^+(t))\}+$$

$$+\frac{1}{\bar{\gamma}_1-\bar{\gamma}_2}\{\mu_1(\bar{\gamma}_2\Psi^-(t)-\Phi^-(t))-\mu_2(\bar{\gamma}_1\Psi^-(t)-\Phi^-(t))\} = M(t) \quad \text{on } C_2. \tag{5.8}$$

Equation (2.3) shows that

$$\bar{\gamma}_1+\bar{\gamma}_2+\frac{1}{\gamma_1}+\frac{1}{\gamma_2} = -\frac{2a_2}{a_3}, \qquad \frac{\bar{\gamma}_1\bar{\gamma}_2}{\gamma_1\gamma_2} = \frac{\bar{a}_3}{a_3}, \tag{5.9}$$

and these relations combined with the definitions of $\lambda_j$ and $\mu_j$ in (3.8) enable (5.8) to be written

$$A\{\Phi^+(t)+\Phi^-(t)\}+B\Psi^+(t)+C\Psi^-(t) = M(t) \quad \text{on } C_2, \tag{5.10}$$

where the complex constant $A$ and the real constants $B$ and $C$ are given by

$$A = a_3\frac{(\gamma_1+\gamma_2)}{\gamma_1\gamma_2}+a_2, \qquad B = a_1-\frac{a_3}{\gamma_1\gamma_2}, \qquad C = a_3\overline{\gamma_1\gamma_2}-a_1. \tag{5.11}$$

Equation (5.7) shows that the complex conjugate of (5.10) is

$$\bar{A}\{\Psi^-(t)+\Psi^+(t)\}+B\Phi^-(t)+C\Phi^+(t) = -\overline{M(t)} \quad \text{on } C_2. \tag{5.12}$$

In order to solve (5.10) and (5.12), numbers $\nu$ are sought which make the equation $[(5.10)+\nu\ (5.12)]$ have the form

$$\kappa\Theta^+(t)+\Theta^-(t) = U(t) \quad \text{on } C_2 \tag{5.13}$$

with
$$\Theta(\zeta) = \Phi(\zeta)+\theta\Psi(\zeta). \tag{5.14}$$

It is easily seen that $\nu$ must satisfy the equation

$$\frac{B+\nu\bar{A}}{A+\nu C} = \frac{C+\nu\bar{A}}{A+\nu B} = \theta, \tag{5.15}$$

which on eliminating $\nu$ gives two values $\theta_1$, $\theta_2$ for $\theta$, namely, the roots of

$$A\theta^2-(B+C)\theta+\bar{A} = 0. \tag{5.16}$$

Equations (5.13) and (5.15) show that the corresponding values of $\nu$ and $\kappa$ are

$$\nu = -\frac{1}{\theta}, \qquad \kappa = \frac{A\theta-C}{A\theta-B} \tag{5.17}$$

and that $\kappa$ satisfies the equation

$$(A\bar{A}-BC)\kappa^2+(B^2+C^2-2A\bar{A})\kappa+(A\bar{A}-BC) = 0. \tag{5.18}$$

By using (5.9) and the conditions $|\gamma_1| < 1$, $|\gamma_2| < 1$ it may easily be shown that $(B+C)^2 > 4A\bar{A}$, which ensures that $\theta_1$, $\theta_2$ are different and $\kappa_1$, $\kappa_2$ are real. When the material is orthotropic then not only are the roots $\kappa_1$, $\kappa_2$ real, but also positive; the proof depends on the conditions imposed on the elastic constants by the positive definiteness of the elastic

energy function, and for orthotropy these conditions are (see Gladwell (4))

$$a_1 > a_3 > 0, \qquad a_4 > 0, \qquad a_4(a_1+a_3) > 2a_2^2. \tag{5.19}$$

The author believes, but has been unable to prove, that $\kappa_1$, $\kappa_2$ are positive in the general case. This certainly is true for the numerical values derived from the elastic constants given for ethylene diamine tartrate and lithium sulphate, which are the only two substances known to the author which have the most general type of anisotropy (4).

Returning to (5.13) it is seen that, in principle, the problem is now solved; the two roots $\theta_1$, $\theta_2$ of (5.16) give two functions $\Theta_j(\zeta)$ which satisfy

$$\Theta_j(\zeta) = \Phi(\zeta)+\theta_j\Psi(\zeta), \tag{5.20}$$

$$\Theta_j^+(t)-\Theta_j^-(t) = 0 \quad \text{on } C_1, \tag{5.21}$$

$$\kappa_j\Theta_j^+(t)+\Theta_j^-(t) = U_j(t) \quad \text{on } C_2, \tag{5.22}$$

$$U_j(t) = (\theta_j M(t)+\overline{M(t)})/(A\theta_j-B), \tag{5.23}$$

and these equations may now be solved by known means to give $\Phi(\zeta)$, $\Psi(\zeta)$, $f_1^0(\zeta_1)$, and $f_2^0(\zeta_2)$. In particular, when $M(t)$ is given by (4.10), it may be shown that

$$U_j(t) = -(\kappa_j+1)\{f_1^*(t)+f_2^*(t)+\theta_j(\gamma_1 f_1^*(t)+\gamma_2 f_2^*(t))\}. \tag{5.24}$$

In order that the stresses should be of an order of infinity of degree less than 1 at the end points of $C_2$, it is necessary that $\Theta_j(\zeta)$ should be bounded there. Restricting attention to the case when the roots $\kappa_1$, $\kappa_2$ are positive and writing $X_j(\zeta)$ for the fundamental solution of the equation

$$\kappa_j X_j^+(t)+X_j^-(t) = 0 \quad \text{on } C_2 \tag{5.25}$$

which is bounded at the end points of $C_2$ and of lowest degree there, the general solution of (5.22) which is bounded both at the end points of $C_2$ and at infinity is

$$\Theta_j(\zeta) = \frac{X_j(\zeta)}{2\pi i\kappa_j}\int_{C_2}\frac{U_j(t)\,dt}{X_j^+(t)(t-\zeta)}. \tag{5.26}$$

Using (5.25), and writing $\Gamma_2$ for the contour $C_2^+ + C_2^-$, equation (5.26) may be written

$$\Theta_j(\zeta) = \frac{X_j(\zeta)}{2\pi i(\kappa_j+1)}\int_{\Gamma_2}\frac{U_j(t)\,dt}{X_j(t)(t-\zeta)}. \tag{5.27}$$

## 6. The mixed boundary condition for the infinite plate with a circular or elliptic hole

The problems for plates occupying these regions may be solved in a way exactly similar to that of the previous section, the only difference being in the definition of the functions $\Phi(\zeta)$ and $\Psi(\zeta)$. If the circle $C$ in the $\zeta$-plane has radius $a$, then $\Phi(\zeta)$, $\Psi(\zeta)$ are sectionally holomorphic

functions defined throughout the $\zeta$-plane, including the point at infinity, by the relations

$$\Phi(\zeta) = \begin{cases} f_1^0(\zeta)+f_2^0(\zeta), & \zeta \text{ in } S^+ \ (|\zeta| > a) \\ -\bar{\gamma}_1\bar{f}_1^0(a^2/\zeta)-\bar{\gamma}_2\bar{f}_2^0(a^2/\zeta), & \zeta \text{ in } S^- \ (|\zeta| < a) \end{cases}, \tag{6.1}$$

$$\Psi(\zeta) = \begin{cases} \gamma_1 f_1^0(\zeta)+\gamma_2 f_2^0(\zeta), & \zeta \text{ in } S^+ \\ -\bar{f}_1^0(a^2/\zeta)-\bar{f}_2^0(a^2/\zeta), & \zeta \text{ in } S^- \end{cases}. \tag{6.2}$$

The equation (5.3) is replaced by

$$\overline{\Phi}(a^2/\zeta) = -\Psi(\zeta), \tag{6.3}$$

but the remainder of section 5 applies unchanged.

## 7. Constant bending moment and shear on part of the real axis

The problem to be solved now, as an application of the theory given in section 5, is that of a plate occupying the upper half-plane, clamped along part of the real axis and acted on by constant bending moment and shear along the remainder (this is type (*b*) of the Introduction) which it is assumed lies wholly in the finite part of the plane. (Note that if this is not assumed then at infinity there are higher infinities in the displacements than normal (see section 3).)

If the bending moment $M$ and shear $S$ are constant then (3.4), (3.5) show that

$$K+izF = Mt-\tfrac{1}{2}iSt^2+iCt+\epsilon, \tag{7.1}$$

and therefore $M(t)$ may be taken to be

$$M(t) = 3(Mt-\tfrac{1}{2}iSt^2)/8h^2. \tag{7.2}$$

For simplicity $C_2$ is taken to be the single segment $|t| < a$. If $\kappa_1$, $\kappa_2$ are positive, then the fundamental solution $X_j(\zeta)$ of (5.25) is

$$X_j(\zeta) = (\zeta/a-1)^{\frac{1}{2}+i\alpha_j}(\zeta/a+1)^{\frac{1}{2}-i\alpha_j}, \qquad \alpha_j = (\log\kappa_j)/2\pi, \tag{7.3}$$

where that branch is taken which is holomorphic in the plane cut along $C_2$, and at infinity has the form

$$X_j(\zeta) = \zeta/a+O(1). \tag{7.4}$$

It may easily be shown by contour integration that

$$\frac{X_j(\zeta)}{2\pi i}\int_{\Gamma_2}\frac{M(t)\,dt}{X_j(t)(t-\zeta)} = -\frac{3}{16h^2}\{(2M\zeta-iS\zeta^2)+X_j(\zeta)[iSa\zeta-2(Ma+Sa^2\alpha_j)]\} \tag{7.5}$$

and from this result $\Theta_j(\zeta)$ may be obtained by using equations (5.23) and (5.27). After simplification it is found that

$$\Theta_1(\zeta) = -\frac{3}{16h^2A(\theta_1-\theta_2)}\times$$

$$\times\{2M(1+\theta_1)[\zeta-aX_1(\zeta)]+iS(1-\theta_1)[\zeta^2-aX_1(\zeta)(\zeta+2ia\alpha_1)]\}, \qquad (7.6)$$

with a similar equation, with the suffixes 1 and 2 interchanged, for $\Theta_2(\zeta)$. Since equations (5.5), (5.6), and (5.14) give

$$f_1(\zeta_1) = \Omega_1'(z_1), \qquad f_2(\zeta_2) = \Omega_2'(z_2) \qquad (7.7)$$

as linear combinations of $\Theta_1(\zeta_1)$, $\Theta_1(\zeta_2)$, $\Theta_2(\zeta_1)$, and $\Theta_2(\zeta_2)$, the problem is now solved.

Problems concerning isolated normal loads may be solved in a similar way; the contour integrals being evaluated by methods similar to those used in (1) for isotropic plates: details may be found in (4), where the uniqueness of the solutions is also considered.

## REFERENCES

1. G. M. L. Gladwell, *Quart. J. Mech. App. Math.* **11** (1958), 159.
2. N. I. Muskhelishvili, *Singular Integral Equations*, 2nd edn. (Moscow, 1946). English edition, P. Noordhoff (Groningen, 1953).
3. A. E. Green and W. Zerna, *Theoretical Elasticity* (Oxford, 1954).
4. G. M. L. Gladwell, Ph.D. Thesis, London, 1957.
5. A. C. Stevenson, *Phil. Mag.* (7) **34** (1943) 105–14.

# SHRINK-FIT STRESSES BETWEEN TUBES HAVING A FINITE INTERVAL OF CONTACT

*By* R. T. SEVERN

(*Dept. of Civil Engineering, University of Bristol*)

[Received 28 November 1957. Revise received 15 May 1958]

SUMMARY

The evaluation of shrinkage stresses when the contact interval between two tubes is infinite has already been discussed elsewhere (**1**). Part I of this paper discusses the evaluation of shrinkage stresses when the contact interval between two infinite tubes is finite. The method considers each tube separately and uses relaxation methods to find the radial displacement distribution along its length due to a unit, axially-symmetric, radial pressure acting on a small length of each of the two surfaces which are in contact. An integral equation is then solved embodying these two displacements to find the shrinkage-stresses. Part II discusses the problem when both tubes are finite (e.g. collar on a shaft) by solving the elastic equations for the stress-functions $\phi$ and $\psi$ (**2**) with special conditions at the contact interface.

## Part I

**1.** We suppose that a tube, shown in section in Fig. 1, occupies the region of space defined by $b \leqslant r \leqslant c$ and $-\infty < z < \infty$ and is subject to a unit axially-symmetric, radial pressure on a small length of its inner surface. The radial ($u$) and longitudinal ($v$) displacements must then satisfy

$$\left.\begin{aligned}(1-\sigma)\left(\frac{\partial^2 u}{\partial r^2}+\frac{1}{r}\frac{\partial u}{\partial r}-\frac{u}{r^2}\right)+\frac{1-2\sigma}{2}\frac{\partial^2 u}{\partial z^2}+\frac{1}{2}\frac{\partial^2 v}{\partial r\partial z}=0\\ \text{and}\qquad (1-\sigma)\frac{\partial^2 v}{\partial z^2}+\frac{1-2\sigma}{2}\left(\frac{\partial^2 v}{\partial r^2}+\frac{1}{r}\frac{\partial v}{\partial r}\right)+\frac{1}{2}\frac{\partial^2 u}{\partial r\partial z}+\frac{1}{2r}\frac{\partial u}{\partial z}=0\end{aligned}\right\} \tag{1}$$

subject to the stress boundary conditions; these may be written in terms of displacements according to

$$\left.\begin{aligned}\frac{1+\sigma}{E}\widehat{rr}=\frac{\partial u}{\partial r}+\frac{\sigma}{1-2\sigma}\left(\frac{\partial u}{\partial r}+\frac{u}{r}+\frac{\partial v}{\partial z}\right)\\ \text{and}\qquad \frac{1+\sigma}{E}\widehat{zr}=\frac{1}{2}\left(\frac{\partial u}{\partial z}+\frac{\partial v}{\partial r}\right)\end{aligned}\right\}, \tag{2}$$

where $\sigma$ is Poisson's ratio.

This system of equations and boundary conditions may be solved by the relaxation method (**2**) in which the boundary $DC$ is moved to the right as computation proceeds so that residuals upon it are of no consequence within the accuracy required. The radial displacement distribution on $r = b$ will be denoted by $U$. If a second tube, occupying the region of

space $a \leqslant r \leqslant b$ and $-\infty < z < \infty$ is subject to a similar unit pressure acting on a small length of $r = b$ in the negative $r$-direction, the displacement distributions may be found in a similar way. The radial displacement on $r = b$ for this inner tube will be denoted by $U'$.

Suppose now that the outer radius of the inner tube is not $b$ but $b+\delta(z)$,

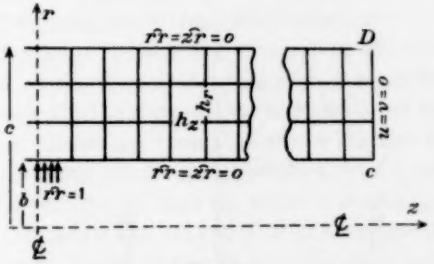


FIG. 1

where $\delta(z) \ll b$ and is zero unless $-l \leqslant z \leqslant l$; this condition defines the contact interval. Then, if the outer and inner tubes are assumed to be fitted together, the shrinkage-stress $\rho(z)$ is given by

$$\delta(z) = \int_{-l}^{l} [U(z-\xi) - U'(z-\xi)]\rho(\xi)\, d\xi, \tag{3}$$

where $U$ and $U'$ have already been found, and $\delta(z)$ is specified. The integral in (3) can be replaced by a summation formula and, if the range of integration is divided into $n$ equal parts, $(n+1)$ simultaneous algebraic equations are obtained each involving all the $(n+1)$ shrinkage-stress values. Such a system is easily solved on an electronic computer although, if $n$ is less than about ten, hand computation is feasible.

**2.** In the numerical example which follows a tube of internal radius one unit and external radius two units is shrink-fitted to a solid shaft of unit radius and of the same material ($\sigma = \frac{1}{4}$), and a contact interval of $-1 \leqslant z \leqslant 1$ with the 'lack-of-fit' $\delta(z)$ taken as a constant such that $E\delta = 10^3$. With mesh-lengths of 0·1 and 0·2 in the $z$- and $r$-directions respectively and the unit pressure applied over a length 0·1 the distributions of $10^3EU$ and $10^3EU'$ are given above the line in Figs. 2 and 3, respectively. The accuracy of these distributions may be checked in the following way. Firstly, if the unit load were to be applied to the whole of the inner surface of the tube, instead of a small part of it, the radial displacement of any point on this surface would be given by an integration of the values given above the line in Fig. 2; the value thereby obtained

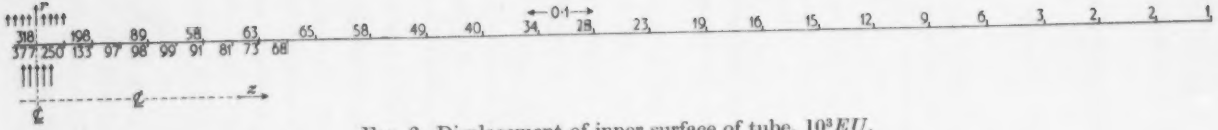


FIG. 2. Displacement of inner surface of tube. $10^3 EU$.

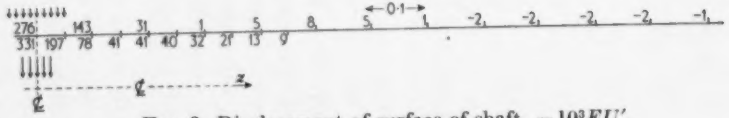


FIG. 3. Displacement of surface of shaft. $-10^3 EU'$.

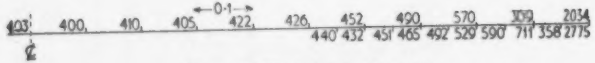


FIG. 4. Shrinkage stresses.

is 1,898. But, if the unit pressure is applied over the whole surface it can easily be shown (by putting $V = 0$ and $u$ independent of $z$ in (1)), that, for plane strain, the radial displacement ($\times 10^3 E$) at any point of the inner surface is 1,875. There is, therefore, a small finite-difference error in the relaxation solution. A similar treatment of the shaft gives 625 as the exact value of the radial displacement ($\times 10^3 E$) on the outer surface compared with 646 given by the relaxation solution.

To find the shrinkage stresses the integral in (3) was replaced by a summation based on the trapezoidal rule with a mesh-length of 0·1; the eleven simultaneous algebraic equations were then solved for the eleven unknown $p$-values. These are presented above the line in Fig. 4. If the contact interval had been infinite and, therefore, $U$, $U'$, and $\rho$ independent of $z$, it is easily shown from (3) that the uniform shrinkage pressure would have been 400. To refine the accuracy of the evaluations of shrinkage stresses it was first necessary to obtain more detailed radial displacement distributions and this was done with mesh-sizes 0·05 and 0·1 in the $z$- and $r$-directions respectively with the same radial load as before now acting over a length 0·05. By the principle of Saint-Venant this redistribution of load will not affect the displacement values at a sufficient distance away and, in the relaxation computation, the finer mesh was extended as far as was necessary. The changed displacement values are given below the line in Figs. 2 and 3. In recalculating the shrinkage stresses close to the end-point of contact it was assumed, because they were close to the value obtained for infinite contact, that the values previously obtained on the coarse mesh for $-0{\cdot}5 \leqslant z \leqslant 0{\cdot}5$ would not be significantly changed. The finer mesh values for the shrinkage stress close to the end-point of contact are given below the line in Fig. 4.

**3.** In the foregoing method the greatest effort is expended in obtaining the radial displacement distributions and it can be noted that these displacements are more easily obtained when the ratio of tube thickness to radius is small. For it can be shown (**3**) that if a thin-walled cylindrical tube, of thickness $t$, is subject to an axially-symmetric band of pressure, the resulting displacements can be obtained by discussing the bending of a beam of unit width, depth $t$ and relevant second moment of area $t^3/R(1-\sigma^2)$ on an elastic foundation whose reaction constant is $Et/R^2$, where $R$ is the radius of the middle surface of the tube. Tables of functions are available (**3**) for use in solution of this second problem so that displacement distributions are readily obtained. Although this method of obtaining displacement distributions requires the ratio of tube thickness to radius to be small it is interesting to consider its application in violation

of this requirement, but for the case of infinite contact between the two tubes considered in the example above. Thus the 'reaction-constants' for outer tube and shaft are $\frac{1}{6}E$ and $4E$ respectively and, if $\delta'$ and $\delta''$ are the (uniform) radial displacements of tube and shaft and $\delta'+\delta''=\delta$, the lack-of-fit, then the shrinkage stress $\rho=\frac{1}{6}E\delta'=4E\delta''$ which gives $\rho=0{\cdot}4E\delta$. This is the result found previously by a different method and this simple way of finding shrinkage stress for infinite contact is valid for tubes of any radius.

## Part II

**4.** The method described in Part I applies generally only when both tubes extend to infinity in the $z$-direction so that one computation of the radial displacement suffices for any position of the load on the contact surface. Prohibitive labour is involved in calculating the different displacement distributions for each position of load application which would be necessary if either tube was finite. If the ratio of thickness to radius is small such a procedure is feasible on the beam on elastic foundation analogy, but the important problem of a collar shrink-fitted to a shaft does not come within this category. Here, a method of solution is given for this type of problem.

If an axially symmetric solid of revolution is subject to axially-symmetric loading, the stress-components can be written in terms of two stress functions, $\phi$ and $\psi$, as (**2**)

$$\left.\begin{aligned} \widehat{rr} &= \frac{1}{r}\left(\frac{\partial\phi}{\partial r}+\frac{\partial\psi}{\partial r}\right)-\frac{1}{r^2}(\psi+(1-\sigma)\phi), \qquad \widehat{zz}=-\frac{1}{r}\frac{\partial\psi}{\partial r} \\ \widehat{\theta\theta} &= \frac{\sigma}{r}\frac{\partial\phi}{\partial r}+\frac{1}{r^2}(\psi+(1-\sigma)\phi) \quad \text{and} \quad \widehat{zr}=\frac{1}{r}\frac{\partial\psi}{\partial z} \end{aligned}\right\}. \tag{4}$$

The stress functions themselves satisfy the simultaneous equations

$$\frac{\partial^2\phi}{\partial r^2}-\frac{1}{r}\frac{\partial\phi}{\partial r}+\frac{\partial^2\phi}{\partial z^2}=0 \quad \text{and} \quad \frac{\partial^2\psi}{\partial r^2}-\frac{1}{r}\frac{\partial\psi}{\partial r}+\frac{\partial^2\psi}{\partial z^2}=\frac{\partial^2\phi}{\partial z^2}. \tag{5}$$

Now
$$\frac{u}{r}=e_{\theta\theta}=\frac{1}{E}[\widehat{\theta\theta}-\sigma(\widehat{rr}+\widehat{zz})]$$

where $E$ is Young's modulus, so that, using (4), we have

$$u=\frac{1+\sigma}{Er}(\psi+(1-\sigma)\phi). \tag{6}$$

Suppose the two tubes (Fig. 5) to be in contact along the whole length of the smaller tube ($AB$) and that the initial lack-of-fit is $\delta(z)$. If $\widehat{zr}=0$ on $AB$ and $s$ is measured round the boundary we have from (4) that $\partial\psi/\partial s=0$

round $ABCD$ and $EFGH$. Thus $\psi$ is a constant round these boundaries and can conveniently be taken as zero. Hence from (6)

$$u = \frac{1-\sigma^2}{Er}\phi \tag{7}$$

on the boundaries and, in particular, on the contact surface $AB$. If $u(z)$ and $u'(z)$ are the radial displacements on the contact surface for the outer

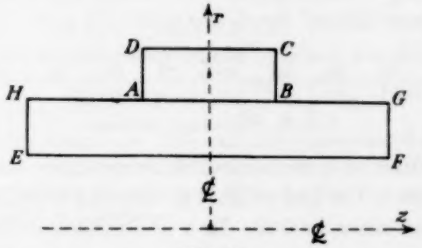


FIG. 5

and inner tubes respectively and $\phi$ and $\phi'$ are the corresponding stress functions, we have

$$u(z)-u'(z) = \delta(z) = \frac{1-\sigma^2}{ER}(\phi-\phi') \tag{8}$$

where $R$ is the radius of the contact surface.

5. On a square mesh, of size $h$, the governing equations (5) can be expressed approximately as

$$\left.\begin{aligned} &\phi_1+\phi_3+(1-\tfrac{1}{2}h/r_0)\phi_2+(1+\tfrac{1}{2}h/r_0)\phi_4-4\phi_0 = 0 \\ \text{and}\quad &\psi_1+\psi_3+(1-\tfrac{1}{2}h/r_0)\psi_2+(1+\tfrac{1}{2}h/r_0)\psi_4-4\psi_0+2\phi_0-\phi_1-\phi_3 = 0 \end{aligned}\right\}. \tag{9}$$

All external boundaries are stress-free so that (4) and the $\psi$-governing equation, which is not otherwise satisfied, can be used to eliminate fictitious stress function values from (9) on these external boundaries (2).

On the interface, if the first equation of (9) is applied to the outer tube, $\phi_4$ is fictitious; similarly $\phi'_2$ is fictitious if this equation is applied to the inner tube. At the interface $\widehat{rr} = \rho(z)$, the unknown shrinkage stress and this condition, stated for both tubes in terms of $\psi$ and $\phi$, from (4), introduces in addition a fictitious $\psi_4$ related to the outer tube, and a fictitious $\psi'_2$ related to the inner tube. At the interface, however, it is necessary to satisfy the equations (9) for both inner and outer tubes and the equation $\widehat{rr} = \rho(z)$ for each tube. It is therefore possible to eliminate the four fictitious stress-function values and the unknown $\rho(z)$ from these six

equations. Using also (8) we obtain

$$\left(1-\frac{h}{2R}\right)(\phi_2+\psi_2)+\left(1+\frac{h}{2R}\right)(\phi_4'+\psi_4')-2\phi_0+$$
$$+\frac{E\delta R}{1-\sigma^2}\left[1+\frac{h}{2R}-\frac{(1-\sigma)h}{R}\left(1-\frac{h^2}{4R^2}\right)\right]=0 \quad (10)$$

for the interface.

**6.** For the example which has been considered, the outer tube occupies the region of space defined by $1 \leqslant r \leqslant 2$, $-1 \leqslant z \leqslant 1$ and is shrink-

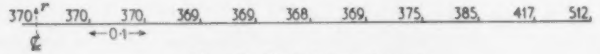


FIG. 6. Shrinkage stresses.

fitted to a solid shaft of unit radius and bounded by $-2 \leqslant z \leqslant 2$. Over the contact surface $\delta$, the lack of fit was assumed constant and $E\delta$ taken to be 1,000; $\sigma$ was taken as 0·25. In a preliminary computation a mesh size of 0·2 was used in both $r$- and $z$-directions but a finer net of 0·1 in both directions was subsequently introduced near the contact interface. The stress-function distributions are not given here but the derived shrinkage stress values are shown in Fig. 6. It is interesting to note that, with the dimensions as above, the shrinkage stress value for infinite contact given by Southwell (**1**) is 375 and that, for finite contact, this value obtains over the greater part of the contact interval. A more detailed solution near the end point of contact could therefore be obtained without involving the greater part of the contact interval with a resultant saving of effort.

## REFERENCES

**1.** R. V. SOUTHWELL, *Theory of Elasticity* (Oxford, 1941).
**2.** D. N. de G. ALLEN, *Relaxation Methods* (McGraw-Hill, 1955).
**3.** M. HETENYI, *Beams on Elastic Foundations* (University of Michigan, 1946).

# AN IMPROVEMENT ON DONNELL'S APPROXIMATION FOR THIN-WALLED CIRCULAR CYLINDERS

*By* L. S. D. MORLEY

(*Royal Aircraft Establishment, Farnborough*)

[Received 30 January 1958]

SUMMARY

Donnell's equation for thin-walled circular cylinders is replaced by

$$\nabla^4(\nabla^2+1)^2w+4K^4\frac{\partial^4w}{\partial x^4}=\frac{a^2}{D}\nabla^4q,$$

where $w$ is a non-dimensional form of the radial displacement and $q$ is the distributed radial loading. This equation retains the essential simplicity of the original but, unlike Donnell's equation, the accuracy does not decrease as the wavelength of circumferential distortion increases.

## 1. Introduction

ALTHOUGH the precise formulation of the linear theory of elastic shells has received considerable attention and is still the subject of controversy, it remains apparent that when numerical values are required for a particular problem it is often necessary, and indeed sufficient, to resort to relatively simple equations in order that the computations should not be too laborious. For example, as long ago as 1933, Donnell (**1**) derived a simple set of equations which he used to investigate the stability of thin-walled circular cylinders under torsion and obtained an acceptable agreement with experiment.

More recently, these same equations have been employed by Hoff (**2**, **3**) and his collaborators for the solution of equilibrium problems of the thin-walled circular cylinder, using eigenfunctions which are trigonometric either along a generator or around a circumference. However, it is well known that as the wavelength of circumferential distortion increases so does the error in Donnell's equations and, with this in mind, Hoff (**4**) later determined the limiting values of the parameters beyond which the error becomes intolerable. For this purpose the more accurate, and more complex, equations derived by Flügge (**5**) were used as the standard for comparison.

The purpose of the present paper is to remove the source of the error by improving on Donnell's approximation and yet retaining the essential simplicity. With equilibrium problems in mind, it is then demonstrated that the resulting eigenfunctions are quite accurate for all values of the parameters.

The application of the new equations to the solution of other types of problems is not considered.

## 2. Statement of Flügge's equations

Flügge's (5) equations for the thin-walled circular cylinder, shown in Fig. 1, are used later as the standard for comparison of the approximate equations. It is therefore appropriate to begin by listing them.

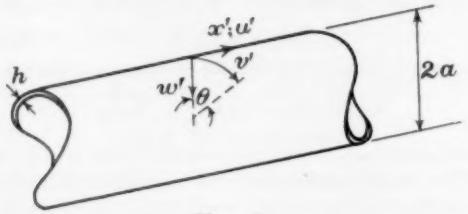


FIG. 1

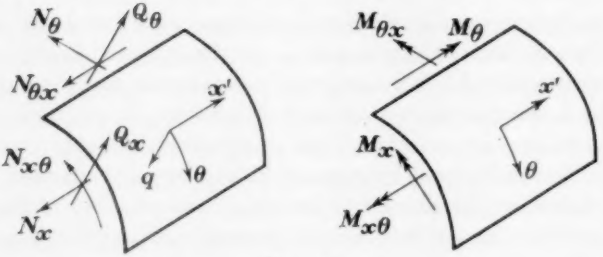


FIG. 2

The equilibrium equations for the element shown in Fig. 2 are, in terms of the displacements,

$$\nabla^4 w+2w_{,\theta\theta}+w+\tfrac{1}{2}(3-\nu)v_{,x\theta}+u_{,xxx}-\tfrac{1}{2}(1-\nu)u_{,x\theta\theta}+$$
$$+12\left(\frac{a}{h}\right)^2(w-v_{,\theta}-\nu u_{,x})=\frac{a^3}{D}q, \quad (1)$$

$$u_{,xx}+\tfrac{1}{2}(1-\nu)u_{,\theta\theta}+\tfrac{1}{2}(1+\nu)v_{,x\theta}-\nu w_{,x}+$$
$$+\frac{1}{12}\left(\frac{h}{a}\right)^2\{w_{,xxx}-\tfrac{1}{2}(1-\nu)(w_{,x\theta\theta}-u_{,\theta\theta})\}=0, \quad (2)$$

$$v_{,\theta\theta}+\tfrac{1}{2}(1-\nu)v_{,xx}+\tfrac{1}{2}(1+\nu)u_{,x\theta}-w_{,\theta}+\frac{1}{12}\left(\frac{h}{a}\right)^2\{\tfrac{1}{2}(3-\nu)w_{,xx\theta}+\tfrac{3}{2}(1-\nu)v_{,xx}\}=0, \quad (3)$$

where the subscripts following a comma indicate differentiation. In these equations, $h$ is the thickness and $a$ is the mean radius of the shell, $\nu$ is

Poisson's ratio, $\nabla^2$ is Laplace's operator

$$\nabla^2 = \frac{\partial^2}{\partial x^2} + \frac{\partial^2}{\partial \theta^2},$$

and the flexural rigidity is $D = \dfrac{Eh^3}{12(1-\nu^2)}$,

where $E$ is Young's modulus. The distributed radial load is $q$ per unit area and the non-dimensional distances and displacements are defined by the equations

$$x = \frac{x'}{a}, \quad u = \frac{u'}{a}, \quad v = \frac{v'}{a}, \quad w = \frac{w'}{a}, \tag{4}$$

where $x'$ is the distance measured along a generator, $a\theta$ that measured around a circumference, and $u'$, $v'$, $w'$ are the displacements respectively along a generator, a circumference, and a radius.

Flügge further shows that significant simplifications can be made for thin shells where the parameter $(h/a)^2$ can be neglected in comparison with unity. In fact, the equilibrium equations (1), (2), and (3) can then be rewritten in the more convenient form

$$\nabla^8 w + 4K^4 w_{,xxxx} + 2\nu w_{,xxxxxx} + 6w_{,xxxx\theta\theta} + \\ + 2(4-\nu) w_{,xx\theta\theta\theta\theta} + 2(2-\nu) w_{,xx\theta\theta} + 2w_{,\theta\theta\theta\theta\theta\theta} + w_{,\theta\theta\theta\theta} = \frac{a^3}{D} \nabla^4 q, \tag{5}$$

$$\nabla^4 u = \nu w_{,xxx} - w_{,x\theta\theta} + \frac{1}{12}\left(\frac{h}{a}\right)^2 \left\{ w_{,x\theta\theta\theta} - w_{,xxxxx} + \frac{3(1-\nu)}{2} \frac{1}{12}\left(\frac{h}{a}\right)^2 w_{,xxx\theta\theta} \right\}, \tag{6}$$

$$\nabla^4 v = (2+\nu) w_{,xx\theta} + w_{,\theta\theta\theta} - \frac{1}{12}\left(\frac{h}{a}\right)^2 \{2w_{,xxxx\theta} + 2w_{,xx\theta\theta\theta}\}. \tag{7}$$

In equation (5), the parameter $K$ is defined by

$$4K^4 = 12(1-\nu^2)\left(\frac{a}{h}\right)^2. \tag{8}$$

To complete this list, the stress resultants in terms of the displacements are, according to Flügge,

$$N_x = \frac{Eh}{1-\nu^2}\left\{ u_{,x} + \nu(v_{,\theta} - w) + \frac{1}{12}\left(\frac{h}{a}\right)^2 w_{,xx} \right\}, \tag{9}$$

$$N_\theta = \frac{Eh}{1-\nu^2}\left\{ v_{,\theta} - w + \nu u_{,x} - \frac{1}{12}\left(\frac{h}{a}\right)^2 (w_{,\theta\theta} + w) \right\}, \tag{10}$$

$$N_{x\theta} = \frac{Eh}{2(1+\nu)}\left\{ u_{,\theta} + v_{,x} + \frac{1}{12}\left(\frac{h}{a}\right)^2 (w_{,x\theta} + v_{,x}) \right\}, \tag{11}$$

$$N_{\theta x} = \frac{Eh}{2(1+\nu)}\left\{ u_{,\theta} + v_{,x} - \frac{1}{12}\left(\frac{h}{a}\right)^2 (w_{,x\theta} - u_{,\theta}) \right\}, \tag{12}$$

while the moment resultants are

$$M_x = -\frac{D}{a}\{w_{,xx}+\nu(w_{,\theta\theta}+v_{,\theta})+u_{,x}\}, \tag{13}$$

$$M_\theta = -\frac{D}{a}\{w_{,\theta\theta}+w+\nu w_{,xx}\}, \tag{14}$$

$$M_{x\theta} = \frac{D}{a}(1-\nu)\{w_{,x\theta}+v_{,x}\}, \tag{15}$$

$$M_{\theta x} = -\frac{1}{2}\frac{D}{a}(1-\nu)\{2w_{,x\theta}+v_{,x}-u_{,\theta}\}, \tag{16}$$

and the shear stress resultants which accompany these moments are

$$Q_x = -\frac{D}{a^2}\{w_{,xxx}+w_{,x\theta\theta}+u_{,xx}-\tfrac{1}{2}(1-\nu)u_{,\theta\theta}+\tfrac{1}{2}(1+\nu)v_{,x\theta}\}, \tag{17}$$

$$Q_\theta = -\frac{D}{a^2}\{w_{,\theta\theta\theta}+w_{,xx\theta}+w_{,\theta}+(1-\nu)v_{,xx}\}. \tag{18}$$

## 3. Donnell's approximation

Flügge's equations are often avoided because of the laborious calculations which are associated with them. On the other hand, the approximate equations given by Donnell (**1**) have met with fairly wide application.

Donnell's approximation will not be discussed in detail here. In a summarized form it is equivalent to the neglect of:

(i) the terms in $(h/a)^2$ appearing in equations (9) to (12) for the stress resultants,

(ii) the terms in $u$, $v$, $w$ and their first derivatives in equations (13) to (16) for the moment resultants,

(iii) the terms in the first and second derivatives of $u$, $v$, $w$ in the equations (17) and (18) for the shear stress resultants.

With these modifications, the equations of equilibrium in terms of the displacements become

$$\nabla^8 w+4K^4 w_{,xxxx} = \frac{a^3}{D}\nabla^4 q, \tag{19}$$

$$\nabla^4 u = \nu w_{,xxx}-w_{,x\theta\theta}, \tag{20}$$

$$\nabla^4 v = (2+\nu)w_{,xx\theta}+w_{,\theta\theta\theta}. \tag{21}$$

## 4. The improved approximation

It is well known that as the wavelength of circumferential distortion increases so does the error in Donnell's approximation. However, a close examination of Hoff's results (**4**) reveals that this error is only significant for that particular class of eigenfunctions which becomes increasingly independent of position $x$ along a generator. Under such circumstances,

it is clearly inadvisable to neglect the terms in $v$ and $w$ and their derivatives in the equations (13) to (18) for the moment and shear stress resultants.

If the above-mentioned terms are retained and the usual substitutions made, it is possible to obtain a new set of equilibrium equations in terms of the displacements but, unfortunately, they are just as difficult to solve as those derived by Flügge. However, in an approximate analysis such as this, there is no particular virtue in striving for the elegance of a system of equilibrium equations which are necessarily consistent when they are expressed in terms of either the displacements or the stress resultants. Instead, the aim is for the greatest simplicity at each stage consistent with the degree of approximation. With this in mind, the following system of equilibrium equations is proposed,

$$\nabla^4(\nabla^2+1)^2 w+4K^4 w_{,xxxx} = \frac{a^3}{D}\nabla^4 q, \tag{22}$$

$$\nabla^4 u = \nu w_{,xxx} - w_{,x\theta\theta}, \tag{23}$$

$$\nabla^4 v = (2+\nu) w_{,xx\theta} + w_{,\theta\theta\theta}, \tag{24}$$

the justification of which is given below.

If the Flügge equilibrium equation (5) is taken as the standard for comparison, it is noticed that the term

$$-2(1-\nu)(w_{,xxxxxx} - w_{,xx\theta\theta\theta\theta} - w_{,xx\theta\theta}) \tag{25}$$

is neglected in arriving at equation (22). Now, if a further comparison is made, and the usual 'order of magnitude' arguments are applied, it is seen that the constituents of equation (25) are of the same order as those neglected in obtaining Donnell's equation (19). Thus, equation (22) corresponds at least to the same degree of approximation as Donnell's equation (19). Furthermore, as pointed out at the beginning of this section, the error in Donnell's approximation only grows significantly for the class of eigenfunctions which becomes increasingly independent of the position $x$ along a generator. Therefore, in arriving at equation (22) account is taken of the fact that terms in $w_{,\theta}$ are more important than terms in $w_{,x}$—hence the final neglect of the term (25).

The remaining equations (23) and (24) are identical with those of Donnell and there is no necessity here for their modification.

## 5. Eigenfunction solution with trigonometric expressions along a generator

Hoff and his collaborators (**2, 3**) have shown that solutions to many equilibrium problems can be conveniently obtained with the aid of eigenfunctions which are trigonometric either along a generator or around a circumference.

Following an identical procedure, the solution of the homogeneous equation (22) is obtained for the case when the eigenfunctions are trigonometric along a generator, i.e.

$$w = e^{p\theta}\cos nx, \tag{26}$$

where $n$ is real. When this expression is substituted into equation (22) one obtains the auxiliary equation

$$(p^2-n^2)^2(p^2-n^2+1)^2+4K^4n^4 = 0 \tag{27}$$

which is quartic in $p^2$. From this, the following expressions can be written down for the roots $p_1^2$, $p_2^2$, $p_3^2$, and $p_4^2$.

$$p_1^2,\ p_2^2,\ p_3^2,\ p_4^2 = n^2-\tfrac{1}{2}\pm(\tfrac{1}{4}\pm 2iK^2n^2)^{\frac{1}{2}} \tag{28}$$

and, since it often occurs that $n > 0{\cdot}17$ we have the approximations

$$p_1^2,\ p_2^2,\ p_3^2,\ p_4^2 = n^2-\tfrac{1}{2}\pm\left\{\left(Kn+\frac{1}{16Kn}\right)\pm i\left(Kn-\frac{1}{16Kn}\right)\right\} \tag{29}$$

which in the limiting case of $n = 0{\cdot}17$ are as inaccurate as neglecting $(h/a)^2$ in comparison with unity.† The roots of Donnell's equation (19) are

$$p_{1D}^2,\ p_{2D}^2,\ p_{3D}^2,\ p_{4D}^2 = n^2\pm(Kn\pm iKn), \tag{30}$$

and since Donnell's equation is rarely valid for $n \leqslant 0{\cdot}17$ it is seen that there is no loss of simplicity here.

For purposes of comparison, some numerical values of the roots calculated from equation (28) are tabulated in Table 1 below along with values of the roots obtained from Donnell's equation and those from the more accurate Flügge equation (taking Poisson's ratio as $\nu = 0{\cdot}3$). Following Hoff (4), three values are assumed for $K$, namely 5, 10, and 50. When $K$ is smaller than 5, then the assumptions of thin shell theory are invalid and $(h/a)^2$ cannot be neglected in comparison with unity. When $K$ is greater than 50, the shell is so thin walled that it can hardly fulfil structural requirements.

† The limiting factor is derived from the consideration that

$$(\tfrac{1}{4}\pm 2iK^2n^2)^{\frac{1}{2}} = Kn(1\pm i)\left(1\mp\frac{i}{8K^2n^2}\right)^{\frac{1}{2}}$$

$$\doteqdot Kn(1\pm i)\left\{\left(1+\frac{1}{512K^4n^4}-\ldots\right)\mp\frac{i}{16K^2n^2}\left(1-\frac{1}{512K^4n^4}+\ldots\right)\right\},$$

where the term $1/512K^4n^4$ can be neglected provided that it is sufficiently small in comparison with unity. On substituting from equation (8), we find that

$$\frac{1}{512K^4n^4} \equiv \frac{(h/a)^2}{1536(1-\nu^2)n^4},$$

but we have agreed that $(h/a)^2$ can be neglected in comparison with unity and so $1/512K^4n^4$ can likewise be neglected in comparison with unity provided that

$$1536(1-\nu^2)n^4 \geqslant 1,$$

or, for $\nu = 0{\cdot}3$, provided that $\qquad n \geqslant 0{\cdot}17.$

TABLE 1

*Roots when w is trigonometric along a generator* ($w = e^{v\theta}\cos nx$)

| $K$ | $n$ | | $p_1, p_2$ | $p_3, p_4$ |
|---|---|---|---|---|
| 5 | 0·01 | Present | 0·0506+0·0494*i* | 0·0025+1·0000*i* |
| | | Flügge | 0·0510+0·0490*i* | 0·0025+1·0000*i* |
| | | Donnell | 0·2458+0·1017*i* | 0·1018+0·2455*i* |
| 5 | 0·10 | Present | 0·5316+0·3696*i* | 0·1825+1·0767*i* |
| | | Flügge | 0·5330+0·3662*i* | 0·1812+1·0783*i* |
| | | Donnell | 0·7824+0·3195*i* | 0·3241+0·7714*i* |
| 5 | 1·00 | Present | 2·5441+0·9801*i* | 1·0520+2·3704*i* |
| | | Flügge | 2·5469+0·9694*i* | 1·0455+2·3749*i* |
| | | Donnell | 2·6278+0·9514*i* | 1·0962+2·2807*i* |
| 5 | 10·00 | Present | 12·3921+2·0172*i* | 7·7414+3·2290*i* |
| | | Flügge | 12·3952+1·9456*i* | 7·7458+3·2942*i* |
| | | Donnell | 12·4120+2·0142*i* | 7·7689+3·2180*i* |
| 10 | 0·01 | Present | 0·1012+0·0987*i* | 0·0100+1·0002*i* |
| | | Flügge | 0·1014+0·0985*i* | 0·0100+1·0002*i* |
| | | Donnell | 0·3476+0·1439*i* | 0·1440+0·3473*i* |
| 10 | 0·10 | Present | 0·9153+0·5133*i* | 0·3619+1·2982*i* |
| | | Flügge | 0·9157+0·5121*i* | 0·3611+1·2987*i* |
| | | Donnell | 1·1026+0·4535*i* | 0·4567+1·0948*i* |
| 10 | 1·00 | Present | 3·5360+1·4131*i* | 1·4640+3·4131*i* |
| | | Flügge | 3·5371+1·4097*i* | 1·4613+3·4146*i* |
| | | Donnell | 3·5963+1·3993*i* | 1·4923+3·3506*i* |
| 10 | 10·00 | Present | 14·5372+3·4394*i* | 7·0534+7·0887*i* |
| | | Flügge | 14·5388+3·4209*i* | 7·0534+7·1011*i* |
| | | Donnell | 14·5535+3·4356*i* | 7·0711+7·0711*i* |
| 50 | 0·01 | Present | 0·5254+0·3741*i* | 0·1818+1·0812*i* |
| | | Flügge | 0·5254+0·3740*i* | 0·1818+1·0812*i* |
| | | Donnell | 0·7769+0·3217*i* | 0·3218+0·7768*i* |
| 50 | 0·10 | Present | 2·3723+1·0512*i* | 0·9808+2·5425*i* |
| | | Flügge | 2·3723+1·0511*i* | 0·9807+2·5426*i* |
| | | Donnell | 2·4585+1·0169*i* | 1·0183+2·4550*i* |
| 50 | 1·00 | Present | 7·7964+3·2065*i* | 3·2293+7·7414*i* |
| | | Flügge | 7·7965+3·2063*i* | 3·2290+7·7415*i* |
| | | Donnell | 7·8237+3·1954*i* | 3·2409+7·7139*i* |
| 50 | 10·00 | Present | 26·2692+9·5168*i* | 10·9573+22·8158*i* |
| | | Flügge | 26·2695+9·5158*i* | 10·9566+22·8163*i* |
| | | Donnell | 26·2776+9·5138*i* | 10·9616+22·8069*i* |

It is seen from Table 1 that for all values of $n$ the numerical results obtained from equation (28) are quite close to those from the more accurate Flügge equation (5). The accuracy does deteriorate as $K$ decreases but in connexion with this it should be noted that the value $K = 5$ corresponds, for example, to a cylinder which is five feet in diameter with a wall thickness of nearly two inches. The error in Donnell's roots is intolerable for the lower values of $n$.

The roots of Flügge's equation (5) which are given in Table 1 above were calculated with the aid of an electronic digital computer but, in the absence of such a device they could have been approximated by

$$p_F = (1+\epsilon)p, \tag{31}$$

where

$$\epsilon = \frac{(1-\nu)n^2(p^4+p^2-n^4)}{2p^2\{2(p^2-n^2+\frac{1}{2})(p^2-n^2+1)(p^2-n^2)-(1-\nu)n^2(2p^2+1)\}}$$

from Newton's approximation. In the case when $n$ increases indefinitely it is easily checked that the error term $\epsilon$ tends to zero. On the other hand, when $n = 0$, both equation (22) and Flügge's equation (5) reduce to that defining the behaviour of a circular ring.

## 6. Eigenfunction solution with trigonometric expressions in the circumferential direction

When the eigenfunctions are trigonometric in the circumferential direction, the displacement $w$ is taken to be

$$w = e^{px}\cos n\theta, \tag{32}$$

where $n$ is an integral number for a closed cylinder. Substitution of this into the homogeneous differential equation (25) yields the auxiliary equation

$$(p^2-n^2)^2(p^2-n^2+1)^2+4K^4p^4 = 0 \tag{33}$$

which is again quartic in $p^2$. The roots $p_1^2$, $p_2^2$, $p_3^2$, $p_4^2$ are found to be

$$\left.\begin{aligned} p_1^2,\, p_3^2 &= n^2-\tfrac{1}{2}+iK^2\left[1\pm\left\{1-\frac{i(2n^2-1)}{K^2}\right\}^{\frac{1}{2}}\right], \\ p_2^2,\, p_4^2 &= n^2-\tfrac{1}{2}-iK^2\left[1\pm\left\{1+\frac{i(2n^2-1)}{K^2}\right\}^{\frac{1}{2}}\right]. \end{aligned}\right\} \tag{34}$$

The roots $\pm p_{1D}$, $\pm p_{2D}$, $\pm p_{3D}$, $\pm p_{4D}$ of Donnell's equation (19) are calculated from the quadratic equations

$$p_D^2\pm(1\pm i)Kp_D-n^2 = 0. \tag{35}$$

Again, for purposes of comparison, some numerical values of the roots calculated from equation (34) are given in Table 2 below along with values of the roots obtained from Donnell's equation and those of the more accurate Flügge equation. The same values of $K$ are taken as for Table 1, while $n$ assumes the values 0, 1, 2, 3, 4, and 10 appropriate to a closed cylinder.

As before, it is seen from Table 2 that for all values of $n$ the numerical results obtained from equation (34) are quite close to those from the more accurate Flügge equation (5). There is a deterioration in accuracy as $K$ decreases. The error in Donnell's roots $p_3$ and $p_4$ is hardly tolerable for $n = 1, 2, 3$.

Again, the eigenvalues $p_{1F}$, etc., for the Flügge equation (5) which are given in Table 2 were calculated with the aid of an electronic digital computer, but they could have been approximated by

$$p_F = (1+\epsilon)p, \tag{36}$$

## TABLE 2

*Roots when w is trigonometric around a circumference* ($w = e^{pz} \cos n\theta$)

| $K$ | $n$ | | $p_1, p_2$ | $p_3, p_4$ |
|---|---|---|---|---|
| 5 | 0 | Present | 4·9502 + 5·0502$i$ | — — |
| | | Flügge | 4·9854 + 5·0154$i$ | — — |
| | | Donnell | 5·0000 + 5·0000$i$ | — — |
| 5 | 1 | Present | 5·0502 + 4·9502$i$ | 0 |
| | | Flügge | 5·0848 + 4·9148$i$ | 0 |
| | | Donnell | 5·1019 + 4·9021$i$ | 0·1019 + 0·0979$i$ |
| 5 | 2 | Present | 5·3700 + 4·6764$i$ | 0·3669 + 0·3195$i$ |
| | | Flügge | 5·4026 + 4·6387$i$ | 0·3646 + 0·3220$i$ |
| | | Donnell | 5·4261 + 4·6359$i$ | 0·4261 + 0·3641$i$ |
| 5 | 3 | Present | 5·9358 + 4·3180$i$ | 0·9348 + 0·6800$i$ |
| | | Flügge | 5·9607 + 4·2780$i$ | 0·9509 + 0·6582$i$ |
| | | Donnell | 5·9931 + 4·2893$i$ | 0·9931 + 0·7107$i$ |
| 5 | 4 | Present | 6·7075 + 3·9845$i$ | 1·7072 + 1·0141$i$ |
| | | Flügge | 6·7354 + 3·9374$i$ | 1·7001 + 1·0260$i$ |
| | | Donnell | 6·7605 + 3·9670$i$ | 1·7605 + 1·0330$i$ |
| 5 | 10 | Present | 12·4943 + 3·1249$i$ | 7·4947 + 1·8745$i$ |
| | | Flügge | 12·5167 + 3·0368$i$ | 7·4812 + 1·9264$i$ |
| | | Donnell | 12·5194 + 3·1238$i$ | 7·5194 + 1·8762$i$ |
| 10 | 0 | Present | 9·9750 + 10·0250$i$ | — — |
| | | Flügge | 9·9926 + 10·0076$i$ | — — |
| | | Donnell | 10·0000 + 10·0000$i$ | — — |
| 10 | 1 | Present | 10·0250 + 9·9750$i$ | 0 |
| | | Flügge | 10·0425 + 9·9575$i$ | 0 |
| | | Donnell | 10·0502 + 9·9503$i$ | 0·0502 + 0·0497$i$ |
| 10 | 2 | Present | 10·1779 + 9·8281$i$ | 0·1761 + 0·1701$i$ |
| | | Flügge | 10·1950 + 9·8102$i$ | 0·1758 + 0·1704$i$ |
| | | Donnell | 10·2038 + 9·8042$i$ | 0·2038 + 0·1958$i$ |
| 10 | 3 | Present | 10·4413 + 9·5943$i$ | 0·4406 + 0·4049$i$ |
| | | Flügge | 10·4579 + 9·5761$i$ | 0·4430 + 0·4023$i$ |
| | | Donnell | 10·4683 + 9·5718$i$ | 0·4683 + 0·4282$i$ |
| 10 | 4 | Present | 10·8243 + 9·2922$i$ | 0·8240 + 0·7074$i$ |
| | | Flügge | 10·8406 + 9·2732$i$ | 0·8227 + 0·7088$i$ |
| | | Donnell | 10·8522 + 9·2719$i$ | 0·8522 + 0·7281$i$ |
| 10 | 10 | Present | 15·2678 + 7·4347$i$ | 5·2678 + 2·5652$i$ |
| | | Flügge | 15·2808 + 7·4080$i$ | 5·2633 + 2·5744$i$ |
| | | Donnell | 15·2909 + 7·4293$i$ | 5·2909 + 2·5707$i$ |
| 50 | 0 | Present | 49·9950 + 50·0050$i$ | — — |
| | | Flügge | 49·9985 + 50·0015$i$ | — — |
| | | Donnell | 50·0000 + 50·0000$i$ | — — |
| 50 | 1 | Present | 50·0050 + 49·9950$i$ | 0 |
| | | Flügge | 50·0085 + 49·9915$i$ | 0 |
| | | Donnell | 50·0100 + 49·9900$i$ | 0·0100 + 0·0100$i$ |
| 50 | 2 | Present | 50·0350 + 49·9650$i$ | 0·0347 + 0·0346$i$ |
| | | Flügge | 50·0385 + 49·9615$i$ | 0·0347 + 0·0346$i$ |
| | | Donnell | 50·0400 + 49·9600$i$ | 0·0400 + 0·0400$i$ |
| 50 | 3 | Present | 50·0851 + 49·9151$i$ | 0·0850 + 0·0847$i$ |
| | | Flügge | 50·0886 + 49·9116$i$ | 0·0850 + 0·0847$i$ |
| | | Donnell | 50·0902 + 49·9102$i$ | 0·0902 + 0·0898$i$ |
| 50 | 4 | Present | 50·1555 + 49·8455$i$ | 0·1554 + 0·1544$i$ |
| | | Flügge | 50·1590 + 49·8420$i$ | 0·1554 + 0·1544$i$ |
| | | Donnell | 50·1605 + 49·8405$i$ | 0·1605 + 0·1595$i$ |
| 50 | 10 | Present | 51·0140 + 49·0255$i$ | 1·0140 + 0·9744$i$ |
| | | Flügge | 51·0174 + 49·0220$i$ | 1·0139 + 0·9745$i$ |
| | | Donnell | 51·0192 + 49·0208$i$ | 1·0192 + 0·9792$i$ |

where

$$\epsilon = \frac{(1-\nu)(p^4-n^4+n^2)}{2\{2(p^2-n^2+\frac{1}{2})(p^2-n^2+1)(p^2-n^2)+4K^4p^2-(1-\nu)(3p^4-n^4+n^2)\}}.$$

## 7. Solution of the inhomogeneous equation

As pointed out by Hoff (4), when the distributed radial load $q$ is represented by a double-trigonometric series then the displacements can be expressed in the same form. The procedure is so simple that there is little reason to make use of approximate equations in preference to that of Flügge, but Hoff goes on to show that the inhomogeneous Donnell equation (19) should not, in any case, be used when the cylinder length is

TABLE 3

*Double-trigonometric solution of the inhomogeneous equations*

| $K$ | $n$ | $s$ | $A_F/A$ | $A_F/A_D$ |
|---|---|---|---|---|
| 5 | 1 | 0 | — | — |
| 5 | 2 | 0 | 1·0000 | 1·7778 |
| 5 | 3 | 0 | 1·0000 | 1·2656 |
| 5 | 1 | 0·5 | 0·9999 | 1·0148 |
| 5 | 2 | 0·5 | 1·0157 | 1·4520 |
| 5 | 3 | 0·5 | 1·0020 | 1·2557 |
| 5 | 1 | 1·0 | 0·9999 | 1·0042 |
| 5 | 2 | 1·0 | 1·0053 | 1·0833 |
| 5 | 3 | 1·0 | 1·0095 | 1·1904 |
| 5 | 10 | 1·0 | 1·0001 | 1·0202 |
| 10 | 1 | 0 | — | — |
| 10 | 2 | 0 | 1·0000 | 1·7778 |
| 10 | 3 | 0 | 1·0000 | 1·2656 |
| 10 | 1 | 0·5 | 1·0000 | 1·0010 |
| 10 | 2 | 0·5 | 1·0020 | 1·0561 |
| 10 | 3 | 0·5 | 1·0030 | 1·1835 |
| 10 | 1 | 1·0 | 1·0000 | 1·0003 |
| 10 | 2 | 1·0 | 1·0004 | 1·0060 |
| 10 | 3 | 1·0 | 1·0020 | 1·0417 |
| 10 | 10 | 1·0 | 1·0001 | 1·0202 |

greater than the diameter. However, this restriction does not apply to the equation (22) for its solution is nearly the same as that of the more exact Flügge equation (5). If the radial load $q$ is assumed to be

$$q = \cos sx \cos n\theta \tag{37}$$

then the displacement $w$ can be expressed as

$$w = A \cos sx \cos n\theta, \tag{38}$$

where $A$, $s$, and $n$ are all constants. Substitution of these two equations into the Flügge equation (5) yields

$$A_F = \frac{(a^3/D)(s^2+n^2)^2}{(s^2+n^2)^2(s^2+n^2-1)^2+4K^4s^4+2(1-\nu)(s^6-s^2n^4+s^2n^2)}, \tag{39}$$

and when substituted into Donnell's equation (19) we find

$$A_D = \frac{(a^3/D)(s^2+n^2)^2}{(s^2+n^2)^4+4K^4s^4}, \tag{40}$$

and, finally, when substituted into the equation (22) we obtain

$$A = \frac{(a^3/D)(s^2+n^2)^2}{(s^2+n^2)(s^2+n^2-1)^2+4K^4s^4}. \tag{41}$$

For purposes of comparison some numerical values of the ratios $A_F/A$ and $A_F/A_D$ have been computed and are tabulated in Table 3 above.

For the particular numerical results given in Table 3 it is seen that the greatest error is only 1·6 per cent when the inhomogeneous form of equation (22) is used in the place of the more accurate Flügge equation (5). The inhomogeneous Donnell equation should only be used with the greatest caution for equilibrium problems.

## REFERENCES

1. L. H. Donnell, *Stability of Thin Walled Tubes under Torsion.* NACA Report No. 479 (1933).
2. N. J. Hoff, Joseph Kempner, and Frederick V. Pohle, 'Line load applied along generators of thin walled circular cylindrical shells of finite length', *Quart. Appl. Math.* **11** (1953) 411.
3. —— 'Boundary-value problems of the thin walled circular cylinder', *J. App. Math.* **21** (1954) 343.
4. —— 'The accuracy of Donnell's equations', *J. App. Math.* **22** (1955), 329.
5. W. Flügge, *Statik und Dynamik der Schalen* (Berlin, 1934), pp. 110 et seq.

# FORMULAE FOR HYPEROSCULATORY INTERPOLATION, DIRECT AND INVERSE

*By* HERBERT E. SALZER

(*Convair Astronautics, California*)

[Received 21 November 1957]

SUMMARY

A convenient new procedure for direct 'hyperosculatory' interpolation for $f(x) = f(x_0+ph) \equiv f$, when values are given for $f(x_i) \equiv f_i, f'(x_i) \equiv f_i'$ and $f''(x_i) \equiv f_i''$ at $n$ equally spaced points $x_i = x_0+ih$, $i = -[\frac{1}{2}(n-1)]$ to $[\frac{1}{2}n]$, is derived from Hermite's $(3n-1)$th degree osculatory interpolation formula, for $n = 2(1)7$ (i.e. up to 20th degree accuracy). Certain fixed auxiliary quantities $a_i$, $b_i$ and $c_i$, which are independent of $p, f_i, f_i'$ and $f_i''$, are tabulated exactly. The method is an extension of the author's earlier adaptation of the simple osculatory interpolation formula, employing both a decomposition and uniqueness property of Hermite's general formula. The remainder term indicates the vast increase in accuracy and permissible size of $h$, when compared with simple osculatory interpolation formulae which are the next most accurate. For inverse interpolation the coefficients of the first ten powers of $r = (f-f_0)/hf_0'$, for $n = 2(1)5$, (i.e. up to 14th degree accuracy in the direct function) are given in terms of $f_i, f_i'$ and $f_i''$. Hyperosculatory interpolation is specially suitable in (1) practical problems in astronautics involving rocket or missile flight, where the acceleration data, or $f_i''$, are available as well as position and velocity data, or $f_i$ and $f'$, and where (2) higher mathematical functions that are tabulated with their first derivatives, are solutions of simple second order differential equations, so that $f_i''$ is readily obtained.

## 1. Introduction

In a series of previous articles (**1**)–(**6**), the writer gave formulae and tables for osculatory interpolation (direct and inverse, for real and complex arguments) which employs both the first derivative as well as the function itself at the interpolation points. The advantages over the ordinary type formulae that employ the functional values only are in the much greater accuracy when the interval of tabulation is the same, and in that, when no increase in accuracy is required, one can interpolate over much larger intervals, thus saving a large amount of required tabulation of the function. Fuller discussion of these advantages is contained in (**1**), p. 212. But every advantage in osculatory interpolation is enhanced to a still greater degree when one can utilize the second derivative as well as the function and its first derivative at the fixed points. Such formulae will be designated as 'hyperosculatory'. The present paper will be concerned with giving (I) a convenient and concise scheme for direct hyperosculatory interpolation for a real function $f(x)$ that is tabulated at equal intervals, with

its first and second derivatives either explicitly tabulated or readily available, and (II) formulae for inverse interpolation under the same conditions.

## 2. Special applications

At this point it is worth considering some of the reasons for giving special attention to formulae that employ second derivatives. One can go on giving new formulae employing derivatives of higher order beyond the second; but there is a reasonable point at which to stop because in practice either higher order derivatives are unavailable or troublesome to calculate, or too much time and effort on the preparation of papers on interpolation yield diminishing returns in proportion to the need. However, there are two very special reasons for developing these hyperosculatory interpolation formulae, apart from the extreme accuracy over comparatively large intervals of interpolation mentioned above:†

(1) In practical problems of astronautics involving rocket or missile flight, where interpolation is desired over the largest possible interval $h$, one often has the acceleration which has been determined by physical means (e.g. in inertial guidance), in addition to the velocity and position. Thus one may take the fullest advantage of the available information by using $f$, $f'$ and $f''$ in any interpolation or extrapolation problems on trajectories, orbits, or any functions that are tabulated with their first and second derivatives. This includes many functions arising in guided missile work that are given with their first derivatives, and where the functions are solutions of various types of second order differential equations for which the second derivative is given fairly explicitly, so that $f''$ is almost as accessible as $f$ and $f'$.

(2) Many higher mathematical functions of widespread importance which are tabulated with their first derivatives satisfy rather simple looking second order differential equations. Thus it would be almost a pity to employ ordinary or osculatory interpolation, when $f''$ for hyperosculatory interpolation is so readily available from the differential

† To get a crude idea as to how much better hyperosculatory interpolation is by comparison with osculatory or even ordinary interpolation, consider just the simplest 2-point formula using $f$, $f'$ and $f''$ at each end-point. Suppose that an ordinary six-point formula at intervals of $h$ is required for solving a problem to the desired accuracy. An osculatory formula using $f$ and $f'$ at three points would be a confluent case of the ordinary formula where the six entries over a total range of $5h$ could be regarded as coalescing in pairs, into three entries of $f$ and $f'$ at intervals of $2\frac{1}{2}h$, so that the interval of interpolation is now $2\frac{1}{2}$ times as great. But suppose in that same six-point formula there is coalescence by threes into two entries of $f$, $f'$ and $f''$ at the two end-points, $5h$ apart. Thus we now have an interval of interpolation that is five times as great as in ordinary interpolation and twice as great as in osculatory interpolation.

equation $f''+f'/x+f=0$ in a table of $J_0(x)$ with $J_1(x)=-J_0'(x)$ (7), or of $Y_0(x)$ with $Y_1(x)=-Y_0'(x)$ (8), or of any linear combination of those two. Also any type of Hankel function that is tabulated together with its derivative (9), is well suited to this hyperosculatory interpolation since it satisfies a simple Bessel-type second order differential equation. Likewise for interpolation in any kind of Hermite, Legendre, Jacobi, Mathieu, or hypergeometric function, where the first derivative is given with the function, one should use $f''$ too, as it is so easily obtained from the differential equation.

### 3. Direct interpolation

In the case of direct interpolation we wish to find $f(x)$, given $f(x_i)\equiv f_i$, $f'(x_i)\equiv f_i'$ and $f''(x_i)\equiv f_i''$ at equally-spaced points $x_i\equiv x_0+ih$, where $h$ is the tabular interval, $x=x_0+ph$, $f(x)=f(x_0+ph)\equiv f_p\equiv f$. For the $n$ points $x_i$, $i$ runs from $-[\frac{1}{2}(n-1)]$ to $[\frac{1}{2}n]$, the symbol $[m]$ denoting the largest integer not exceeding $m$. Then the hyperosculatory confluent form of Lagrange's interpolation formula, or in other words, Hermite's formula as far as the second derivative, which gives the polynomial of degree $3n-1$ having prescribed $f_i$, $f_i'$ and $f_i''$ at $x=x_i$, may be shown to be given by the following formula in terms of the variable $p$:

$$f(x_0+ph)=\sum_{i=-[\frac{1}{2}(n-1)]}^{[\frac{1}{2}n]}\{L_i^{(n)}(p)\}^3\{F_i(p)f_i+hG_i(p)f_i'+h^2H_i(p)f_i''\}+R_{3n}(p), \tag{1}$$

where

$$F_i(p)=1-3L_i^{(n)\prime}(i)(p-i)+(-\tfrac{3}{2}L_i^{(n)\prime\prime}(i)+6\{L_i^{(n)\prime}(i)\}^2)(p-i)^2, \tag{1'}$$

$$G_i(p)=(p-i)\{1-3L_i^{(n)\prime}(i)(p-i)\}, \tag{1''}$$

$$H_i(p)=\tfrac{1}{2}(p-i)^2, \tag{1'''}$$

$$L_i^{(n)}(p)=\prod_{j=-[\frac{1}{2}(n-1)]}^{[\frac{1}{2}n]}{}'\{(p-j)/(i-j)\}, \tag{2}$$

and

$$R_{3n}(p)=h^{3n}f^{(3n)}(\xi)\Big\{\prod_{j=-[\frac{1}{2}(n-1)]}^{[\frac{1}{2}n]}(p-j)\Big\}^3\Big/(3n)!; \tag{3}$$

where $x_{-[\frac{1}{2}(n-1)]}\leqslant\xi\leqslant x_{[\frac{1}{2}n]}$ in the case of *interpolation only*, i.e. for $x_{-[\frac{1}{2}(n-1)]}\leqslant x\leqslant x_{[\frac{1}{2}n]}$, and $\xi$ is in the interval $(x, x_{-[\frac{1}{2}(n-1)]},\dots, x_{[\frac{1}{2}n]})$ for any location of $x$, thus covering *extrapolation* also. Whenever $f^{(3n)}(\xi)$ is difficult to estimate, we may approximate $h^{3n}f^{(3n)}(\xi)$ in (3) by $\Delta^{3n}$, or the $(3n)$th difference of the entries $f_i$.

The derivation of (1) is straightforward from the general existence and uniqueness theorem on Lagrangian interpolation, including all confluent forms (10), and is suggested by the appearance of the explicit formula for

ordinary osculatory interpolation (**10**), (**11**). Thus in any $(3n-1)$th degree polynomial approximation to $f(x_0+ph)$ of the form

$$P(p) \equiv \sum_{i=-[\frac{1}{2}(n-1)]}^{[\frac{1}{2}n]} \{L_i^{(n)}(p)\}^3\{(a_i+b_i(p-i)+c_i(p-i)^2)f_i+$$
$$+h(a_i'+b_i'(p-i)+c_i'(p-i)^2)f_i'+h^2(a_i''+b_i''(p-i)+c_i''(p-i)^2)f_i''\},$$

the factor of $\{L_i^{(n)}(p)\}^3$ makes the coefficient of $f_i$, $f_i'$ or $f_i''$ vanish in $P(j)$, $P'(j)$ or $P''(j)$, for $j \neq i$. The condition $P(i) = f_i$, leads to $a_i = 1$, $a_i' = a_i'' = 0$; the condition

$$\frac{d}{dx}P(p)\bigg|_{x=x_i} = \frac{P'(i)}{h} = f_i',$$

leads to $b_i = -3L_i^{(n)\prime}(i)$, $b_i' = 1$, $b_i'' = 0$; and the condition

$$\frac{d^2}{dx^2}P(p)\bigg|_{x=x_i} = \frac{P''(i)}{h^2} = f_i'',$$

leads to

$$c_i = -\tfrac{3}{2}L_i^{(n)\prime\prime}(i)+6\{L_i^{(n)\prime}(i)\}^2, \quad c_i' = -3L_i^{(n)\prime}(i), \quad c_i'' = \tfrac{1}{2}.$$

This completes the derivation of (1), except for (3), the expression for the remainder term $R_{3n}(p)$, the derivation of which may be found in (**10**).

Some idea as to the extreme accuracy of (1) may be had by a glance at the value of $R_{3n}(p)$ in say the 3-, 5- and 7-point cases for $p = \frac{1}{2}$. Then $R_{3n}(\frac{1}{2})$ would be

$$\sim \frac{\{(\frac{1}{2}-(-1))(\frac{1}{2}-0)(\frac{1}{2}-1)\}^3}{9!}\Delta^9,$$

$$\frac{\{(\frac{1}{2}-(-2))(\frac{1}{2}-(-1))(\frac{1}{2}-0)(\frac{1}{2}-1)(\frac{1}{2}-2)\}^3}{15!}\Delta^{15}$$

and $$\frac{\{(\frac{1}{2}-(-3))(\frac{1}{2}-(-2))(\frac{1}{2}-(-1))(\frac{1}{2}-0)(\frac{1}{2}-1)(\frac{1}{2}-2)(\frac{1}{2}-3)\}^3}{21!}\Delta^{21},$$

or $\sim -1{\cdot}45.10^{-7}\Delta^9$, $2{\cdot}13.10^{-12}\Delta^{15}$ and $-3{\cdot}65.10^{-17}\Delta^{21}$ respectively. The corresponding remainder terms $R_{2n}(\frac{1}{2})$ in ordinary osculatory interpolation turn out to be

$$\sim \frac{\{(\frac{1}{2}-(-1))(\frac{1}{2}-0)(\frac{1}{2}-1)\}^2}{6!}\Delta^6,$$

$$\frac{\{(\frac{1}{2}-(-2))(\frac{1}{2}-(-1))(\frac{1}{2}-0)(\frac{1}{2}-1)(\frac{1}{2}-2)\}^2}{10!}\Delta^{10}$$

and

$$\frac{\{(\frac{1}{2}-(-3))(\frac{1}{2}-(-2))(\frac{1}{2}-(-1))(\frac{1}{2}-0)(\frac{1}{2}-1)(\frac{1}{2}-2)(\frac{1}{2}-3)\}^2}{14!}\Delta^{14},$$

or $\sim 1{\cdot}95.10^{-4}\Delta^6$, $5{\cdot}45.10^{-7}\Delta^{10}$ and $1{\cdot}74.10^{-9}\Delta^{14}$ respectively, which, although still impressively small, are not anywhere near the smallness of

the $R_{3n}(\frac{1}{2})$. For final comparison, we note the corresponding remainder terms $R_n(\frac{1}{2})$ in plain ordinary Lagrangian interpolation, namely,

$$\sim \frac{(\frac{1}{2}-(-1))(\frac{1}{2}-0)(\frac{1}{2}-1)}{3!}\Delta^3,$$

$$\frac{(\frac{1}{2}-(-2))(\frac{1}{2}-(-1))(\frac{1}{2}-0)(\frac{1}{2}-1)(\frac{1}{2}-2)}{5!}\Delta^5$$

$$\frac{(\frac{1}{2}-(-3))(\frac{1}{2}-(-2))(\frac{1}{2}-(-1))(\frac{1}{2}-0)(\frac{1}{2}-1)(\frac{1}{2}-2)(\frac{1}{2}-3)}{7!}\Delta^7,$$

or $\sim -\frac{1}{16}\Delta^3$, $\frac{3}{256}\Delta^5$ and $-\frac{5}{2048}\Delta^7$, which are considerably large by comparison. Another idea as to the power of the hyperosculatory interpolation formula (1) may be furnished from the value of the remainder in extrapolation over one full interval $h$, which is obtained by setting $p = [\frac{1}{2}n]+1$ in (3). Whereas ordinary 3-, 5- and 7-point Lagrangian extrapolation gives remainders $\sim \Delta^3$, $\Delta^5$ and $\Delta^7$ respectively, and the corresponding osculatory extrapolation gives the considerably smaller approximations of $\frac{1}{20}\Delta^6$, $\frac{1}{252}\Delta^{10}$ and $2{\cdot}91.10^{-4}\Delta^{14}$ respectively, here the $R_{3n}([\frac{1}{2}n]+1)$ for hyperosculatory extrapolation gives the exceedingly small remainders of approximately $5{\cdot}95.10^{-4}\Delta^9$, $1{\cdot}32.10^{-6}\Delta^{15}$ and $2{\cdot}51.10^{-9}\Delta^{21}$ respectively.†

Formula (1) as it stands is very cumbersome, involving large amounts of computation for the coefficients of $f_i$, $f_i'$ and $f_i''$. In this present treatment we give a more concise method of using (1) for any $p$, employing a very small schedule of precomputed constants, $a_i$, $b_i$ and $c_i$ which are tabulated below. The use of this new method saves a great amount of labour which would be required in using (1) directly. The principle is almost an extension of that expounded in (**1**), pp. 212–14, the only difference being in the extra term involving $f_i''$, and it will be recapitulated

† This present paper is concerned exclusively with this hyperosculatory or doubly-confluent Lagrangian interpolation and the advantages are shown in comparison with just ordinary and singly-confluent Lagrangian formulae. Thus the table-maker may still be concerned with other aids that are either remotely or not at all related to the ideas here. For example, the use of 'reduced derivatives' which is synonymous with the Taylor series represents a completely confluent Lagrangian formula. There, instead of the function at $n$ distinct points, we employ the function and its first $(n-1)$ derivatives at a single point, which makes it even more accurate than these present formulae. But in practice those higher order derivatives are often either unknown or too difficult to calculate. Some other types of interpolation aids like modified differences and coefficients in economized polynomials (the most popular arising from expansions in terms of Chebyshev polynomials) are based upon the entirely different idea of approximating under suitable conditions a polynomial of higher degree by one of considerably lower degree. Thus, if desired, one may start with the explicit formulae for (1) obtainable from $s, t, u, v,\ldots$ in the section on *Inverse Interpolation* and, with a considerable amount of manipulation, approximate them by lower degree economized polynomials.

only in outline here, for the reader's convenience. Writing (1) in the form

$$f(x_0+ph) = \{L^{(n)}(p)\}^3 \sum_{i=-[\frac{1}{2}(n-1)]}^{[\frac{1}{2}n]} \left\{\left(\frac{A_i^3}{(p-i)^3} - \frac{3A_i^3 L_i^{(n)\prime}(i)}{(p-i)^2} + \right.\right.$$
$$+ \frac{A_i^3(-\frac{3}{2}L_i^{(n)\prime\prime}(i)+6\{L_i^{(n)\prime}(i)\}^2)}{(p-i)}\Big) f_i +$$
$$\left. + h\left(\frac{A_i^3}{(p-i)^2} - \frac{3A_i^3 L_i^{(n)\prime}(i)}{(p-i)}\right) f_i' + \frac{h^2 A_i^3}{2(p-i)} f_i''\right\} + R_{3n}(p), \quad (4)$$

where
$$L^{(n)}(p) \equiv \prod_{j=-[\frac{1}{2}(n-1)]}^{[\frac{1}{2}n]} (p-j) \quad (5)$$

and
$$A_i \equiv \left\{\prod_{j=-[\frac{1}{2}(n-1)]}^{[\frac{1}{2}n]}{}' (i-j)\right\}^{-1}, \quad (6)$$

just as before, by setting $f(x_0+ph) \equiv 1$ and using the uniqueness of representation of any arbitrary $(3n-1)$th degree polynomial, by (4), we obtain

$$\{L^{(n)}(p)\}^{-3} = \sum_{i=-[\frac{1}{2}(n-1)]}^{[\frac{1}{2}n]} \left(\frac{A_i^3}{(p-i)^3} - \frac{3A_i^3 L_i^{(n)\prime}(i)}{(p-i)^2} + \right.$$
$$\left. + \frac{A_i^3(-\frac{3}{2}L_i^{(n)\prime\prime}(i)+6\{L_i^{(n)\prime}(i)\}^2)}{(p-i)}\right). \quad (7)$$

Thus from (4) and (7), it is apparent that (1) may be expressed concisely (omitting remainder $R_{3n}(p)$, and limits of $-[\frac{1}{2}(n-1)]$ to $[\frac{1}{2}n]$ in $\sum$ understood) in the form

$$f \sim \sum (\alpha_i f_i + h\beta_i f_i' + h^2\gamma_i f_i'')/\sum \alpha_i, \quad (8)$$

where

$$\alpha_i = \frac{a_i}{(p-i)^3} + \frac{b_i}{(p-i)^2} + \frac{c_i}{(p-i)}, \quad (9)$$

$$\beta_i = \frac{a_i}{(p-i)^2} + \frac{b_i}{(p-i)}, \quad (10)$$

$$\gamma_i = \frac{a_i}{2(p-i)}, \quad (11)$$

and the fixed quantities $a_i$, $b_i$ and $c_i$ may be defined by

$$a_i = k(n)A_i^3, \quad (12)$$

$$b_i = -3k(n)A_i^3 L_i^{(n)\prime}(i), \quad (13)$$

and
$$c_i = k(n)A_i^3(-\tfrac{3}{2}L_i^{(n)\prime\prime}(i)+6\{L_i^{(n)\prime}(i)\}^2). \quad (14)$$

In (12)–(14), $k(n)$ may be any suitably chosen constant of proportionality which depends only upon $n$, and whose function is merely to express $a_i$, $b_i$ and $c_i$ as exact integers instead of exact rational fractions; this simplifies the computation in (8)–(11).

The table below gives the exact values of $a_i$, $b_i$ and $c_i$ for $n = 2(1)7$, with corresponding accuracy of degrees 5(3)20.

*Table of $a_i$, $b_i$ and $c_i$*

| | | $a_i$ | | $b_i$ | | $c_i$ |
|---|---|---|---|---|---|---|
| 2-point | $a_0$ | −1 | $b_0$ | −3 | $c_0$ | −6 |
| | $a_1$ | 1 | $b_1$ | −3 | $c_1$ | 6 |
| 3-point | $a_{-1}$ | 2 | $b_{-1}$ | 9 | $c_{-1}$ | 24 |
| | $a_0$ | −16 | $b_0$ | 0 | $c_0$ | −48 |
| | $a_1$ | 2 | $b_1$ | −9 | $c_1$ | 24 |
| 4-point | $a_{-1}$ | −6 | $b_{-1}$ | −33 | $c_{-1}$ | −103 |
| | $a_0$ | 162 | $b_0$ | 243 | $c_0$ | 729 |
| | $a_1$ | −162 | $b_1$ | 243 | $c_1$ | −729 |
| | $a_2$ | 6 | $b_2$ | −33 | $c_2$ | 103 |
| 5-point | $a_{-2}$ | 12 | $b_{-2}$ | 75 | $c_{-2}$ | 260 |
| | $a_{-1}$ | −768 | $b_{-1}$ | −1920 | $c_{-1}$ | −5120 |
| | $a_0$ | 2592 | $b_0$ | 0 | $c_0$ | 9720 |
| | $a_1$ | −768 | $b_1$ | 1920 | $c_1$ | −5120 |
| | $a_2$ | 12 | $b_2$ | −75 | $c_2$ | 260 |
| 6-point | $a_{-2}$ | −300 | $b_{-2}$ | −2055 | $c_{-2}$ | −7697 |
| | $a_{-1}$ | 37500 | $b_{-1}$ | 1 21875 | $c_{-1}$ | 3 34375 |
| | $a_0$ | −3 00000 | $b_0$ | −3 00000 | $c_0$ | −13 25000 |
| | $a_1$ | 3 00000 | $b_1$ | −3 00000 | $c_1$ | 13 25000 |
| | $a_2$ | −37500 | $b_2$ | 1 21875 | $c_2$ | −3 34375 |
| | $a_3$ | 300 | $b_3$ | −2055 | $c_3$ | 7697 |
| 7-point | $a_{-3}$ | 600 | $b_{-3}$ | 4410 | $c_{-3}$ | 17549 |
| | $a_{-2}$ | −1 29600 | $b_{-2}$ | −4 98960 | $c_{-2}$ | −14 39424 |
| | $a_{-1}$ | 20 25000 | $b_{-1}$ | 35 43750 | $c_{-1}$ | 112 21875 |
| | $a_0$ | −48 00000 | $b_0$ | 0 | $c_0$ | −196 00000 |
| | $a_1$ | 20 25000 | $b_1$ | −35 43750 | $c_1$ | 112 21875 |
| | $a_2$ | −1 29600 | $b_2$ | 4 98960 | $c_2$ | −14 39424 |
| | $a_3$ | 600 | $b_3$ | −4410 | $c_3$ | 17549 |

The computation of $\alpha_i$, $\beta_i$ and $\gamma_i$ in (9)–(11) is facilitated by the recurrence scheme of first finding $\gamma_i$ by (11), and then

$$\beta_i = \frac{2\gamma_i + b_i}{(p-i)}, \tag{10'}$$

followed by

$$\alpha_i = \frac{\beta_i + c_i}{(p-i)}. \tag{9'}$$

## 4. Inverse interpolation

In $n$-point inverse hyperosculatory interpolation the problem is to find $x = x_0 + ph$ from given values of $f(x_0+ph)$, $f_i$, $f_i'$ and $f_i''$, $i = -[\frac{1}{2}(n-1)]$ to $[\frac{1}{2}n]$. Here the resulting formulae for $p$ are given by the inversion of (1) or the direct (truncated) power series for $f$ in terms of $p$. Since (1) is much more accurate than either the ordinary Lagrange formula or the

simple osculatory formula, the resulting inverse hyperosculatory interpolation formulae for $p$ would be expected to be much more efficient and enable the user to employ very much larger intervals $h$ for sufficient accuracy, surpassing even the permissible size of $h$ in inverse simple osculatory interpolation (**3**). The formulae below apply to all the types of problems cited under *Special Applications* in connexion with direct interpolation. All formulae express $p$ as a rapidly convergent series in powers of a variable $r$ (a suitable linear function of $f$), the coefficients of $r^m$ being very simple functions (and the same for every $n$) of fixed quantities $s$, $t$, $u$, $v$,..., which are given below in terms of $f_i$, $f_i'$ and $f_i''$ for $n = 2$, 3, 4 and 5. Although the direct hyperosculatory interpolation formulae for $n = 4$ and $n = 5$ are of the 11th and 14th degree accuracy, respectively, the inversion formula for $p$ that is given below does not go beyond the 10th degree terms, because in numerical work one rarely goes even that far, and in most practical problems the first few terms will be sufficient. In other words we simply do not employ the coefficient of $p^{11}$ in (1) for $n = 4$ nor the coefficients of $p^{11}$, $p^{12}$, $p^{13}$ and $p^{14}$ in (1) for $n = 5$. For every $n$, we define $r = (f-f_0)/hf_0'$ and $s = hf_0''/2f_0'$, and corresponding to $n = 2$, 3, 4 and 5, quantities $t$, $u$, $v$, $w$, $x$, $y$, $z$ and $\bar{z}$ are defined as follows:†

$$n = 2$$

$$t = [-10(f_0-f_1)-h(6f_0'+4f_1')-\tfrac{1}{2}h^2(3f_0''-f_1'')]/hf_0',$$

$$u = [15(f_0-f_1)+h(8f_0'+7f_1')+\tfrac{1}{2}h^2(3f_0''-2f_1'')]/hf_0',$$

$$v = [-6(f_0-f_1)-3h(f_0'+f_1')-\tfrac{1}{2}h^2(f_0''-f_1'')]/hf_0',$$

$$w = x = y = z = \bar{z} = 0.$$

$$n = 3$$

$$t = [-35(f_{-1}-f_1)-h(11f_{-1}'+48f_0'+11f_1')-h^2(f_{-1}''-f_1'')]/16hf_0',$$

$$u = [48(f_{-1}-2f_0+f_1)+13h(f_{-1}'-f_1')+h^2(f_{-1}''-24f_0''+f_1'')]/16hf_0',$$

$$v = [21(f_{-1}-f_1)+h(9f_{-1}'+24f_0'+9f_1')+h^2(f_{-1}''-f_1'')]/8hf_0',$$

$$w = [-32(f_{-1}-2f_0+f_1)-11h(f_{-1}'-f_1')-h^2(f_{-1}''-12f_0''+f_1'')]/8hf_0',$$

$$x = [-15(f_{-1}-f_1)-h(7f_{-1}'+16f_0'+7f_1')-h^2(f_{-1}''-f_1'')]/16hf_0',$$

$$y = [24(f_{-1}-2f_0+f_1)+9h(f_{-1}'-f_1')+h^2(f_{-1}''-8f_0''+f_1'')]/16hf_0',$$

$$z = \bar{z} = 0.$$

† The inverse interpolation formula for $p$ in powers of $r$ works even for $n = 1$, i.e. given only $f_0$, $f_0'$ and $f_0''$ besides $f$, if we set $t = u = v = w = x = y = z = \bar{z} = 0$.

$$n = 4$$

$$t = [-1136f_{-1} - 7452f_0 + 9072f_1 - 484f_2 - \\ - h(312f'_{-1} + 5832f'_0 + 3240f'_1 - 144f'_2) - \\ - h^2(24f''_{-1} + 972f''_0 - 648f''_1 + 12f''_2)]/1296hf'_0,$$

$$u = [3200f_{-1} - 3645f_0 + 445f_2 + h(828f'_{-1} + 1296f'_0 + 324f'_1 - 138f'_2) + \\ + h^2(60f''_{-1} - 1458f''_0 - 324f''_1 + 12f''_2)]/1296hf'_0,$$

$$v = [-1592f_{-1} + 21627f_0 - 21384f_1 + 1349f_2 - \\ - h(246f'_{-1} - 9477f'_0 - 8262f'_1 + 399f'_2) - \\ - h^2(6f''_{-1} - 2835f''_0 + 1782f''_1 - 33f''_2)]/1296hf'_0,$$

$$w = [-3120f_{-1} - 2025f_0 + 6480f_1 - 1335f_2 - \\ - h(1107f'_{-1} + 3888f'_0 + 2349f'_1 - 414f'_2) - \\ - h^2(99f''_{-1} - 486f''_0 - 1053f''_1 + 36f''_2)]/1296hf'_0,$$

$$x = [3573f_{-1} - 20169f_0 + 17739f_1 - 1143f_2 + \\ + h(1071f'_{-1} - 6399f'_0 - 6885f'_1 + 333f'_2) + \\ + h^2(81f''_{-1} - 2673f''_0 + 1539f''_1 - 27f''_2)]/1296hf'_0,$$

$$y = [-120f_{-1} + 8505f_0 - 9720f_1 + 1335f_2 + \\ + h(54f'_{-1} + 3888f'_0 + 3402f'_1 - 414f'_2) + \\ + h^2(18f''_{-1} + 810f''_0 - 1134f''_1 + 36f''_2)]/1296hf'_0,$$

$$z = [-1390f_{-1} + 5265f_0 - 4050f_1 + 175f_2 - \\ - h(480f'_{-1} - 1215f'_0 - 1620f'_1 + 45f'_2) - \\ - h^2(48f''_{-1} - 729f''_0 + 324f''_1 - 3f''_2)]/1296hf'_0,$$

$$\bar{z} = [688f_{-1} - 4131f_0 + 3888f_1 - 445f_2 + \\ + h(225f'_{-1} - 1296f'_0 - 1377f'_1 + 138f'_2) + \\ + h^2(21f''_{-1} - 486f''_0 + 405f''_1 - 12f''_2)]/1296hf'_0.$$

$$n = 5$$

$$t = [9616(f_{-2} - f_2) - 499712(f_{-1} - f_1) + \\ + h\{2592(f'_{-2} + f'_2) - 172032(f'_{-1} + f'_1) - 622080f'_0\} + \\ + h^2\{192(f''_{-2} - f''_2) - 24576(f''_{-1} - f''_1)\}]/165888hf'_0,$$

$$u = [-5504(f_{-2} + f_2) + 720896(f_{-1} + f_1) - 1430784f_0 + \\ + h\{-1392(f'_{-2} - f'_2) + 221184(f'_{-1} - f'_1)\} + \\ + h^2\{-96(f''_{-2} + f''_2) + 24576(f''_{-1} + f''_1) - 311040f''_0\}]/165888hf'_0,$$

$$v = [-32936(f_{-2}-f_2)+882688(f_{-1}-f_1)+$$
$$+h\{-8976(f'_{-2}+f'_2)+374784(f'_{-1}+f'_1)+902016f'_0\}+$$
$$+h^2\{-672(f''_{-2}-f''_2)+67584(f''_{-1}-f''_1)\}]/165888hf'_0,$$

$$w = [18880(f_{-2}+f_2)-1392640(f_{-1}+f_1)+2747520f_0+$$
$$+h\{4824(f'_{-2}-f'_2)-509952(f'_{-1}-f'_1)\}+$$
$$+h^2\{336(f''_{-2}+f''_2)-67584(f''_{-1}+f''_1)+451008f''_0\}]/165888hf'_0,$$

$$x = [41557(f_{-2}-f_2)-679424(f_{-1}-f_1)+$$
$$+h\{11514(f'_{-2}+f'_2)-290304(f'_{-1}+f'_1)-635040f'_0\}+$$
$$+h^2\{876(f''_{-2}-f''_2)-66048(f''_{-1}-f''_1)\}]/165888hf'_0,$$

$$y = [-23876(f_{-2}+f_2)+1101824(f_{-1}+f_1)-2155896f_0+$$
$$+h\{-6195(f'_{-2}-f'_2)+422400(f'_{-1}-f'_1)\}+$$
$$+h^2\{-438(f''_{-2}+f''_2)+66048(f''_{-1}+f''_1)-317520f''_0\}]/165888hf'_0,$$

$$z = [-23215(f_{-2}-f_2)+256640(f_{-1}-f_1)+$$
$$+h\{-6606(f'_{-2}+f'_2)+104064(f'_{-1}+f'_1)+225504f'_0\}+$$
$$+h^2\{-516(f''_{-2}-f''_2)+28032(f''_{-1}-f''_1)\}]/165888hf'_0,$$

$$\bar{z} = [13388(f_{-2}+f_2)-416768(f_{-1}+f_1)+806760f_0+$$
$$+h\{3561(f'_{-2}-f'_2)-160128(f'_{-1}-f'_1)\}+$$
$$+h^2\{258(f''_{-2}+f''_2)-28032(f''_{-1}+f''_1)+112752f''_0\}]/165888hf'_0.$$

For every $n$, the formula for $p$ is the following:

$$p = r-r^2s+r^3(2s^2-t)+r^4(-5s^3+5st-u)+r^5(14s^4-21s^2t+3t^2+6su-v)+$$
$$+r^6(-42s^5+84s^3t-28st^2-28s^2u+7tu+7sv-w)+$$
$$+r^7(132s^6-330s^4t+180s^2t^2+120s^3u-12t^3-72stu-36s^2v+$$
$$+4u^2+8tv+8sw-x)+$$
$$+r^8(-429s^7+1287s^5t-990s^3t^2-495s^4u+495s^2tu+165st^3+165s^3v-$$
$$-45t^2u-45su^2-90stv-45s^2w+9uv+9tw+9sx-y)+$$
$$+r^9(1430s^8-5005s^6t+5005s^4t^2+2002s^5u-1430s^2t^3-2860s^3tu-$$
$$-715s^4v+55t^4+660st^2u+330s^2u^2+660s^2tv+220s^3w-$$
$$-55tu^2-55t^2v-110suv-110stw-55s^2x+5v^2+$$
$$+10uw+10tx+10sy-z)+$$
$$+r^{10}(-4862s^9+19448s^7t-24024s^5t^2-8008s^6u+10010s^3t^3+$$
$$+15015s^4tu+3003s^5v-1001st^4-6006s^2t^2u-2002s^3u^2-$$
$$-4004s^3tv-1001s^4w+286t^3u+858stu^2+858s^2tw+$$
$$+858st^2v+858s^2uv+286s^2x-22u^3-132tuv-66t^2w-$$
$$-66sv^2-132suw-132stx-66s^2y+11vw+11ux+$$
$$11ty+11sz-\bar{z})+\ldots.$$

## REFERENCES


1. H. E. Salzer, 'New formulas for facilitating osculatory interpolation', *J. Res. Nat. Bur. Stands.* **52** (1954) 211–16.
2. —— 'Osculatory interpolation in the complex plane', ibid. **54** (1955) 263–6.
3. —— 'Formulas for inverse osculatory interpolation', ibid. **56** (1956) 51–54.
4. —— 'Coefficients for complex osculatory interpolation over a cartesian grid', *J. Math. Phys.* **35** (1956) 152–63.
5. —— 'Formulas for inverse osculatory interpolation in the complex plane', *J. Res. Nat. Bur. Stands.* **59** (1957) 233–8.
6. —— 'Tables of osculatory interpolation coefficients', to be published as a Nat. Bur. Stands. Applied Math. Series booklet.
7. National Bureau of Standards, *Table of the Bessel Functions* $J_0(z)$ *and* $J_1(z)$ *for Complex Arguments* (New York, 1947).
8. National Bureau of Standards, *Table of the Bessel Functions* $Y_0(z)$ *and* $Y_1(z)$ *for Complex Arguments* (New York, 1950).
9. Harvard Computation Laboratory, *Tables of the Modified Hankel Functions of Order One-Third and of their Derivatives* (Cambridge, Mass., 1945).
10. T. Fort, *Finite Differences* (Oxford, Clarendon Press, 1948), pp. 85–88.
11. J. F. Steffensen, *Interpolation* (Baltimore, 1927), pp. 33–34.

# ON 'BEST' NINE-POINT LAPLACE DIFFERENCE ANALOGUES ON RECTANGULAR GRIDS

*By* D. GREENSPAN (*Mathematics Department, Purdue University, Lafayette, Indiana, U.S.A.*)

[Received 14 November 1957]

SUMMARY

A known nine-point difference analogue of Laplace's equation is rederived for rectangular grids in such a fashion that it is readily established as a 'best' difference analogue by elementary methods.

## 1. Introduction

A POPULAR technique for the numerical solution of a Dirichlet problem involves the replacement of the Laplace equation†

$$u_{xx}+u_{yy}=0, \tag{1}$$

by the nine-point difference analogue

$$-20u_0+4(u_1+u_2+u_3+u_4)+u_5+u_6+u_7+u_8=0, \tag{2}$$

where

$$u_0=u(x_0,y_0),\quad u_1=u(x_0+h,y_0),\quad u_2=u(x_0,y_0+h),$$
$$u_3=u(x_0-h,y_0),\quad u_4=u(x_0,y_0-h),\quad u_5=u(x_0+h,y_0+h),$$
$$u_6=u(x_0-h,y_0+h),\quad u_7=u(x_0-h,y_0-h),\quad u_8=u(x_0+h,y_0-h),$$

and $h$ is the positive grid constant. (See, for example, reference (1), chapters 8 and 10.) Also, it is known that equation (2) is a 'best' nine-point analogue of equation (1), subject to certain assumptions and definitions (see reference (2)).

The primary object here is to determine a 'best' nine-point analogue of Laplace's equation for which the grid size $h$, in the $x$-direction, need not necessarily be the same as the grid size $d$, in the $y$-direction.

The concept of 'best', as used here, will be completely defined and studied in section 3. Intuitively, a difference approximation is 'best' if no higher order difference approximation of the same type exists.

## 2. Derivation of the difference analogue

Let the grid sizes in the $x$ and $y$ directions be $h$ and $d$, respectively. The following notation will be used:

$$u_0=u(x_0,y_0),\qquad u_1=u(x_0+h,y_0),\qquad u_2=u(x_0,y_0+d),$$

† Suffixes denote partial derivatives.

$$u_3 = u(x_0-h, y_0), \quad u_4 = u(x_0, y_0-d), \qquad u_5 = u(x_0+h, y_0+d),$$
$$u_6 = u(x_0-h, y_0+d), \quad u_7 = u(x_0-h, y_0-d), \quad u_8 = u(x_0+h, y_0-d) \tag{3}$$

$$A_{m,n} \equiv \frac{1}{m!\,n!}\frac{\partial^{m+n}u}{\partial x^m \partial y^n}. \tag{4}$$

Since $h$ and $d$ are positive constants, let

$$h = pd \quad (h > 0,\ d > 0,\ p > 0). \tag{5}$$

Since $u$ is harmonic, it follows from (2), p. 426, that

$$\left.\begin{aligned}
A_{2,0} &= -A_{0,2} & A_{3,2} &= -2A_{1,4}\\
A_{3,0} &= -\tfrac{1}{3}A_{1,2} & A_{2,3} &= -10A_{0,5}\\
A_{2,1} &= -3A_{0,3} & A_{6,0} &= -A_{0,6}\\
A_{4,0} &= A_{0,4} & A_{5,1} &= A_{1,5}\\
A_{3,1} &= -A_{1,3} & A_{4,2} &= 15A_{0,6}\\
A_{2,2} &= -6A_{0,4} & A_{3,3} &= -\tfrac{10}{3}A_{1,5}\\
A_{5,0} &= \tfrac{1}{5}A_{1,4} & A_{2,4} &= -15A_{0,6}\\
A_{4,1} &= 5A_{0,5}
\end{aligned}\right\} \tag{6}$$

For future reference, note that by use of (4), (5), and (6), the Taylor series about $(x_0, y_0)$ may be written

$$\left.\begin{aligned}
u_0 &= A_{0,0}\\
u_1 &= A_{0,0}+A_{1,0}pd-A_{0,2}p^2d^2-\tfrac{1}{3}A_{1,2}p^3d^3+A_{0,4}p^4d^4+\tfrac{1}{5}A_{1,4}p^5d^5-\\
&\qquad -A_{0,6}p^6d^6+O(d^7)\\
u_2 &= A_{0,0}+A_{0,1}d+A_{0,2}d^2+A_{0,3}d^3+A_{0,4}d^4+A_{0,5}d^5+A_{0,6}d^6+O(d^7)\\
u_3 &= A_{0,0}-A_{1,0}pd-A_{0,2}p^2d^2+\tfrac{1}{3}A_{1,2}p^3d^3+A_{0,4}p^4d^4-\tfrac{1}{5}A_{1,4}p^5d^5-\\
&\qquad -A_{0,6}p^6d^6+O(d^7)\\
u_4 &= A_{0,0}-A_{0,1}d+A_{0,2}d^2-A_{0,3}d^3+A_{0,4}d^4-A_{0,5}d^5+A_{0,6}d^6+O(d^7)\\
u_5 &= A_{0,0}+d[pA_{1,0}+A_{0,1}]+d^2[pA_{1,1}+A_{0,2}(1-p^2)]+\\
&\quad +d^3[A_{1,2}(p-\tfrac{1}{3}p^3)+A_{0,3}(1-3p^2)]+\\
&\quad +d^4[A_{0,4}(p^4-6p^2+1)+A_{1,3}(p-p^3)]+\\
&\quad +d^5[A_{0,5}(5p^4-10p^2+1)+A_{1,4}(\tfrac{1}{5}p^5-2p^3+p)]+\\
&\quad +d^6[A_{0,6}(1-15p^2+15p^4-p^6)+A_{1,5}(p^5-\tfrac{10}{3}p^3+p)]+O(d^7)\\
u_6 &= A_{0,0}+d[-pA_{1,0}+A_{0,1}]+d^2[-pA_{1,1}+A_{0,2}(1-p^2)]+\\
&\quad +d^3[A_{1,2}(\tfrac{1}{3}p^3-p)+A_{0,3}(1-3p^2)]+\\
&\quad +d^4[A_{0,4}(p^4-6p^2+1)+A_{1,3}(p^3-p)]+\\
&\quad +d^5[A_{0,5}(5p^4-10p^2+1)+A_{1,4}(2p^3-p-\tfrac{1}{5}p^5)]+\\
&\quad +d^6[A_{0,6}(1-15p^2+15p^4-p^6)+A_{1,5}(\tfrac{10}{3}p^3-p-p^5)]+O(d^7)
\end{aligned}\right\} \tag{7}$$

$$\left.\begin{aligned}
u_7 = A_{0,0}&+d[-pA_{1,0}-A_{0,1}]+d^2[pA_{1,1}+A_{0,2}(1-p^2)]+\\
&+d^3[A_{1,2}(\tfrac{1}{3}p^3-p)+A_{0,3}(3p^2-1)]+\\
&+d^4[A_{0,4}(p^4-6p^2+1)+A_{1,3}(p-p^3)]+\\
&+d^5[A_{0,5}(10p^2-5p^4-1)+A_{1,4}(2p^3-\tfrac{1}{5}p^5-p)]+\\
&+d^6[A_{0,6}(1-15p^2+15p^4-p^6)+A_{1,5}(p^5-\tfrac{10}{3}p^3+p)]+O(d^7)\\
u_8 = A_{0,0}&+d[pA_{1,0}-A_{0,1}]+d^2[-pA_{1,1}+A_{0,2}(1-p^2)]+\\
&+d^3[A_{1,2}(p-\tfrac{1}{3}p^3)+A_{0,3}(3p^2-1)]+\\
&+d^4[A_{0,4}(p^4-6p^2+1)+A_{1,3}(p^3-p)]+\\
&+d^5[A_{0,5}(10p^2-5p^4-1)+A_{1,4}(\tfrac{1}{5}p^5-2p^3+p)]+\\
&+d^6[A_{0,6}(1-15p^2+15p^4-p^6)+A_{1,5}(\tfrac{10}{3}p^3-p^5-p)]+O(d^7).
\end{aligned}\right\}$$

Now let

$$L(u) = \sum_0^8 \alpha_i u_i. \tag{8}$$

Substitution of (7) into (8), and rearrangement yield

$$\left.\begin{aligned}
L(u) = A_{0,0}&(\alpha_0+\alpha_1+\alpha_2+\alpha_3+\alpha_4+\alpha_5+\alpha_6+\alpha_7+\alpha_8)\\
&+d\{A_{1,0}p(\alpha_1-\alpha_3+\alpha_5-\alpha_6-\alpha_7+\alpha_8)+\\
&\qquad +A_{0,1}(\alpha_2-\alpha_4+\alpha_5+\alpha_6-\alpha_7-\alpha_8)\}+\\
&+d^2\{A_{0,2}[-\alpha_1p^2+\alpha_2-\alpha_3p^2-\alpha_4+(1-p^2)(\alpha_5+\alpha_6+\alpha_7+\alpha_8)]+\\
&\qquad +A_{1,1}p(\alpha_5-\alpha_6+\alpha_7-\alpha_8)\}+\\
&+d^3\{\tfrac{1}{3}pA_{1,2}[-\alpha_1p^2+\alpha_3p^2+(3-p^2)(\alpha_5-\alpha_6-\alpha_7+\alpha_8)]+\\
&\qquad +A_{0,3}[\alpha_2-\alpha_4+(1-3p^2)(\alpha_5+\alpha_6-\alpha_7-\alpha_8)]\}+\\
&+d^4\{A_{1,3}(p-p^3)(\alpha_5-\alpha_6+\alpha_7-\alpha_8)+\\
&+A_{0,4}[\alpha_1p^4+\alpha_2+\alpha_3p^4+\alpha_4+(p^4-6p^2+1)(\alpha_5+\alpha_6+\alpha_7+\alpha_8)]\}+\\
&+d^5\{\tfrac{1}{5}pA_{1,4}[\alpha_1p^4-\alpha_3p^4+(p^4-10p^2+5)(\alpha_5-\alpha_6-\alpha_7+\alpha_8)]+\\
&\qquad +A_{0,5}[\alpha_2-\alpha_4+(5p^4-10p^2+1)(\alpha_5+\alpha_6-\alpha_7-\alpha_8)]\}+\\
&+d^6\{A_{1,5}(p^5-\tfrac{10}{3}p^3+p)(\alpha_5-\alpha_6+\alpha_7-\alpha_8)+A_{0,6}[-\alpha_1p^6+\alpha_2-\\
&\quad -\alpha_3p^6+\alpha_4+(1-15p^2+15p^4-p^6)(\alpha_5+\alpha_6+\alpha_7+\alpha_8)]\}+O(d^7)
\end{aligned}\right\} \tag{9}$$

In order to make $L(u)$, in (9), of as high an order as possible in $d$, consider the following system of linear equations

$$\left.\begin{aligned}
\alpha_0+\alpha_1+\alpha_2+\alpha_3+\alpha_4+\alpha_5+\alpha_6+\alpha_7+\alpha_8 &= 0\\
\alpha_1-\alpha_3+\alpha_5-\alpha_6-\alpha_7+\alpha_8 &= 0\\
\alpha_2-\alpha_4+\alpha_5+\alpha_6-\alpha_7-\alpha_8 &= 0\\
-\alpha_1p^2+\alpha_2-\alpha_3p^2+\alpha_4+(1-p^2)(\alpha_5+\alpha_6+\alpha_7+\alpha_8) &= 0\\
\alpha_5-\alpha_6+\alpha_7-\alpha_8 &= 0\\
-\alpha_1p^2+\alpha_3p^2+(3-p^2)(\alpha_5-\alpha_6-\alpha_7+\alpha_8) &= 0\\
\alpha_2-\alpha_4+(1-3p^2)(\alpha_5+\alpha_6-\alpha_7-\alpha_8) &= 0\\
\alpha_1p^4+\alpha_2+\alpha_3p^4+\alpha_4+(p^4-6p^2+1)(\alpha_5+\alpha_6+\alpha_7+\alpha_8) &= 0
\end{aligned}\right\}. \tag{10}$$

The solution to this system, in terms of $\alpha_0$, is

$$\alpha_1 = \alpha_3 = \tfrac{1}{10}\alpha_0\left(\frac{p^2-5}{p^2+1}\right); \qquad \alpha_2 = \alpha_4 = \tfrac{1}{10}\alpha_0\left(\frac{1-5p^2}{p^2+1}\right);$$

$$\alpha_5 = \alpha_6 = \alpha_7 = \alpha_8 = -\tfrac{1}{20}\alpha_0.$$

Hence, from (8)

$$L(u) \equiv \alpha_0 u_0 + \tfrac{1}{10}\alpha_0\left(\frac{p^2-5}{p^2+1}\right)(u_1+u_3) + \\ + \tfrac{1}{10}\alpha_0\left(\frac{1-5p^2}{p^2+1}\right)(u_2+u_4) - \tfrac{1}{20}\alpha_0(u_5+u_6+u_7+u_8) \quad (11)$$

while from (9):

$$L(u) \equiv O(d^6). \quad (12)$$

Hence

$$\alpha_0 u_0 + \tfrac{1}{10}\alpha_0\left(\frac{p^2-5}{p^2+1}\right)(u_1+u_3) + \tfrac{1}{10}\alpha_0\left(\frac{1-5p^2}{p^2+1}\right)(u_2+u_4) - \\ - \tfrac{1}{20}\alpha_0(\alpha_5+\alpha_6+\alpha_7+\alpha_8) \equiv O(d^6). \quad (13)$$

Finally, letting $\alpha_0 = -20$ and discarding the terms $O(d^6)$, (13) yields the following difference analogue:

$$-20u_0 + 2\left(\frac{5-p^2}{1+p^2}\right)(u_1+u_3) + 2\left(\frac{5p^2-1}{1+p^2}\right)(u_2+u_4) + (u_5+u_6+u_7+u_8) = 0. \quad (14)$$

One may note immediately that for $h = d$, i.e. for $p = 1$, equation (14) reduces to equation (2).

### 3. Establishment of equation (14) as a 'best' difference analogue for Laplace's equation

It is now assumed that in equation (5), the only predetermined constant is the mesh ratio $p$, that is, $p$ is a fixed positive constant independent of $h$ and $d$. Hence, by (5), $h$ is a function only of $d$ and $h \to 0$ as $d \to 0$. This assumption also allows discussions which involve $h$, or $h$ and $d$, to be replaced by discussions involving $d$ alone. This is readily utilized in what follows.

An allowable difference equation analogue, for present purposes, is defined to be an equation of the form

$$\sum_0^8 \alpha_i u_i = 0,$$

where the $u_i$ are given by (3) and $\lim_{d\to 0} \alpha_i \neq 0$ for at least one value of $i = 0, 1, 2, \ldots, 8$. (For heuristic considerations concerning this definition, see reference (**2**), p. 428.) If, in the preceding discussion, one constructs in place of (13), say (13′)

$$\sum_0^8 \alpha_i u_i \equiv O(d^n) \quad (13')$$

and, correspondingly, in place of (14), the analogue

$$\sum_{0}^{8} \alpha_i u_i = 0 \tag{14'}$$

where (14') is an allowable analogue, then (14') is called an approximation of order $(n-1)$.

It will now be shown that (14) is a 'best' difference analogue in that both the following theorems are valid.

THEOREM 1. *If $p = 1$, then equation* (14) *is an allowable* 7*th order analogue and there does not exist an allowable* 8*th order analogue.* (For proof, see (2), pp. 428–30.)

THEOREM 2. *If $p \neq 1$, then equation* (14) *is an allowable* 5*th order analogue and there does not exist an allowable* 6*th order analogue.*

*Proof.* The fact that (14) is an allowable 5th order analogue follows from equation (13). We proceed, now, using proof by contradiction.

Suppose that there exists an *allowable* 6th order analogue. Then let us consider in detail equation (9).

From equations (6), it follows that $A_{0,2}$, $A_{1,2}$, $A_{0,3}$, $A_{1,3}$, $A_{0,4}$, $A_{1,4}$, $A_{0,5}$, $A_{1,5}$, $A_{0,6}$ may be considered as independent parameters. Moreover, since $A_{0,0}$, $A_{1,0}$, $A_{0,1}$ are independent of $d$, it follows that one may consider $A_{0,0}$, $A_{0,1}$, $A_{1,0}$, $A_{0,2}$, $A_{1,2}$, $A_{0,3}$, $A_{1,3}$, $A_{0,4}$, $A_{1,4}$, $A_{0,5}$, $A_{1,5}$, $A_{0,6}$ as independent parameters. Now, by assumption, there exists an allowable 6th order analogue, which implies that the right-hand side of equation (9) is of order at least 7 in $d$. Since the $A_{i,j}$'s which occur in equation (9) are those which we are considering to be independent parameters, it must follow then that

$$\alpha_0+\alpha_1+\alpha_2+\alpha_3+\alpha_4+\alpha_5+\alpha_6+\alpha_7+\alpha_8 = \epsilon_1 = O(d^7), \tag{15.1}$$

$$\alpha_1-\alpha_3+\alpha_5-\alpha_6-\alpha_7+\alpha_8 = \epsilon_2 = O(d^6), \tag{15.2}$$

$$\alpha_2-\alpha_4+\alpha_5+\alpha_6-\alpha_7-\alpha_8 = \epsilon_3 = O(d^6), \tag{15.3}$$

$$-\alpha_1 p^2+\alpha_2-\alpha_3 p^2+\alpha_4+(1-p^2)(\alpha_5+\alpha_6+\alpha_7+\alpha_8) = \epsilon_4 = O(d^5), \tag{15.4}$$

$$\alpha_5-\alpha_6+\alpha_7-\alpha_8 = \epsilon_5 = O(d^5), \tag{15.5}$$

$$-\alpha_1 p^2+\alpha_3 p^2+(3-p^2)(\alpha_5-\alpha_6-\alpha_7+\alpha_8) = \epsilon_6 = O(d^4), \tag{15.6}$$

$$\alpha_2-\alpha_4+(1-3p^2)(\alpha_5+\alpha_6-\alpha_7-\alpha_8) = \epsilon_7 = O(d^4), \tag{15.7}$$

$$\alpha_1 p^4+\alpha_2+\alpha_3 p^4+\alpha_4+(p^4-6p^2+1)(\alpha_5+\alpha_6+\alpha_7+\alpha_8) = \epsilon_8 = O(d^3), \tag{15.8}$$

$$\alpha_1 p^4-\alpha_3 p^4+(p^4-10p^2+5)(\alpha_5-\alpha_6-\alpha_7+\alpha_8) = \epsilon_9 = O(d^2), \tag{15.9}$$

$$\alpha_2-\alpha_4+(5p^4-10p^2+1)(\alpha_5+\alpha_6-\alpha_7-\alpha_8) = \epsilon_{10} = O(d^2), \tag{15.10}$$

$$-\alpha_1 p^6+\alpha_2-\alpha_3 p^6+\alpha_4+(1-15p^2+15p^4-p^6)(\alpha_5+\alpha_6+\alpha_7+\alpha_8) = \epsilon_{11} = O(d). \tag{15.11}$$

Recall, of course, that $O(d^n)$ represents a function of order at least $n$ in $d$.

If one now considers equations (15.1), (15.2), (15.3), (15.4), (15.5), (15.6), (15.7), (15.8), and (15.11), then the determinant of this sub-system of equations is $-5184p^6(p^2+1)(p^2-1)$. Since $p$ is a constant and $p \neq 0$, $p \neq \pm 1$, this determinant is not zero, so that from these equations, one can explicitly and uniquely calculate $\alpha_0, \alpha_1, \alpha_2, \ldots, \alpha_8$. By Cramer's Rule, these values have the form:

$$\alpha_i = \frac{\pm \begin{vmatrix} O(d^7) & . & . & . \\ . & . & . & . \\ O(d) & . & . & . \end{vmatrix}}{-5184p^6(p^2+1)(p^2-1)} = \frac{\pm d \begin{vmatrix} \beta_1 & . & . & . \\ . & . & . & . \\ \beta_9 & . & . & . \end{vmatrix}}{-5184p^6(p^2+1)(p^2-1)} \quad (i = 0, 1, 2, \ldots, 8);$$

from which it follows that $\lim_{d \to 0} \alpha_i = 0$, for each $i = 0, 1, 2, \ldots, 8$. This, however, contradicts the assumption that an *allowable* 6th order analogue existed. Hence, a contradiction has been reached and the theorem is proved.

## REFERENCES

1. W. E. Milne, *Numerical Solution of Differential Equations* (New York, 1953).
2. D. Greenspan, 'On a 'best' 9-point difference equation analogue of Laplace's equation', *J. Franklin Institute*, **263** (1957) 425–30.

# ON THE NUMERICAL SOLUTION OF DIRICHLET PROBLEMS

*By* DONALD GREENSPAN

(*Purdue University Mathematics Dept., Lafayette, Indiana, U.S.A.*)

[Received 23 January 1958]

SUMMARY

Generalizations to a rectangular grid are given of some fundamental lemmas and theorems of S. Gerschgorin. The popular five-point technique for the numerical resolution of boundary-value problems associated with the Laplace equation is extended. The Dirichlet problem is replaced by the problem of solving a system of linear, algebraic equations, which, it is shown, has a unique solution. It is proved finally that the numerical solution converges to the analytic solution as the mesh constants converge to zero.

## 1. Introduction

In 1930 S. Gerschgorin proved some fundamental theorems germane to the numerical solution of elliptic differential equations (**1**). Since then, the vast advances in the field of computational machinery have added to the importance of that paper. One present need, and the intent here, is to generalize part of Gerschgorin's work, which was accomplished for the square grid, to the rectangular grid.

Let $G$, then, be a closed, bounded, simply connected plane region whose interior is denoted by $R$ and whose boundary curve is denoted by $S$. Let $g(x, y)$ be defined and continuous on $S$. The Dirichlet problem is to produce a function $u(x, y)$ such that both $(a)$ and $(b)$, as follow, are satisfied:

$(a)$ on $G$, $u(x, y)$ satisfies the Laplace equation, that is:

$$u_{xx}+u_{yy} = 0, \tag{1.1}$$

$(b)$ on $S$, $u(x, y) \equiv g(x, y)$.

Under general conditions, there exists a unique solution (**2** and **3**), and only such problems will be considered here. However, the analytical determination of $u(x, y)$ is quite another story from that of its existence and usually offers what are at present insurmountable problems. Hence the approach here is through numerical analysis.

## 2. General method

Let $h$ and $d$ be fixed positive constants and let $(x_0, y_0)$ be an arbitrary, but fixed, point of $G$. Denote by $G_h$ the set of all points of the form

$(x_0+mh, y_0+nd)$, contained in $G$, where $m$ and $n$ are integers. Two points $(x_1, y_1)$ and $(x_2, y_2)$ of $G_h$ are called adjacent if and only if

$$(a) \quad x_2 = x_1, \qquad |y_2 - y_1| = d;$$

or

$$(b) \quad y_2 = y_1, \qquad |x_2 - x_1| = h.$$

The interior of $G_h$, denoted by $R_h$, is the set of all points of $G_h$ which have four adjacent points which also belong to $G_h$. The boundary of $G_h$, denoted by $S_h$, and called the lattice boundary, is defined by

$$S_h = G_h - R_h.$$

The numerical method, then, is as follows. Suppose $G_h$ consists of $n$ points. Number these points in a one to one fashion with the integers 1, 2, 3,..., $n$. Denote the coordinates of the point numbered $k$ by $(x_k, y_k)$ and the unknown function $u$ at $(x_k, y_k)$ by

$$u(x_k, y_k) \equiv u_k, \quad \text{for} \quad k = 1, 2, 3, \ldots, n.$$

Let $(x_i, y_i)$ be an arbitrary point of $S_h$. Approximate $u_i$ by $g(x', y')$, where $(x', y')$ is the nearest point of $S$ to $(x_i, y_i)$. If $(x', y')$ is not unique, choose any one of the set of nearest points and use it. The problem of finding numerical approximations to $u(x, y)$ on the lattice boundary is, though crudely done, adequate for present purposes. We require then that at each point $(x_i, y_i)$ of $R_h$, the function $u$ satisfy

$$-2u(x_i, y_i) + \frac{1}{1+p^2}[u(x_i+h, y_i) + u(x_i-h, y_i)] + \\ + \frac{p^2}{1+p^2}[u(x_i, y_i+d) + u(x_i, y_i-d)] = 0, \quad (2.1)$$

where

$$h = pd \quad (h > 0, d > 0, p > 0). \quad (2.2)$$

Application of (2.1) to each point of $R_h$ results in a system of linear equations which, when solved, yields the remaining numerical approximations. What remains to be shown then is the derivation of (2.1), the fact that the linear system just described has a unique solution and general conditions under which the numerical solution converges to the analytic solution.

## 3. Derivation of the difference analogue (2.1)

The grid sizes, by the construction of $G_h$, are $h$ in the $x$-direction and $d$ in the $y$-direction. The following notation is used throughout:

$$u_0 = u(x, y), \quad u_1 = u(x+h, y), \quad u_2 = u(x, y+d),$$

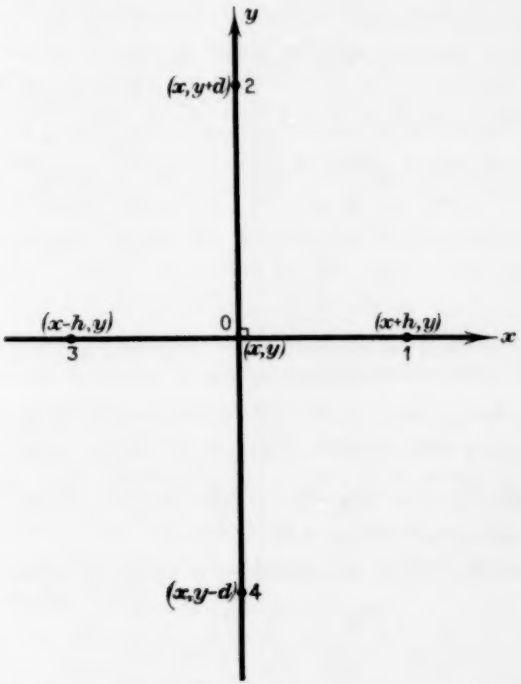


FIG. 1

$$u_3 = u(x-h, y), \quad u_4 = u(x, y-d) \quad \text{(see diagram)}, \tag{3.1}$$

$$A_{m,n} = [1/(m!\,n!)]\frac{\partial^{m+n}u}{\partial x^m \partial y^n}. \tag{3.2}$$

Since $u$ is harmonic, it follows from (4, p. 426), that

$$\left.\begin{array}{ll}
(a)\ A_{2,0} = -A_{0,2} & (i)\ A_{3,2} = -2A_{1,4} \\
(b)\ A_{3,0} = -\tfrac{1}{3}A_{1,2} & (j)\ A_{2,3} = -10A_{0,5} \\
(c)\ A_{2,1} = -3A_{0,3} & (k)\ A_{6,0} = -A_{0,6} \\
(d)\ A_{4,0} = A_{0,4} & (l)\ A_{5,1} = A_{1,5} \\
(e)\ A_{3,1} = -A_{1,3} & (m)\ A_{4,2} = 15A_{0,6} \\
(f)\ A_{2,2} = -6A_{0,4} & (n)\ A_{3,3} = -\tfrac{10}{3}A_{1,5} \\
(g)\ A_{5,0} = \tfrac{1}{5}A_{1,4} & (o)\ A_{2,4} = -15A_{0,6} \\
(h)\ A_{4,1} = 5A_{0,5} &
\end{array}\right\}. \tag{3.3}$$

For future reference, we note by use of Taylor's theorem and by (2.2):

$$\left.\begin{aligned}
u_0 &= A_{0,0} \\
u_1 &= A_{0,0}+A_{1,0}pd+A_{2,0}p^2d^2+A_{3,0}p^3d^3+A_{4,0}p^4d^4+ \\
&\qquad +A_{5,0}p^5d^5+A_{6,0}p^6d^6+O(d^7) \\
u_2 &= A_{0,0}+A_{0,1}d+A_{0,2}d^2+A_{0,3}d^3+A_{0,4}d^4+A_{0,5}d^5+A_{0,6}d^6+O(d^7) \\
u_3 &= A_{0,0}-A_{1,0}pd+A_{2,0}p^2d^2-A_{3,0}p^3d^3+A_{4,0}p^4d^4-A_{5,0}p^5d^5+ \\
&\qquad +A_{6,0}p^6d^6+O(d^7) \\
u_4 &= A_{0,0}-A_{0,1}d+A_{0,2}d^2-A_{0,3}d^3+A_{0,4}d^4-A_{0,5}d^5+A_{0,6}d^6+O(d^7)
\end{aligned}\right\} \cdot \quad (3.4)$$

Now let
$$L(u) = \sum_0^4 a_i u_i. \qquad (3.5)$$

Substitution of (3.4) into (3.5), and then substitution of (3.3) into this result, yield, after recombination:

$$\begin{aligned}
L(u) = {} & A_{0,0}(a_0+a_1+a_2+a_3+a_4)+d[A_{1,0}p(a_1-a_3)+A_{0,1}(a_2-a_4)]+ \\
& +d^2A_{0,2}[(a_2+a_4)-p^2(a_1+a_3)]+d^3[A_{0,3}(a_2-a_4)-(1/3)p^3A_{1,2}(a_1-a_3)]+ \\
& +d^4A_{0,4}[p^4(a_1+a_3)+(a_2+a_4)]+d^5[A_{0,5}(a_2-a_4)+(1/5)p^5A_{1,4}(a_1-a_3)]+ \\
& +d^6A_{0,6}[(a_2+a_4)-p^6(a_1+a_3)]+O(d^7). \qquad (3.6)
\end{aligned}$$

In order to make (3.6) of as high an order in $d$ as possible, consider

$$\begin{aligned}
a_0+a_1+a_2+a_3+a_4 &= 0, \\
a_1-a_3 &= 0, \\
a_2-a_4 &= 0, \\
a_2+a_4-p^2(a_1+a_3) &= 0.
\end{aligned}$$

If one lets $a_0 = -2$, then the solution of this system is

$$a_1 = a_3 = 1/(1+p^2), \qquad a_2 = a_4 = p^2/(1+p^2).$$

Hence, (3.5) becomes

$$L(u) = -2u_0+\frac{1}{1+p^2}(u_1+u_3)+\frac{p^2}{1+p^2}(u_2+u_4) \qquad (3.7)$$

while (3.6) becomes
$$L(u) = O(d^4). \qquad (3.8)$$

Then, from (3.7) and (3.8),

$$-2u_0+\frac{1}{1+p^2}(u_1+u_3)+\frac{p^2}{1+p^2}(u_2+u_4) \equiv O(d^4). \qquad (3.9)$$

Discarding the terms $O(d^4)$ in identity (3.9) and recalling the definitions of $u_0$, $u_1$, $u_2$, $u_3$, $u_4$ yield the difference equation approximation (2.1).

Note, of course, that for a square grid, that is, for $p = 1$, (2.1) is equivalent to the usual five-point analogue of Laplace's equation, that is:

$$-4u_0+u_1+u_2+u_3+u_4 = 0.$$

## 4. Theorems on the numerical method described in section 2

In this section let $u(x,y)$ be the analytic solution of the Dirichlet problem under consideration and let $U(x,y)$ be the solution of the numerical method described in section 2. This latter assumption means that if $(x,y)$ is any point of $R_h$, then

$$-2U_0+\frac{1}{1+p^2}(U_1+U_3)+\frac{p^2}{1+p^2}(U_2+U_4)=0 \tag{4.1}$$

where

$$U_0=U(x,y),\quad U_1=U(x+h,y),\quad U_2=U(x,y+d),$$
$$U_3=U(x-h,y),\quad U_4=U(x,y-d).$$

THEOREM 1. *The solution of the system of linear equations which results by application of the process of section* 2 *is unique.*

*Proof.* It is sufficient to show that the determinant of the system of linear equations is not zero and this is done by demonstrating that the only solution of the homogeneous system which results by considering $g(x,y)\equiv 0$ on $S$ is the zero vector. Suppose then there exists a non-trivial solution for the homogeneous system. For some point of $R_h$, $U\neq 0$. Suppose, without loss of generality, $U>0$. Let the largest value $M$ occur at $(x_0,y_0)$. Then:

$$2U_0=\frac{1}{1+p^2}(U_1+U_3)+\frac{p^2}{1+p^2}(U_2+U_4) \tag{4.2}$$

and
$$M=U_0\geqslant U_i\quad (i=1,2,3,4). \tag{4.3}$$

*Case* 1. Suppose $U_1=U_2=U_3=U_4$. Then from (4.2) and (4.3), $U_0=U_1=M$.

*Case* 2. Suppose not all of $U_1$, $U_2$, $U_3$, $U_4$ are equal. Then there exists a maximum. Suppose that $U_1$ is the maximum. Hence

$$U_2=U_1-t_2,\quad U_3=U_1-t_3,\quad U_4=U_1-t_4, \tag{4.4}$$

where $t_2$, $t_3$, $t_4$ are non-negative and at least one is positive. Substitution of (4.4) into (4.2) yields

$$2U_0=2U_1-\frac{t_3}{1+p^2}-\frac{t_2p^2}{1+p^2}-\frac{t_4p^2}{1+p^2}$$

from which it follows that $U_1>U_0$, by the nature of $t_2$, $t_3$, $t_4$. Hence, (4.3) is contradicted. A similar contradiction is reached if $U_2$, $U_3$, or $U_4$ is selected as the maximum. Hence, in any case, $U_0=U_1=M$.

Applying the same argument, a finite number of times, one may continue this result and show that $U$ at a boundary point is equal to $M$. But this is also a contradiction, since $g(x,y)\equiv 0$ on $S$ implies $U=0$ at each point of $S_h$. Hence the theorem is proved.

DEFINITION. Let

$$L[v(x,y)] \equiv \frac{h^2+d^2}{h^2d^2}\Big\{-2v(x,y)+\frac{1}{1+p^2}[v(x+h,y)+v(x-h,y)]+ \\ +\frac{p^2}{1+p^2}[v(x,y+d)+v(x,y-d)]\Big\}.$$

LEMMA 1. *If $L[v] \leqslant 0$ on $R_h$ and $v \geqslant 0$ on $S_h$, then $v \geqslant 0$ on $R_h$.* The proof follows easily as in (**5**, p. 156).

LEMMA 2. *If $-|L[v_1]| \geqslant L[v_2]$ on $R_h$ and $|v_1| \leqslant v_2$ on $S_h$, then $|v_1| \leqslant v_2$ on $R_h$.* The proof again follows easily as in (**5**, p. 156).

LEMMA 3. *If $|L[v]| \leqslant A$ on $R_h$ and if $|v| \leqslant B$ on $S_h$ and if $r$ is the radius of any circle which contains $G$, then $|v| \leqslant \frac{1}{4}(Ar^2)+B$ on $R_h$.*

*Proof.* Let

$$w(x,y) = \Big[\tfrac{1}{4}(Ar^2)\Big\{1-\frac{(x-a)^2+(y-b)^2}{r^2}\Big\}+B\Big],$$

where $(x-a)^2+(y-b)^2 = r^2$ is the equation of a circle which contains $G$.

Direct calculation yields: $L(w) = -A$. Also, $w \geqslant B$ on $S_h$. Now since $|L[v]| \leqslant A$ on $R_h$, by assumption, and $L[w] = -A$, it follows that, on $R_h$, $|L[v]| \leqslant -L[w]$. Also, $|v| \leqslant B$ on $S_h$ and $w \geqslant B$ on $S_h$, so that $w \geqslant |v|$ on $S_h$. Hence $-|L[v]| \geqslant L[w]$ on $R_h$ and $w \geqslant |v|$ on $S_h$. By Lemma 2, then, $w \geqslant |v|$ on $R_h$, or $|v| \leqslant w \leqslant \frac{1}{4}(Ar^2)+B$, on $R_h$. Hence the lemma is proved.

THEOREM 2. *If $u$ denotes the solution of the Dirichlet problem described in section* 1, *$U$ denotes the solution of the linear system of the method described in section* 2, *then if $(x_i, y_i)$ is any point of $R_h$, it follows that*

$$|U(x_i,y_i)-u(x_i,y_i)| \leqslant \frac{M_4 r^2(h^2+d^2)}{48}+M_1(h+d) \tag{4.5}$$

*where*

$$M_4 = \max_{(x,y)\in G}[|u_{4,0}(x,y)|, |u_{0,4}(x,y)|], \qquad M_1 = \max_{(x,y)\in G}[|u_{1,0}(x,y), u_{0,1}(x,y)|],$$

*$r$ = radius of any fixed circle which contains $G$,*

$$u_{m,n} = \frac{\partial^{m+n}u}{\partial x^m \partial y^n}.$$

*Proof.* Let $Q = L[u]-(u_{xx}+u_{yy})$. Substitution of the finite Taylor series expansions for $u_1$, $u_2$, $u_3$, $u_4$ in $L[u]$ yields

$$Q = \frac{u_{4,0}(\xi_1,y)h^2}{4!}+\frac{u_{4,0}(\xi_2,y)h^2}{4!}+\frac{u_{0,4}(x,\eta_1)d^2}{4!}+\frac{u_{0,4}(x,\eta_2)d^2}{4!}.$$

Hence

$$|Q| \leqslant \frac{M_4(h^2+d^2)}{12}.$$

Note, of course, that

$$|L[u]+(u_{xx}+u_{yy})| = |L[u]| = |Q|.$$

Also, for any point of $S_h$, $U$ was taken as the value $g(x', y')$ at the nearest point $(x', y')$ on the boundary $S$, and $g(x', y') = u(x', y')$ on $S$. Thereby, for any point $(x, y)$ of $S_h$ we have

$$|U(x,y)-u(x,y)| = |g(x',y')-u(x,y)| = |u(x',y')-u(x,y)|$$

where $(x', y')$ is a point of $S$ and

$$(x-x')^2+(y-y')^2 \leqslant 2h^2, \quad \text{or} \quad (x-x')^2+(y-y')^2 \leqslant 2d^2.$$

Therefore

$$\begin{aligned} |U(x,y)-u(x,y)| &= |u(x',y')-u(x,y')+u(x,y')-u(x,y)| \\ &\leqslant |u_x(\xi_3, y')(x-x')|+|u_y(x,\eta_3)(y-y')| \\ &\leqslant M_1[|x-x'|+|y-y'|] \leqslant M_1(h+d). \end{aligned} \tag{4.6}$$

It must also be noted that $L[U] = 0$, by (4.1). Hence

$$|L[U-u]| = |L[U]-L[u]| = |L[u]| = |Q|. \tag{4.7}$$

Applying Lemma 3 to (4.6) and (4.7), then, on $R_h$

$$|U-u| \leqslant (\tfrac{1}{4}r^2)\frac{M_4(h^2+d^2)}{12}+M_1(h+d) = \frac{M_4 r^2(h^2+d^2)}{48}+M_1(h+d) \tag{4.8}$$

which proves the theorem.

THEOREM 3. *Under the conditions of Theorem 2, the numerical solution $U$ converges to the analytical solution $u$, as $(h^2+d^2)$ converges to zero.*

The proof for points of $R_h$ follows immediately from inequality (4.8), while the proof for points of $S_h$ follows directly from the numerical procedure described for such points.

## REFERENCES


1. S. GERSCHGORIN, 'Fehlerabschätzung für das Differenzenverfahren zur Lösung partieller Differentialgleichungen', *Z. f. angew. Math. und Mech.* **10** (1930) 373–82.
2. D. L. BERNSTEIN, *Existence Theorems in Partial Differential Equations*, Annals of Mathematics Study Number 23, Princeton Univ. Press, 1950, pp. 179–92.
3. I. G. PETROVSKY, *Lectures on Partial Differential Equations* (English edition) (Cambridge, 1954).
4. D. GREENSPAN, 'On a "best" 9-point difference equation analogue of Laplace's equation', *J. Franklin Inst.* **263** (1957) 425–30.
5. —— 'On the numerical evaluation of the Stokes' stream function', *Mathematical Tables and Other Aids to Computation*, **11** (1957) 150–60.

# THE SIMPLE PENDULUM UNDER PERIODIC DISTURBANCE

*By* HAROLD JEFFREYS

(*St. John's College, Cambridge*)

[Received 7 November 1957]

SUMMARY

The motion of a pendulum with a periodic disturbance is examined. When higher powers of the displacement are retained there may be one or three periodic solutions according to the amplitude and period of the disturbing force. The elementary solution far from resonance corresponds to two different branches of the general solution, one of which ceases to exist when the resonance is sufficiently close.

**1.** WHEN a small horizontal periodic force is applied to a pendulum, the displacement satisfies a differential equation of the form, with $\epsilon$ small,

$$\ddot{x}+\sigma^2 \sin x = \epsilon \cos x \sin t. \tag{1}$$

If $x^2$ is neglected this has the elementary solution

$$x = \frac{\epsilon \sin t}{\sigma^2-1} \tag{2}$$

and this is certainly a good approximation in most cases. However, when $\sigma^2$ passes through 1 the coefficient of $\sin t$ changes sign; this would suggest that the amplitude either passes through 0 or becomes infinite, and neither alternative is plausible—in fact the former does not satisfy the exact differential equation.

The problem has been studied by E. W. Brown (**1**, **2**, **3**) who shows that when $\sigma^2 = 1$ and higher powers of $x$ are retained there is a periodic solution of (1) with amplitude of order $\epsilon^{\frac{1}{3}}$, and there is a suggestion that the amplitude for all $\sigma$ is at most of this order, but this has not been proved. In any case little is known about the behaviour in the range of transition. This paper concerns the existence and stability of periodic solutions.

*Case* 1. $\sigma^2 \gg 1$. In the first place we notice that if $\sigma^2 > 1$ and $\epsilon = 0$, there is an amplitude $a$ that makes the period $2\pi$. In this motion $x$ is an odd function of $t+\alpha$, where $\alpha$ is constant. Write it as $X(t+\alpha)$. This is a first approximation to $x$; but if

$$E = \tfrac{1}{2}\dot{x}^2+\sigma^2(1-\cos x), \tag{3}$$

$$[E]_0^t = \int_0^t \epsilon \cos x \sin t \, \dot{x} \, dt, \tag{4}$$

and at least for amplitude $\leqslant \frac{1}{2}\pi$ this increases indefinitely with $t$ unless $\dot{x}$, considered as a Fourier series, contains no term in $\sin t$ and therefore $x$ no term in $\cos t$. For a suitable first approximation to a periodic motion we must therefore take $\alpha = 0$ or $\pi$. For higher accuracy put

$$x = X(t)+y \tag{5}$$

with $y$ small. Then to the first order in $\epsilon$ and $y$

$$\ddot{y}+\sigma^2\cos X.y = \epsilon\cos X\sin t. \tag{6}$$

The complementary function is of the form

$$Au(t)+Bv(t), \tag{7}$$

where $u(t)$, $v(t)$ are an even and an odd function of $t$, and their Wronskian $u\dot{v}-\dot{u}v$ can be made 1. Then to order $\epsilon$

$$y = Au(t)+Bv(t)-\int_0^t \{u(t)v(\tau)-u(\tau)v(t)\}\epsilon\cos X(\tau)\sin\tau\, d\tau. \tag{8}$$

The integral is an odd function of $t$; then we find that $y(\pi) = y(-\pi)$, $\dot{y}(\pi) = \dot{y}(-\pi)$, if

$$A = 0, \quad Bv(\pi)-\int_0^{\pi} \{u(\pi)v(\tau)-u(\tau)v(\pi)\}\epsilon\cos X(\pi)\sin\tau\, d\tau = 0. \tag{9}$$

Then $y$ is an odd periodic function. $v(t)$ is not periodic, and $v(\pi) \neq 0$; hence $B$ is determined and there are two periodic solutions of the form

$$x = X(t)+\epsilon\theta(t), \qquad x = -X(t)+\epsilon\theta(t) \tag{10}$$

where $\theta(t)$ is an odd periodic function.

Hence for $\sigma^2 \gg 1$ there are three periodic solutions of (1), the elementary one and two large ones given by (10). For $\sigma^2 \ll 1$ there is no analogue of the second pair, since any free motion would have a speed $< \sigma$.

If $\sigma^2$ is near 1 the method fails because the amplitude of $X$ is small and so is $v(\pi)$. Hence $B$ is the ratio of two small quantities and might not be small.

*Case* 2. $\sigma^2$ near 1. To investigate the transition we put

$$\sigma^2-1 = \mu$$

with $\mu$ small, and neglect powers of $x$ above the third. Then (1) becomes

$$\ddot{x}+x = \tfrac{1}{6}\sigma^2x^3-\mu x+\epsilon(1-\tfrac{1}{2}x^2)\sin t. \tag{11}$$

We shall put $$x = \epsilon^{\frac{1}{3}}z; \quad \mu = \epsilon^{\frac{1}{3}}\nu; \quad \epsilon^{\frac{1}{3}} = \eta. \tag{12}$$

Then to the lowest powers of $\epsilon$

$$\ddot{z}+z = \eta(\tfrac{1}{6}z^3-\nu z+\sin t), \tag{13}$$

where $\eta$ is small but $\nu$ is unrestricted. Substitute

$$z = a\sin t+c\sin 3t \tag{14}$$

and assume $c = o(a)$. The terms in $\sin t$ and $\sin 3t$ give

$$\tfrac{1}{8}a^3 - \tfrac{1}{8}a^2c - \nu a + 1 = 0, \tag{15}$$

$$8c \equiv \eta(-\tfrac{1}{24}a^3 + \tfrac{1}{6}a^2c - \nu c), \tag{16}$$

whence $c$ is small of order $\eta a^3$; and we have to consider the cubic

$$a^3 - 8\nu a + 8 = 0. \tag{17}$$

$\nu = 0$ ($\sigma^2 = 1$) gives $a = -2$, and the coefficient of $\sin t$ in $x$ is $-2\epsilon^{\frac{1}{2}}$, agreeing with Brown's result. There is always a negative root.

For $\nu > 0$ there are two positive roots if

$$\nu > \tfrac{3}{8}.2^{\frac{2}{3}} = 3.2^{-\frac{4}{3}},$$

otherwise none. The critical value makes them coalesce at $a = 2^{\frac{1}{3}}$. When $\nu$ becomes large the smaller corresponds to the elementary solution, the larger to one of the large solutions. The negative root gives the other large solution.

For $\nu < 0$ there are never three solutions. But with $\nu \ll 0$ the solution approximates to the elementary one $a = 1/\nu$.

To investigate the variation of $a$ with $\nu$ we have

$$\frac{da}{d\nu} = \frac{8a}{3a^2 - 8\nu}. \tag{18}$$

For $\nu < 0$, $a < 0$ this is always negative. Hence as $\nu$ increases from $-\infty$ to 0 the magnitude of $a$ increases steadily to 2. As $\nu$ proceeds to positive values the increase continues; $3a^2 - 8\nu$ never vanishes for the negative root of (17), since the left side would be

$$-\tfrac{16}{3}\nu a + 8 > 8$$

for $\nu > 0$, $a < 0$. Hence the elementary solution for $\nu < 0$ passes continuously, with increasing amplitude, into the large negative solution for $\nu > 0$. For $\nu < 3.2^{-\frac{4}{3}}$ (nearly 1) this is the only periodic solution possible.

For larger $\nu$ there are two solutions with positive $a$, the smaller of which approximates to the elementary solution, but as $\nu$ decreases through the critical value these disappear. If the motion has been periodic and near one of them, and $\nu$ decreases, the further motion cannot be periodic at all; it may be described as an oscillation about the solution with negative $a$, but with period only approximately $2\pi$. The latter solution has $a = -2.2^{\frac{1}{3}} = -3{\cdot}3$ nearly.

Search has been made for other small solutions whose leading terms are of the form $a \sin pt$ with $p \neq 1$; all attempts led to contradictions.

## 2. Stability of solutions

If $z$ is slightly disturbed from a periodic solution the disturbance may or may not ultimately become large. We write

$$z = a\sin t+\zeta; \tag{19}$$

then
$$\ddot{\zeta}+\zeta = \eta(\tfrac{1}{2}a^2\sin^2 t-\nu)\zeta = \eta(\tfrac{1}{4}a^2-\nu-\tfrac{1}{4}a^2\cos 2t)\zeta, \tag{20}$$

which is a Mathieu equation. It is known that the solutions of

$$\ddot{\zeta}+(R-2q\cos 2t)\zeta = 0 \tag{21}$$

contain real exponential factors if $R$ (near 1) lies between the values $a_1$, $b_1$

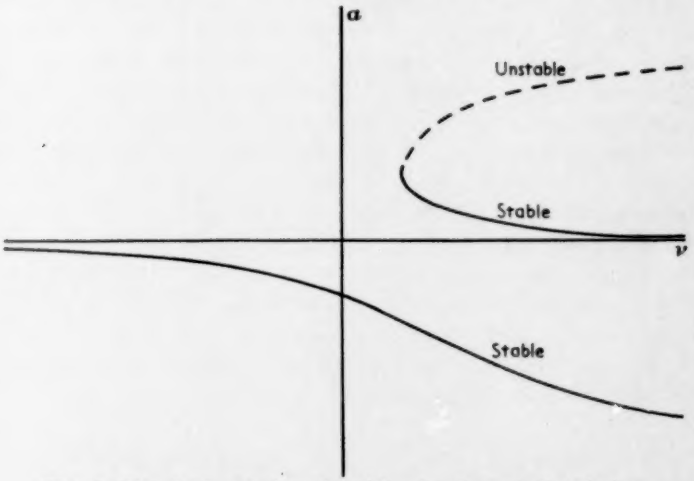


FIG. 1. Sketch of variation of $a$ with $\nu$ for the periodic solutions.

that make an even and an odd periodic solution exist, namely (4, pp. 16, 76, 103)

$$a_1 = 1+q-\tfrac{1}{8}q^2\ldots, \tag{22}$$

$$b_1 = 1-q-\tfrac{1}{8}q^2\ldots. \tag{23}$$

Here
$$q = \tfrac{1}{8}a^2, \quad R = 1-\tfrac{1}{4}a^2+\nu, \tag{24}$$

$$a_1 = 1+\tfrac{1}{8}a^2\ldots, \quad b_1 = 1-\tfrac{1}{8}a^2\ldots.$$

Then $R = b_1$ if $\frac{1}{8}a^2 = \nu$, and $R = a_1$ if $\frac{3}{8}a^2 = \nu$. The instability condition is

$$\tfrac{1}{8}a^2 < \nu < \tfrac{3}{8}a^2.$$

From (17), $\nu-\frac{1}{8}a^2$ has the sign of $a$. Hence the condition is never satisfied for $\nu$ positive or negative if $a$ is negative. The solution with negative $a$ is always stable. For positive $a$ the first inequality is satisfied and stability depends on the sign of $\frac{3}{8}a^2-\nu$. Since the vanishing of this

quantity is the condition for equal roots, when two positive values of $a$ exist the smaller gives a stable solution and the larger an unstable one.

The conclusions are therefore rather peculiar. If we imagine a sequence of systems with varying $\nu$, and start with large negative $\nu$ ($\sigma^2 \ll 1$) the elementary solution starts by being a good approximation. As $\nu$ increases the amplitude increases in magnitude and is $2\epsilon^{\frac{1}{2}}$ when $\nu = 0$, but it continues to increase as $\nu$ becomes positive and may become large—but *not* at the values that make the elementary solution large. This corresponds (with a slight change of parameters) to the development of a large amplitude in a swing.

If $\nu$ is large and positive, and the solution is the large one with negative $a$, decreasing $\nu$ will simply retrace the above process. But more usually the solution in this case will initially correspond to the small elementary one. With decreasing $\nu$ the amplitude increases, but near $\nu = 1$ the solution ceases to exist. With further decrease of $\nu$ the motion will be a non-periodic one, oscillating slowly about the solution with negative $a$. Presumably damping will remove this oscillation in time.

A term in $x^2$ in the differential equation would not affect the main features of the solution. For on separation into harmonic parts it will give a constant and a term in $\cos 2t$, neither of which would affect the coefficient of $\sin t$, and (17) would be unaltered. The solution would contain a constant and a term in $\cos 2t$, and would thus cease to be exactly an odd function of $t$, but the conclusions about the ranges of existence of the solutions and their stability would be hardly affected.

In writing this paper I have benefited greatly from discussions with Professor J. E. Littlewood and Dr. Mary Cartwright. In particular they provided topological proofs of the existence of the solutions that are given approximately above.

## REFERENCES

1. E. W. Brown, Rice Institute Pamphlets, **19**, 1932.
2. —— *Elements of the Theory of Resonance* (Cambridge, 1932).
3. —— and C. A. Shook, *Planetary Theory* (Cambridge, 1933).
4. N. W. McLachlan, *Theory and Application of Mathieu Functions* (Oxford, 1947).

A descriptive [illegible] equations of [illegible] its recent [illegible]
MECHANICS [illegible]

[illegible]

This book [illegible] dynamics and [illegible] importance. [illegible]
APPLIED MATH[illegible]

[illegible]

A simple [illegible] and [illegible] their [illegible]
CAMBRIDGE [illegible] AND
MATHEMAT[illegible]

[illegible]

An intro[illegible] those [illegible] applications

[illegible]

quantity is the condition for equal roots, when two positive values of $a$ exist the smaller gives a stable solution and the larger an unstable one.

The conclusions are therefore rather peculiar. If we imagine a sequence of systems with varying $v$, and start with large negative $v$ ($a^2 = 1$) the elementary solution starts by being a good approximation. As $v$ increases the amplitude increases in magnitude and is $2\epsilon^{\frac{1}{2}}$ when $v = 0$, but it continues to increase as $v$ becomes positive and may become large—but *not* at the values that make the elementary solution large. This corresponds (with a slight change of parameters) to the development of a large amplitude in a swing.

If $v$ is large and positive, and the solution is the large one with negative $a$, decreasing $v$ will simply retrace the above process. But more usually the solution in this case will initially correspond to the small elementary one. With decreasing $v$ the amplitude increases, but near $v = 1$ the solution ceases to exist. With further decrease of $v$ the motion will be a non-periodic one, oscillating slowly about the solution with negative $a$. Presumably damping will remove this oscillation in time.

A term in $x^2$ in the differential equation would not affect the main features of the solution. For on separation into harmonic parts it will give a constant and a term in $\cos 2t$, neither of which would affect the coefficient of $\sin t$, and (17) would be unaltered. The solution would contain a constant and a term in $\cos 2t$, and would thus cease to be exactly an odd function of $t$, but the conclusions about the ranges of existence of the solutions and their stability would be hardly affected.

In writing this paper I have benefited greatly from discussions with Professor J. E. Littlewood and Dr. Mary Cartwright. In particular they provided topological proofs of the existence of the solutions that are given approximately above.

## REFERENCES

1. E. W. Brown, Rice Institute Pamphlets, **19**, 1932.
2. ——, *Elements of the Theory of Resonance* (Cambridge, 1932).
3. —— and C. A. Shook, *Planetary Theory* (Cambridge, 1933).
4. N. W. McLachlan, *Theory and Application of Mathieu Functions* (Oxford, 1947).

THE QUARTERLY JOURNAL OF MECHANICS AND APPLIED MATHEMATICS

VOLUME XII PART 1 FEBRUARY 1959

# CONTENTS



*The Editorial Board gratefully acknowledge the support given by: Blackburn & General Aircraft Limited; Bristol Aeroplane Company; Courtaulds Scientific and Educational Trust Fund; English Electric Company; Hawker Siddeley Group Limited; Imperial Chemical Industries Limited; Metropolitan-Vickers Electrical Company Limited; The Shell Petroleum Co. Limited; Vickers-Armstrongs (Aircraft) Limited.*